



Netherlands Enterprise Agency

Seismic Hazard Assessment

Ten noorden van de Waddeneilanden Wind Farm Zone

*>> Sustainable. Agricultural. Innovative.
International.*





RVO Approval for Publication

Document Characteristics

Version	Title	Date of Publication	Reference Contractor NGI	Reference RVO	Pages
Rev0	Ten Noorden van de Waddeneilanden Wind Farm Zone Seismic Hazard Assessment	May 26 th , 2021	Doc. No.: 20190798-03-TN	WOZ2200196	85 (NGI report) 8 (DNV report) 2 (cover) 1 (approval)

Approval

Approval for public disclosure	Position
Frank van Erp	Executive Expert Offshore Wind Energy
Matté Brijder	Programme Manager RVO Offshore Wind Energy



TEN NOORDEN VAN DE WADDENEILANDEN (TNW) WIND FARM ZONE

Certification Report

Site Conditions

Seismic Hazard Assessment

Netherlands Enterprise Agency

Report No.: CR-SC-DNVGL-SE-0190-06281-0_Seismic Hazard

Date: 2021-09-13



Project name: Ten noorden van de Waddeneilanden (TNW) Wind Farm Zone DNV Energy Systems
Renewables Certification

Report title: Certification Report DNV Denmark A/S
Site Conditions Tuborg Parkvej 8
Seismic Hazard Assessment 2900 Hellerup

Customer: Netherlands Enterprise Agency, Denmark
Croeselaan 15 Tel: +45 39 45 48 00
3521 BJ Utrecht The Netherlands

Customer contact: Huygen van Steen (RVO)

Date of issue: 2021-09-13

Project No.: 10151362

Report No.: CR-SC-DNVGL-SE-0190-06281-0_Seismic Hazard

Applicable contract(s) governing the provision of this Report: 201805104/TN198682. PO WOZ2190149

Objective: To confirm that the Seismic Hazard Assessment at Ten noorden van de Waddeneilanden (TNW) Wind Farm Zone has been derived in line with the requirements as stated in DNVGL-SE-0190:2020 for site conditions. The Seismic Hazard Assessment is to be used for design for Ten noorden van de Waddeneilanden (TNW) Wind Farm Zone.

Prepared by:	Verified by:	Approved by:
Hunt, Helena Jane 2021.09.13 12:35:05 +02'00'	Wagner, Michael 2021.09.13 13:56:03 +02'00'	Redanz, Pia Digitally signed by Redanz, Pia Date: 2021.09.13 18:20:06 +02'00'
Helena Hunt Principal Engineer	Michael Wagner Senior Engineer	Pia Redanz Project Sponsor, Head of Section

Copyright © DNV 2021. All rights reserved. Unless otherwise agreed in writing: (i) This publication or parts thereof may not be copied, reproduced or transmitted in any form, or by any means, whether digitally or otherwise; (ii) The content of this publication shall be kept confidential by the customer; (iii) No third party may rely on its contents; and (iv) DNV undertakes no duty of care toward any third party. Reference to part of this publication which may lead to misinterpretation is prohibited.

DNV Distribution: OPEN. Unrestricted distribution, internal and external. INTERNAL use only. Internal DNV document. CONFIDENTIAL. Distribution within DNV according to applicable contract.* SECRET. Authorized access only.

Keywords: TNW Site Conditions Seismic Hazard Assessment

*Specify distribution: DNV Renewables Certification

Rev. No.	Date	Reason for Issue	Prepared by	Verified by	Approved by
0	2021-09-13	First issue	HEHU	MICWAG	PR



Table of contents

1	EXECUTIVE SUMMARY.....	1
2	CERTIFICATION SCHEME	1
3	SCOPE OF EVALUATION.....	1
4	CONDITIONS.....	1
5	OUTSTANDING ISSUES.....	1
6	CONCLUSION	1
Appendix A	Seismic Hazard Assessment	

1 EXECUTIVE SUMMARY

The Ten noorden van de Waddeneilanden (TNW) Wind Farm Zone is located in the Dutch Sector of the North Sea, approximately 50 km from the coastline. As part of the tender preparations, the Netherlands Enterprise Agency (Rijksdienst voor Ondernemend Nederland, RVO) has requested a Seismic Hazard Assessment of the Ten noorden van de Waddeneilanden (TNW) Wind Farm Zone.

DNV was assigned to validate this Seismic Hazard Assessment and its use within a Design Basis for Offshore Wind Turbine Structures in accordance with DNVGL-ST-0437 and DNVGL-ST-0126.

2 CERTIFICATION SCHEME

Document No.	Title
DNVGL-SE-0190:2020-09	Project certification of wind power plants

3 SCOPE OF EVALUATION

The scope and interface of the evaluation covered by the report is the Seismic Hazard Assessment within the Site Conditions Assessment.

The Appendix to this report comprises the detailed DNV evaluation which include references to standards, list of documentation and the conclusion of the DNV evaluation.

4 CONDITIONS

No conditions have been identified.

5 OUTSTANDING ISSUES

No outstanding issues have been identified.

6 CONCLUSION

The verification work performed by DNV confirms that the seismic hazard assessment as described by the documents listed in the Annex A section "Documentation from customer" related to the Ten noorden van de Waddeneilanden Offshore Wind Farm zone fulfils the relevant demands set up in the Certification Scheme DNVGL-SE-0190:2020-09 and the codes and standards listed in the Annex A section "Basis for the evaluation".

APPENDIX A

Seismic Hazard Assessment

Evaluation of Seismic Hazard Assessment for Ten noorden van de Waddeneilanden (TNW) Wind Farm Zone

A1 Description of verified component/system

This evaluation report documents the verification activities performed by DNV, as Certification Body, to approve the seismic hazard assessment for the Ten noorden van de Waddeneilanden (TNW) offshore wind farm (OWF) zone according to the DNVGL-SE-0190:2020-09 certification scheme.

The TNW OWF zone is located in the Dutch Sector of the North Sea, approximately 50 km from the coastline of Schiermonnikoog. It is in an extended stable continental region far from any tectonic plate boundaries. The largest earthquake within 300 km of the site is the 1931 Dogger Bank earthquake which occurred 274 km from the site off the coast of England.

“Seismic hazard assessment” covers the evaluation of potential seismic sources, the rate of occurrence of earthquake magnitudes for each source, the distribution of source-to-site distances for each source, the intensity measure for all combinations of magnitude, distance and uncertainties, and computation of annualized rate of exceedance within the project area.

A2 Interface to other systems/components:

Evaluation of seismic hazard forms part of geotechnical Design Basis Evaluation (DBE) which is a general term and covers the evaluation of water depth and seabed mobility, geological and geophysical surveys, geotechnical investigation and laboratory test results, and seismic considerations. After data collection, all site investigation results are condensed (to e.g. characteristic design values) and brought into a systematic form which can be used for the purpose of geotechnical and structural foundation design in the Design Evaluation (DE) module.

A3 Basis for the evaluation

Applied codes and standards:

Document No.	Revision	Title
DNVGL-ST-0126	July 2018	Support structures for wind turbines
ISO 19901-2	Nov 2017	Petroleum and natural gas industries – Specific requirements for offshore structures – Part 2: Seismic action procedures and criteria. International Organization for Standardization, Geneva, Switzerland.

The evaluation has been based on the following loads, design basis as well as other specific criteria:

Document No.	Revision	Title
N/A		

A4 Documentation from customer

List of reports:

Document No.	Revision	Title
20190798-03-TN	0 2021-05-26	Technical Note – Seismic Hazard Assessment

List of drawings:

Document No.	Revision	Title
N/A		

List of specifications/manuals/instructions:

Document No.	Revision	Title
N/A		

List of documents taken for information only:

Document No.	Revision	Title
N/A		

A5 Evaluation work

Verification activities

The DNV verification is primarily based on document review. DNV's communication with the client during the verification process has been through Verification Comment Sheets (VCS, reference TNW_644325-VCS-22-rev01-Seismic Study) to the document(s) that constitutes the Design Basis Evaluation for the TNW OWF.

Seismic conditions

Both simplified and detailed seismic action determination procedures were performed by the designer for the TNW OWF site. The simplified procedure was conducted following ISO 19901-2, with horizontal and vertical design spectra at the soil surface estimated for a 1000-year return period earthquake. Both Abnormal Level Earthquake (ALE) and Extreme Level Earthquake (ELE) scenarios for exposure levels L1 and L2 were evaluated. For the detailed seismic action procedure, the designer performed a probabilistic seismic hazard analysis (PSHA) for the project site. The analysis employed 4 different seismic source models were adopted and 5 unique ground motion models (GMMs). The results showed that the source controlling the hazard was the source in which the site is located. The controlling magnitude-distance scenario for short spectral periods was for moment magnitudes between 4.8 and 5.3, at a distance between 50km and 90km. That for long spectral periods was for moment magnitudes between 5.6 and 6.1, at a distance between 140km and 180km. In all cases, the simplified seismic action procedure predicted larger ground motions than the detailed seismic action procedure. This was expected because the simplified seismic action procedure was designed to be conservative.

DNV have verified the seismic hazard assessment performed by the designer, through document review, to confirm its compliance with the applied codes and standards which form the basis for this evaluation. We further note that a wide collection of results based on different return periods (95-year, 475-year, 700-year, 1000-year, 1150-year, 1675-year, 2500-year and 3000-year), different analysis methods (simplified and detailed), different foundation types and different



exposure levels are included in the same study, from which subsequent seismic design for the different assets within the TNW OWF may selectively utilize.

A 6 Conditions to be considered in other certification phases

No conditions have been identified.

A7 Outstanding issues

No outstanding issues have been identified.

A8 Conclusion

The verification work performed by DNV confirms that the seismic hazard assessment as described by the documents listed in the section "Documentation from customer" related to the Ten noorden van de Waddeneilanden Offshore Wind Farm zone fulfils the relevant demands set up in the Certification Scheme DNVGL-SE-0190:2020-09 and the codes and standards listed in the section "Basis for the evaluation".



About DNV

DNV is the independent expert in risk management and assurance, operating in more than 100 countries. Through its broad experience and deep expertise DNV advances safety and sustainable performance, sets industry benchmarks, and inspires and invents solutions.

Whether assessing a new ship design, optimizing the performance of a wind farm, analyzing sensor data from a gas pipeline or certifying a food company's supply chain, DNV enables its customers and their stakeholders to make critical decisions with confidence.

Driven by its purpose, to safeguard life, property, and the environment, DNV helps tackle the challenges and global transformations facing its customers and the world today and is a trusted voice for many of the world's most successful and forward-thinking companies.

To: Ministerie van Economische Zaken en Klimaat, Rijksdienst voor Ondernemend Nederland (RVO)

Attn.: Frank van Erp

Date: 2021-05-26

Revision no./Rev.date: 0 /

Document no.: 20190798-03-TN

Project: Ten noorden van de Waddeneilanden Wind Farm Zone

Project manager: Carl Fredrik Forsberg

Prepared by: Brian Carlton, Yunsup Shin, Valentina Leoncino

Reviewed by: Amir M Kaynia

Seismic hazard assessment

Contents

1	Introduction	4
1.1	Background	4
1.2	Scope of work	4
1.3	Organisation of the report	5
1.4	Abbreviations	5
2	Simplified seismic action procedure	8
3	Previous studies	17
3.1	Global Seismic Hazard Assessment Program (GSHAP)	17
3.2	Bungum et al. 2000	19
3.3	Seismic Hazard Harmonization in Europe (SHARE)	20
3.4	HKW PSHA report	22
4	Overview of PSHA methodology	24
5	Tectonic setting	26
5.1	Overview	26
5.2	Regional geologic structures	26
5.3	Induced seismicity	27
6	Source characterization	28
6.1	Background	28
6.2	Source characterisation based on Fugro (2020)	29
6.3	Earthquake catalogue	36
7	Ground motion models	48
7.1	Background	48
7.2	Selected GMMs	49
8	Characterisation of uncertainty	54
8.1	Aleatory variability and epistemic uncertainty	54
8.2	Logic tree	55

9	Design hazard levels	55
10	PSHA results	57
10.1	Hazard curves	57
10.2	Horizontal design uniform hazard spectra (UHS)	65
10.3	Hazard fractiles	67
10.4	Deaggregation	70
10.5	Comparison with other studies	73
10.6	Vertical design spectra and spectra for other damping ratios	75
11	Conclusions	76
12	References	77

Review and reference page

Summary

NGI performed both a simplified and detailed seismic action procedure according to ISO 19901-2:2017 for the middle (5.699° East 54.022° North) of the Ten Noorden van de Waddeneilanden (TNW) Wind Farm Zone off the north coast of The Netherlands. NGI performed analyses for the Extreme Level Earthquake (ELE) and Abnormal Level Earthquake (ALE), L1 and L2 exposure levels, and assuming both deep steel foundations and shallow concrete foundations. These correspond to return periods of 700, 1000, 1150, 1675, 2500 and 3000 years. In addition, the client requested results for return periods of 95 and 475 years.

The TNW wind farm zone is in the Dutch sector of the North Sea in an extended stable continental region far from any tectonic plate boundaries. The largest earthquake within 300 km of the site is the 1931 Dogger Bank earthquake ($M_w = 5.87$), which occurred 274 km from the site off the coast of England.

For the detailed seismic action procedure NGI performed a probabilistic seismic hazard analysis (PSHA) using the computer program HAZ45.2 developed by Professor Norman Abrahamson (Abrahamson, 2017; Hale et al., 2018). This program implements the PSHA methodology developed principally by Cornell (1968) and refined by McGuire (1974; 1978). NGI developed three seismic source models based on the three areal source models from Fugro (2020) for the HKW wind farm zone, but extended to the north and east to cover a circle 300 km in radius centred on the site. In addition, NGI developed one seismic source model using smoothed gridded seismicity based on an earthquake catalogue merged from The Netherlands, Belgian, German and British national seismic catalogues, as well as the ISC and EMEC catalogues. NGI used the same five ground motion models (GMMs) with the same logic tree weights as Fugro (2020) for the HKW wind farm zone. The GMMs are Akkar et al. (2014), Bindi et al. (2017), Cauzzi et al. (2015), Campbell and Bozorgnia (2014) and Yenier and Atkinson (2015), with weights of 0.25, 0.25, 0.20, 0.20 and 0.10, respectively.

The results show that the source controlling the hazard is the source in which the site is located, and the controlling magnitude-distance scenario for short spectral periods is $M_w = 4.8-5.3$ and $R = 50-90$ km, and for long spectral periods is $M_w = 5.6-6.1$ and $R = 140-180$ km. The table below lists the peak ground acceleration (PGA) values for the eight selected design return periods. In general, the values for TNW are about 70% of the values for HKW, which is expected based on past regional studies. The detailed seismic action procedure predicts lower hazard than the simplified seismic action procedure.

Peak ground acceleration (g) for eight different design return periods (years)

Period (s)	95	475	700	1000	1150	1675	2500	3000
PGA	0.0031	0.0124	0.0167	0.0216	0.0237	0.0304	0.0397	0.0448

1 Introduction

1.1 Background

The Netherlands Enterprise Agency "Rijksdienst voor Ondernemend Nederland" (RVO), is developing offshore wind farms in the Dutch sector of the North Sea. RVO awarded the Norwegian Geotechnical Institute (NGI) the contract to develop a Geological Ground Model and an Integrated Ground Model for the Ten Noorden van de Waddeneilanden (TNW) wind farm zone. This technical note describes the seismic hazard assessment performed by NGI for TNW as part of the Geological Ground Model.

There are currently no internationally recognized codes governing the seismic design of offshore wind farms. However, it has been standard practice to use ISO 19901-2:2017, which is the code governing seismic design of offshore oil and gas structures. Figure 1-1 outlines the procedure to perform seismic design according to ISO 19901-2:2017. The first step is to determine the 5% damped spectral acceleration at an oscillator period of 1.0 second ($S_{a,map}(1.0)$), return period of 1000 years and for a reference rock condition ($V_{S30} > 750$ m/s) for the project location. These values are provided by ISO 19901-2:2017 as shown in Figure 1-2a for offshore locations around the world. For the project location (red star in Figure 1-2), $S_{a,map}(1.0) = 0.02$ g. This value corresponds to a site seismic zone = 0 and seismic risk category (SRC) = 1, regardless of the exposure level of the structure. According to ISO 19901-2:2017, for SRC = 1, no seismic hazard evaluation is required because the seismic hazard is very low.

1.2 Scope of work

Even though no seismic hazard evaluation is required according to ISO 19901-2:2017, RVO requested NGI to perform a simplified seismic action procedure (Clause 7 in ISO 19901-2:2017) and a detailed seismic action procedure (Clause 8 in ISO 19901-2:2017). In addition, RVO requested NGI to perform the detailed seismic action procedure for return periods of 95 years, 475 years, and for the Extreme Level Earthquake (ELE) and Abnormal Level Earthquake (ALE) return periods for both L1 and L2 exposure levels. NGI performed the analyses for the middle of the wind farm, at 5.699° East 54.022° North.

RVO also requested that NGI perform a simplified seismic hazard assessment according to EN 1998-1:2004, which is the code governing seismic design of onshore structures in most countries in Europe. However, there is no national annex for The Netherlands specifying the necessary input parameters. Therefore, strictly speaking, a simplified seismic hazard assessment according to EN 1998-1:2004 cannot be performed for the project location.

1.3 Organisation of the report

Section 2 describes the simplified seismic action procedure according to Clause 7 in ISO 19901-2:2017. Section 3 presents previous seismic hazard studies that encompass or are near the project location. Section 4 outlines the basic components of a site specific probabilistic seismic hazard analysis (PSHA), which is the core of the detailed seismic action procedure according to Clause 8 in ISO 19901-2:2017. Section 5 provides an overview of the geologic and tectonic setting of the study area. Section 6 describes the source characterization based on recorded and historical earthquake events as well as seismic source models from available relevant past studies. Section 7 summarizes the ground motion models used in the PSHA. Section 8 explains the characterisation of uncertainty and the use of a logic tree in PSHA. Section 9 describes the selection of the ELE and ALE return period according to ISO 19901-2:2017 for both L1 and L2 exposure levels, and assuming both shallow concrete and deep steel foundations. Section 10 presents the results of the PSHA, including hazard curves, uniform hazard spectra (UHS), hazard curve and UHS fractiles, deaggregation plots, and comparisons with the results of the simplified seismic action procedure, and the results of the PSHA performed by Fugro (2020) for the HKW wind farm zone. Section 11 summarises the main findings and conclusions of the report.

1.4 Abbreviations

Below is a list of abbreviations used in this report.

- ↗ ALE: Abnormal Level Earthquake
- ↗ BGS: British Geological Survey
- ↗ ELE: Extreme Level Earthquake
- ↗ EMEC: The European and Mediterranean Earthquake Catalogue
- ↗ GMM: Ground motion models
- ↗ GSHAP: Global Seismic Hazard Assessment Program
- ↗ HKW: Hollandse Kust West
- ↗ IM: Intensity measure
- ↗ ISC: International Seismological Centre
- ↗ KNMI: Royal Netherlands Meteorological Institute
- ↗ NGI: Norwegian Geotechnical Institute
- ↗ PGA: Peak ground acceleration
- ↗ PSHA: Probabilistic seismic hazard analysis
- ↗ RESORCE: Reference Database for Seismic Ground-Motion in Europe
- ↗ ROB: Royal Observatory of Belgium
- ↗ RP: Return period
- ↗ RVO: The Netherlands Enterprise Agency "Rijksdienst voor Ondernemend Nederland"
- ↗ SCPT: Seismic cone penetration test
- ↗ SHARE: Seismic Hazard Harmonization in Europe
- ↗ SRC: Seismic risk category
- ↗ TNW: Ten Noorden van de Waddeneilanden
- ↗ UHS: Uniform hazard spectrum

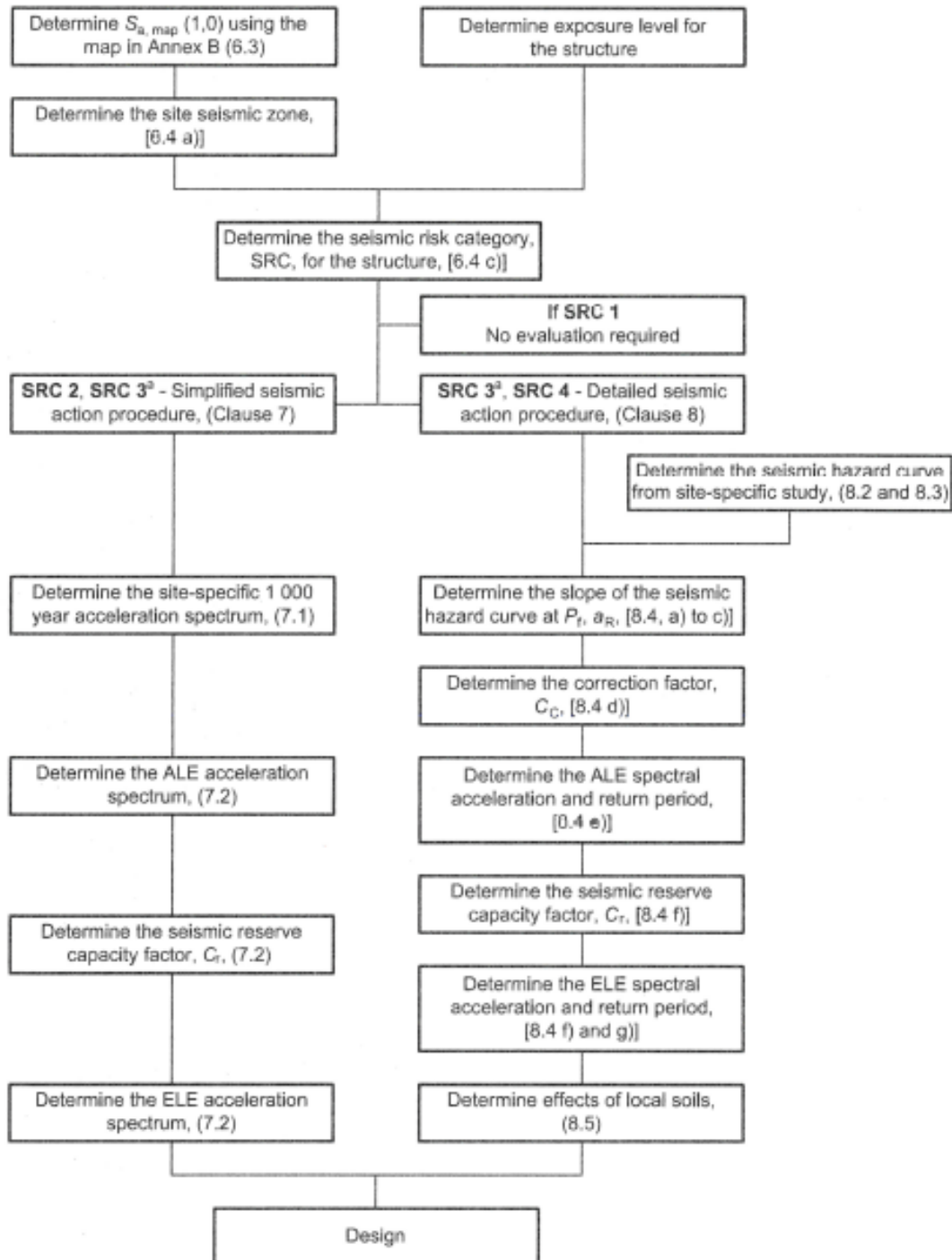
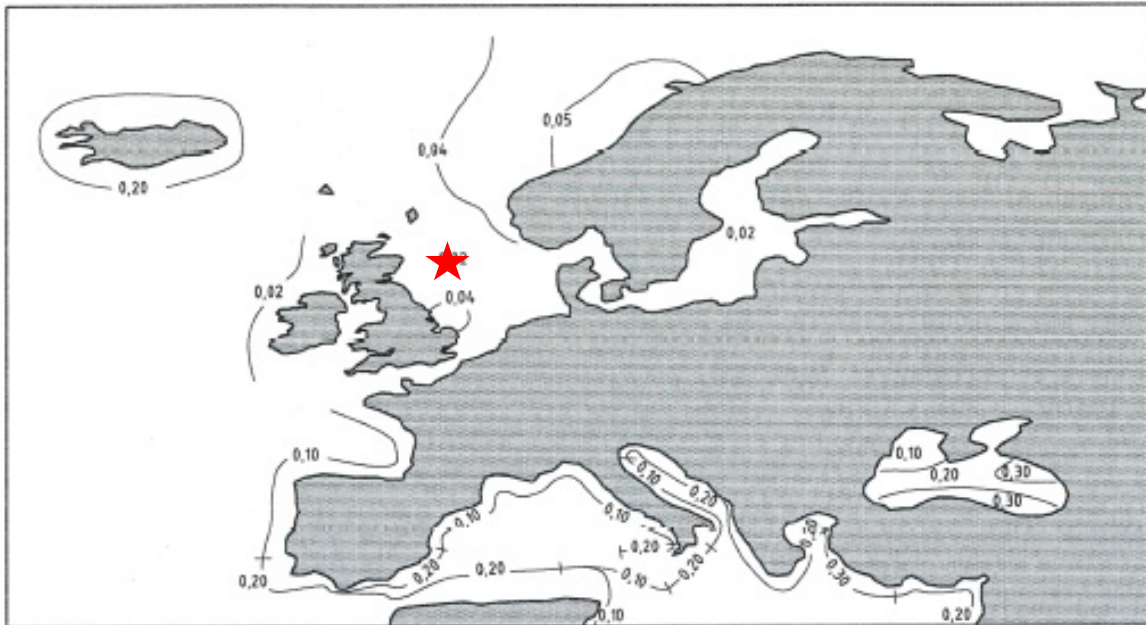
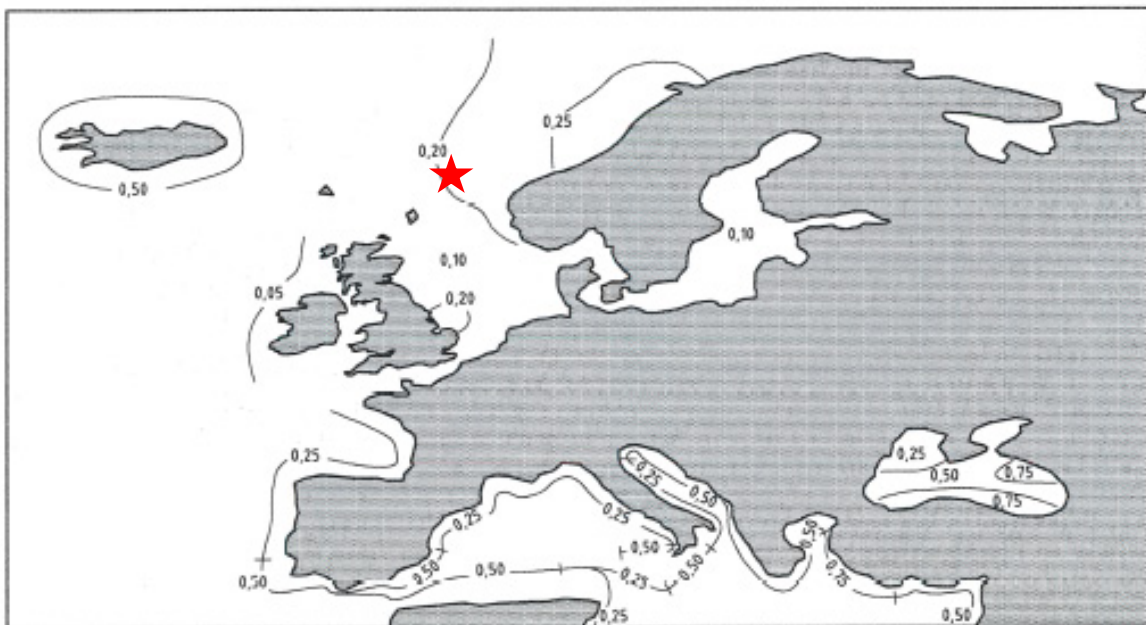


Figure 1-1 Seismic action procedures according to ISO 19901-2:2017



a) 1,0 s oscillator periods



b) 0,2 s oscillator periods

Figure 1-2 a) $S_{a,map}(1.0)$ and b) $S_{a,map}(0.2)$ according to ISO 19901-2:2017. Red star denotes the project location.

2 Simplified seismic action procedure

NGI estimated the horizontal and vertical design spectra at the soil surface for a 1000 year return period earthquake, as well as ALE and ELE scenarios for both L1 and L2 exposure levels using the simplified seismic action procedure according to ISO 19901-2:2017. NGI assumed both shallow and deep pile foundations according to ISO 19901-2:2017.

The left side of Figure 1-1 describes the simplified seismic action procedure. The first step of the simplified seismic action procedure is to select $S_{a,map}(0.2)$ and $S_{a,map}(1.0)$ from Figure 1-2 for the project location. For the TNW location, these values correspond to 0.1 g and 0.03 g, respectively.

The second step of the simplified seismic action procedure is to determine the site class according to either the time averaged shear wave velocity over the top 30 meters (V_{S30}), cone penetration resistance, or undrained shear strength. Figure 2-1 shows the shear wave velocity profiles with depth for all available SCPT measurements across the TNW wind farm zone. The shear wave profiles are similar, therefore, NGI recommends using one representative design V_{S30} value for the entire site. V_{S30} is calculated as:

$$V_{S30} = \frac{30}{\sum_{i=1}^n d_i / V_{S_i}} \quad (2-1)$$

where n is the number of soil layers in the top 30 meters, d_i is the thickness of layer i in meters, and V_{S_i} is the shear wave velocity of layer i in m/s. NGI estimated V_{S30} from the median shear wave velocity of all SCPT for one meter depth intervals. NGI calculated a V_{S30} value of 265 m/s, which is defined as site class D, "stiff to very stiff soil". For site class D and assuming deep pile foundations the site coefficients are $C_a = 1$ and $C_v = 1.2$, and for shallow foundations they are $C_a = 1.6$ and $C_v = 2.4$.

Using the values of $S_{a,map}(0.2)$, $S_{a,map}(1.0)$, C_a and C_v described above, NGI then calculated the design spectrum for a 1000 year return period ground motion and 5% damping using Figure 2-2.

To estimate design spectra for ELE and ALE, NGI used exposure levels L1 and L2, as defined by the client. Exposures levels are based on the life safety category and consequence category of the structure, as shown in Figure 2-1. The exposure level controls the value of N_{ALE} , which is the scale factor that the 1000 year return period response spectrum is multiplied by to estimate the ALE response spectrum. For L1, $N_{ALE} = 1.6$, and for L2, $N_{ALE} = 1.15$.

Finally, to estimate the design spectrum for ELE, the ALE response spectrum is divided by the seismic reserve capacity (C_r) of the structural system. The value of C_r depends on the structure material and configuration. If single-legged structures made predominately out of steel are used (i.e. monopiles), then according to ISO 19902:2020, $C_r = 1.1$. For

concrete structures with continuity and good ductility, ISO 19903:2019 states that a minimum value of $C_r = 1.4$ can be assumed. Therefore, for the scenario assuming deep foundations, NGI used $C_r = 1.1$ assuming steel monopiles, and for the scenario assuming shallow foundations, NGI assumed concrete structures with $C_r = 1.4$. These values represent conservative estimates of C_r .

Table 2-2 lists the input parameters for the four different simplified seismic action procedure scenarios (exposure level L1 and deep foundations, exposure level L2 and deep foundations, exposure level L1 and shallow foundations, exposure level L2 and shallow foundations). Figure 2-3 shows the horizontal design spectra for all four scenarios and ELE, ALE and 1000 year return period ground motions.

Table 2-3 through Table 2-6 list the horizontal and vertical design spectra for 5% damping and 1000 year return period, ALE and ELE scenarios. For projects located in seismic zones = 0, the vertical design spectra are $\frac{1}{2}$ the horizontal design spectra.

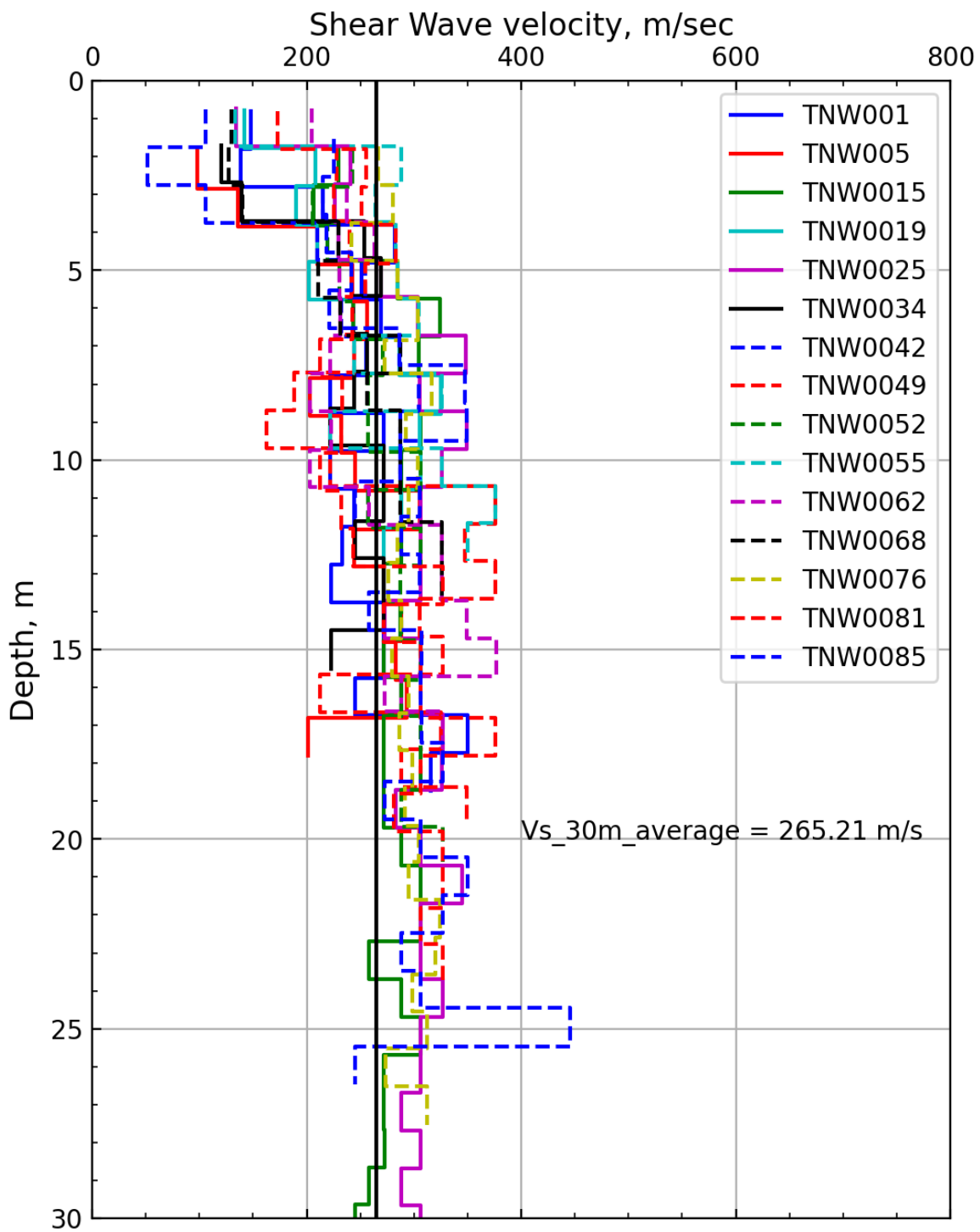


Figure 2-1 Shear wave velocity profiles from all available SCPT measurements at TNW

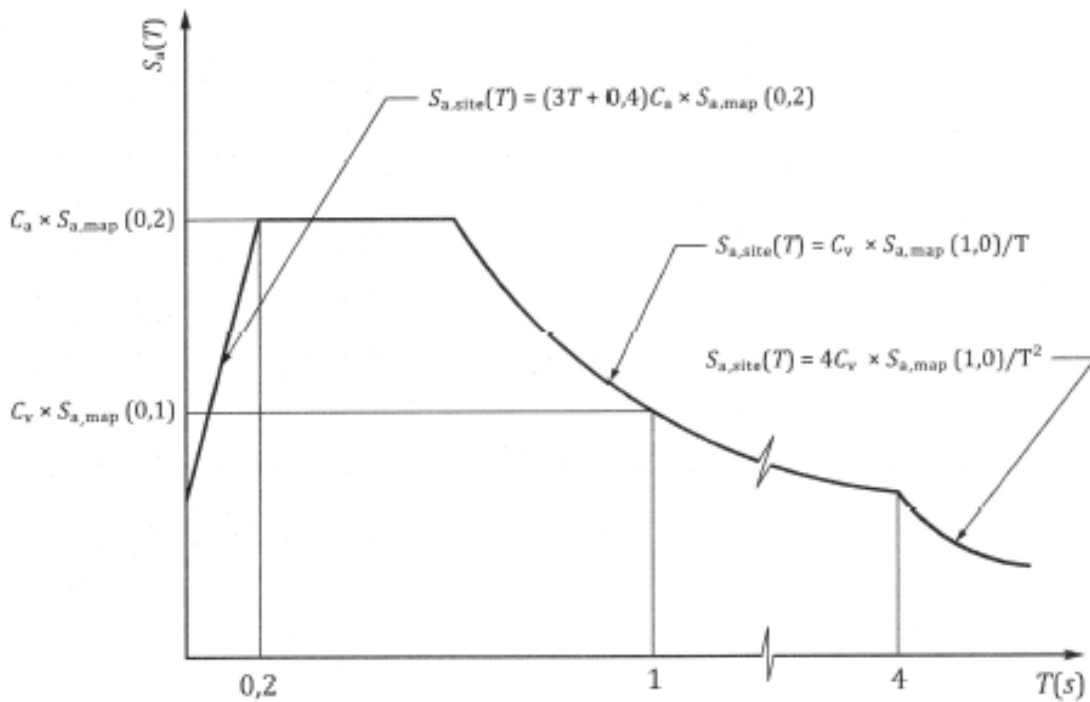


Figure 2-2 Procedure to develop design spectrum for 1000 year return period and 5% damping (Figure 2 in ISO 19901-2:2017)

Table 2-1 Exposure levels according to life safety and consequence categories (ISO 19902)

Life-safety category	Consequence category		
	C1 High consequence	C2 Medium consequence	C3 Low consequence
S1 Manned non-evacuated	L1	L1	L1
S2 Manned evacuated	L1	L2	L2
S3 Unmanned	L1	L2	L3

Table 2-2 Input parameters for the simplified seismic action procedure

Parameter	L1 Deep	L2 Deep	L1 Shallow	L2 Shallow
$S_{a,map}(0.2)$	0.10	0.10	0.10	0.10
$S_{a,map}(1.0)$	0.02	0.02	0.02	0.02
C_a	1	1	1.6	1.6
C_v	1.2	1.2	2.4	2.4
N_{ALE}	1.6	1.15	1.6	1.15
C_r	1.1	1.1	1.4	1.4

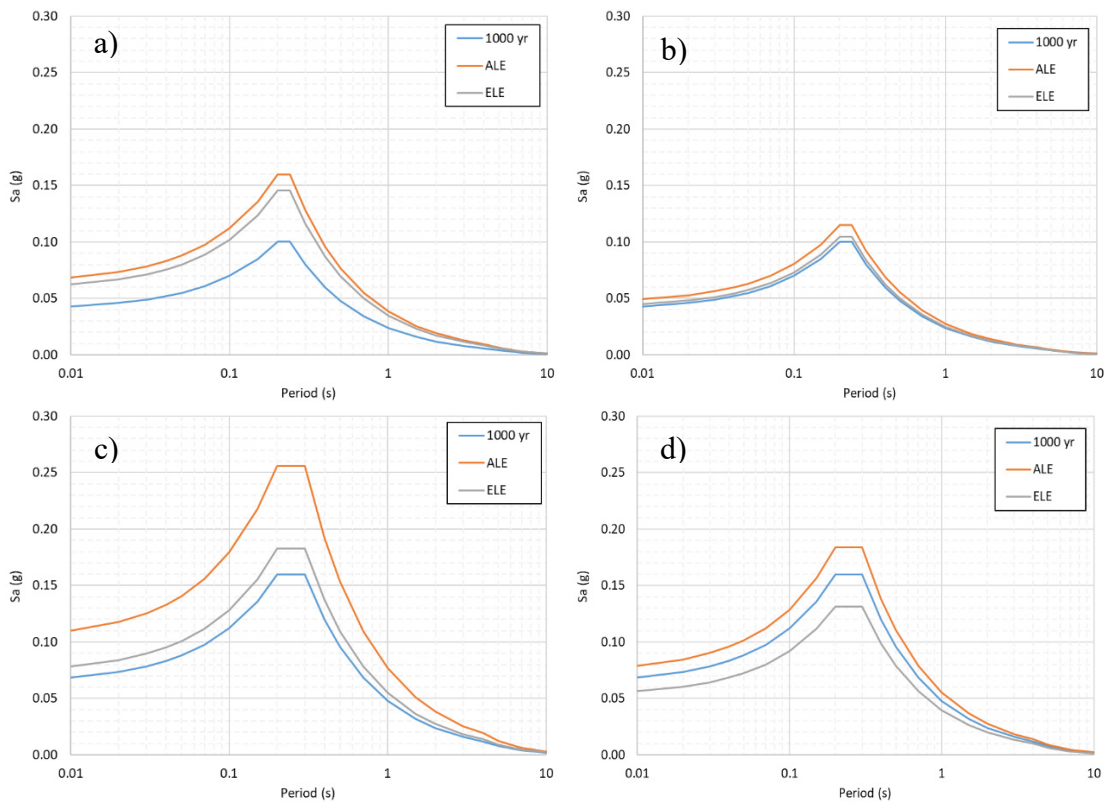


Figure 2-3 Horizontal design response spectra for 5% damping according to the simplified seismic action procedure for a) exposure level L1 and deep foundations, b) exposure level L2 and deep foundations, c) exposure level L1 and shallow foundations and d) exposure level L2 and shallow foundations.

Table 2-3 Horizontal and vertical design spectra for 5% damping and different hazard levels (1000 year return period, ALE and ELE) for exposure level L1 and deep foundations.

T (s)	Horizontal Sa (g)			Vertical Sa (g)		
	1000 yr	ALE	ELE	1000 yr	ALE	ELE
0.01	0.0430	0.0688	0.0625	0.0215	0.0344	0.0313
0.02	0.0460	0.0736	0.0669	0.0230	0.0368	0.0335
0.03	0.0490	0.0784	0.0713	0.0245	0.0392	0.0356
0.04	0.0520	0.0832	0.0756	0.0260	0.0416	0.0378
0.05	0.0550	0.0880	0.0800	0.0275	0.0440	0.0400
0.07	0.0610	0.0976	0.0887	0.0305	0.0488	0.0444
0.1	0.0700	0.1120	0.1018	0.0350	0.0560	0.0509
0.15	0.0850	0.1360	0.1236	0.0425	0.0680	0.0618
0.2	0.1000	0.1600	0.1455	0.0500	0.0800	0.0727
0.24	0.1000	0.1600	0.1455	0.0500	0.0800	0.0727
0.3	0.0800	0.1280	0.1164	0.0400	0.0640	0.0582
0.4	0.0600	0.0960	0.0873	0.0300	0.0480	0.0436
0.5	0.0480	0.0768	0.0698	0.0240	0.0384	0.0349
0.7	0.0343	0.0549	0.0499	0.0171	0.0274	0.0249
1	0.0240	0.0384	0.0349	0.0120	0.0192	0.0175
1.5	0.0160	0.0256	0.0233	0.0080	0.0128	0.0116
2	0.0120	0.0192	0.0175	0.0060	0.0096	0.0087
3	0.0080	0.0128	0.0116	0.0040	0.0064	0.0058
4	0.0060	0.0096	0.0087	0.0030	0.0048	0.0044
5	0.0038	0.0061	0.0056	0.0019	0.0031	0.0028
7	0.0020	0.0031	0.0028	0.0010	0.0016	0.0014
10	0.0010	0.0015	0.0014	0.0005	0.0008	0.0007

Table 2-4 Horizontal and vertical design spectra for 5% damping and different hazard levels (1000 year return period, ALE and ELE) for exposure level L2 and deep foundations.

T (s)	Horizontal Sa (g)			Vertical Sa (g)		
	1000 yr	ALE	ELE	1000 yr	ALE	ELE
0.01	0.0430	0.0495	0.0450	0.0215	0.0247	0.0225
0.02	0.0460	0.0529	0.0481	0.0230	0.0265	0.0240
0.03	0.0490	0.0564	0.0512	0.0245	0.0282	0.0256
0.04	0.0520	0.0598	0.0544	0.0260	0.0299	0.0272
0.05	0.0550	0.0633	0.0575	0.0275	0.0316	0.0288
0.07	0.0610	0.0702	0.0638	0.0305	0.0351	0.0319
0.1	0.0700	0.0805	0.0732	0.0350	0.0403	0.0366
0.15	0.0850	0.0978	0.0889	0.0425	0.0489	0.0444
0.2	0.1000	0.1150	0.1045	0.0500	0.0575	0.0523
0.24	0.1000	0.1150	0.1045	0.0500	0.0575	0.0523
0.3	0.0800	0.0920	0.0836	0.0400	0.0460	0.0418
0.4	0.0600	0.0690	0.0627	0.0300	0.0345	0.0314
0.5	0.0480	0.0552	0.0502	0.0240	0.0276	0.0251
0.7	0.0343	0.0394	0.0358	0.0171	0.0197	0.0179
1	0.0240	0.0276	0.0251	0.0120	0.0138	0.0125
1.5	0.0160	0.0184	0.0167	0.0080	0.0092	0.0084
2	0.0120	0.0138	0.0125	0.0060	0.0069	0.0063
3	0.0080	0.0092	0.0084	0.0040	0.0046	0.0042
4	0.0060	0.0069	0.0063	0.0030	0.0035	0.0031
5	0.0038	0.0044	0.0040	0.0019	0.0022	0.0020
7	0.0020	0.0023	0.0020	0.0010	0.0011	0.0010
10	0.0010	0.0011	0.0010	0.0005	0.0006	0.0005

Table 2-5 Horizontal and vertical design spectra for 5% damping and different hazard levels (1000 year return period, ALE and ELE) for exposure level L1 and shallow foundations.

T (s)	Horizontal Sa (g)			Vertical Sa (g)		
	1000 yr	ALE	ELE	1000 yr	ALE	ELE
0.01	0.0688	0.1101	0.0786	0.0344	0.0550	0.0393
0.02	0.0736	0.1178	0.0841	0.0368	0.0589	0.0421
0.03	0.0784	0.1254	0.0896	0.0392	0.0627	0.0448
0.04	0.0832	0.1331	0.0951	0.0416	0.0666	0.0475
0.05	0.0880	0.1408	0.1006	0.0440	0.0704	0.0503
0.07	0.0976	0.1562	0.1115	0.0488	0.0781	0.0558
0.1	0.1120	0.1792	0.1280	0.0560	0.0896	0.0640
0.15	0.1360	0.2176	0.1554	0.0680	0.1088	0.0777
0.2	0.1600	0.2560	0.1829	0.0800	0.1280	0.0914
0.24	0.1600	0.2560	0.1829	0.0800	0.1280	0.0914
0.3	0.1600	0.2560	0.1829	0.0800	0.1280	0.0914
0.4	0.1200	0.1920	0.1371	0.0600	0.0960	0.0686
0.5	0.0960	0.1536	0.1097	0.0480	0.0768	0.0549
0.7	0.0686	0.1097	0.0784	0.0343	0.0549	0.0392
1	0.0480	0.0768	0.0549	0.0240	0.0384	0.0274
1.5	0.0320	0.0512	0.0366	0.0160	0.0256	0.0183
2	0.0240	0.0384	0.0274	0.0120	0.0192	0.0137
3	0.0160	0.0256	0.0183	0.0080	0.0128	0.0091
4	0.0120	0.0192	0.0137	0.0060	0.0096	0.0069
5	0.0077	0.0123	0.0088	0.0038	0.0061	0.0044
7	0.0039	0.0063	0.0045	0.0020	0.0031	0.0022
10	0.0019	0.0031	0.0022	0.0010	0.0015	0.0011

Table 2-6 Horizontal and vertical design spectra for 5% damping and different hazard levels (1000 year return period, ALE and ELE) for exposure level L2 and shallow foundations

T (s)	Horizontal Sa (g)			Vertical Sa (g)		
	1000 yr	ALE	ELE	1000 yr	ALE	ELE
0.01	0.0688	0.0791	0.0565	0.0344	0.0396	0.0283
0.02	0.0736	0.0846	0.0605	0.0368	0.0423	0.0302
0.03	0.0784	0.0902	0.0644	0.0392	0.0451	0.0322
0.04	0.0832	0.0957	0.0683	0.0416	0.0478	0.0342
0.05	0.0880	0.1012	0.0723	0.0440	0.0506	0.0361
0.07	0.0976	0.1122	0.0802	0.0488	0.0561	0.0401
0.1	0.1120	0.1288	0.0920	0.0560	0.0644	0.0460
0.15	0.1360	0.1564	0.1117	0.0680	0.0782	0.0559
0.2	0.1600	0.1840	0.1314	0.0800	0.0920	0.0657
0.24	0.1600	0.1840	0.1314	0.0800	0.0920	0.0657
0.3	0.1600	0.1840	0.1314	0.0800	0.0920	0.0657
0.4	0.1200	0.1380	0.0986	0.0600	0.0690	0.0493
0.5	0.0960	0.1104	0.0789	0.0480	0.0552	0.0394
0.7	0.0686	0.0789	0.0563	0.0343	0.0394	0.0282
1	0.0480	0.0552	0.0394	0.0240	0.0276	0.0197
1.5	0.0320	0.0368	0.0263	0.0160	0.0184	0.0131
2	0.0240	0.0276	0.0197	0.0120	0.0138	0.0099
3	0.0160	0.0184	0.0131	0.0080	0.0092	0.0066
4	0.0120	0.0138	0.0099	0.0060	0.0069	0.0049
5	0.0077	0.0088	0.0063	0.0038	0.0044	0.0032
7	0.0039	0.0045	0.0032	0.0020	0.0023	0.0016
10	0.0019	0.0022	0.0016	0.0010	0.0011	0.0008

3 Previous studies

3.1 Global Seismic Hazard Assessment Program (GSHAP)

The Global Seismic Hazard Assessment Program (GSHAP) was an international project that ran from 1992 until 1998. It aimed to develop regionally coordinated and homogeneous seismic hazard maps for all onshore locations world-wide. Grünthal et al (1999) presents the results for GSHAP region 3, which includes most of central and northern Europe. The Grünthal et al. (1999) study is based on a catalogue of merged national earthquake databases and 196 seismic source zones merged from different national studies (Figure 3-1). Grünthal et al. (1999) used three different sets of ground motion models, one for the Fennoscandian Shield, one for the Vrancea area in Romania, and one set of ground motion models for the rest of the study area.

Figure 3-2 shows the seismic hazard map calculated by Grünthal et al. (1999) for the project location. Estimated PGA values range from 0.0 to 0.02 g for the closest and surrounding onshore areas for a return period of 475 years on rock.

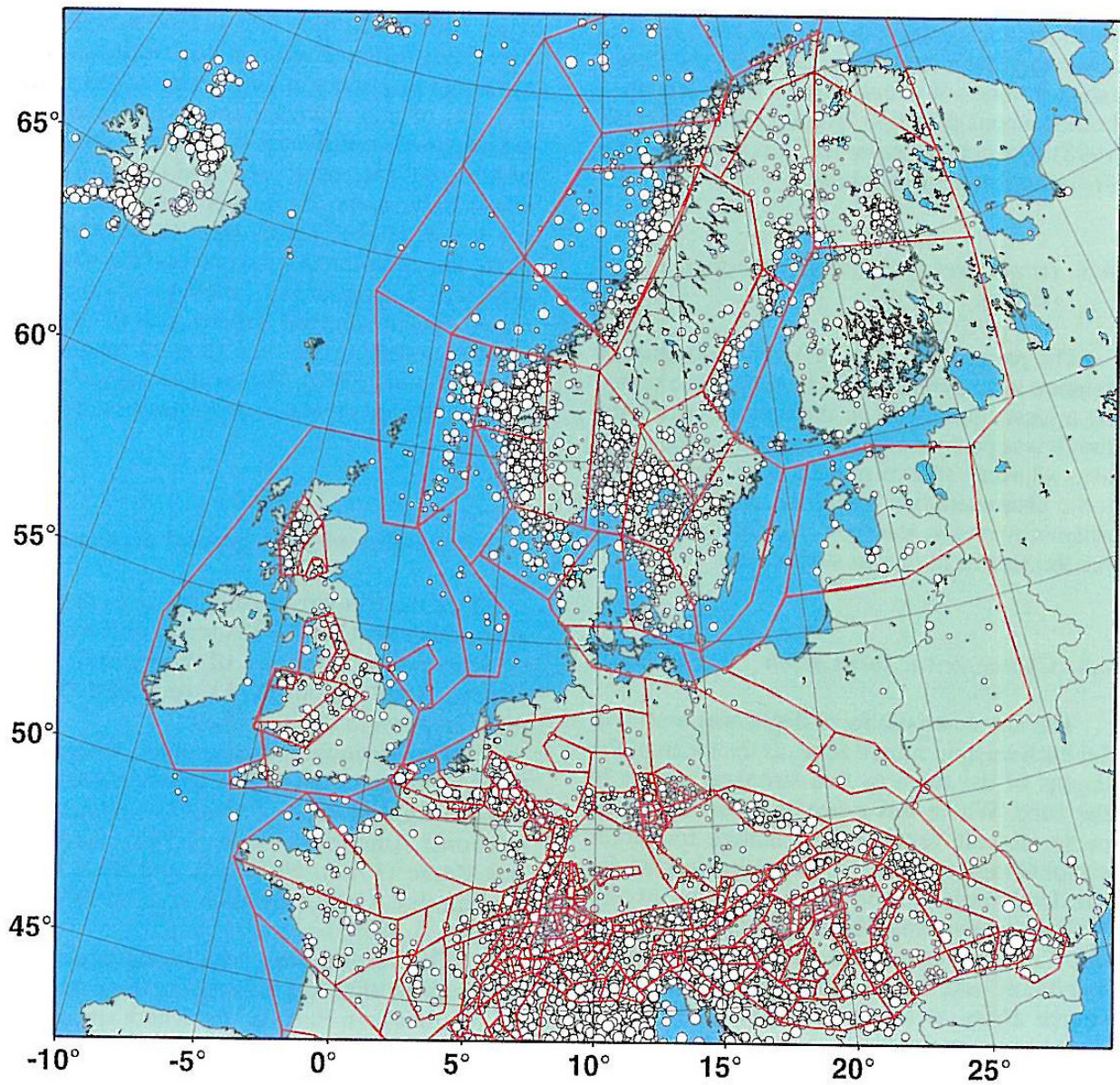


Figure 3-1 Seismic source model used in GSHAP region 3 (Grünthal et al., 1999)

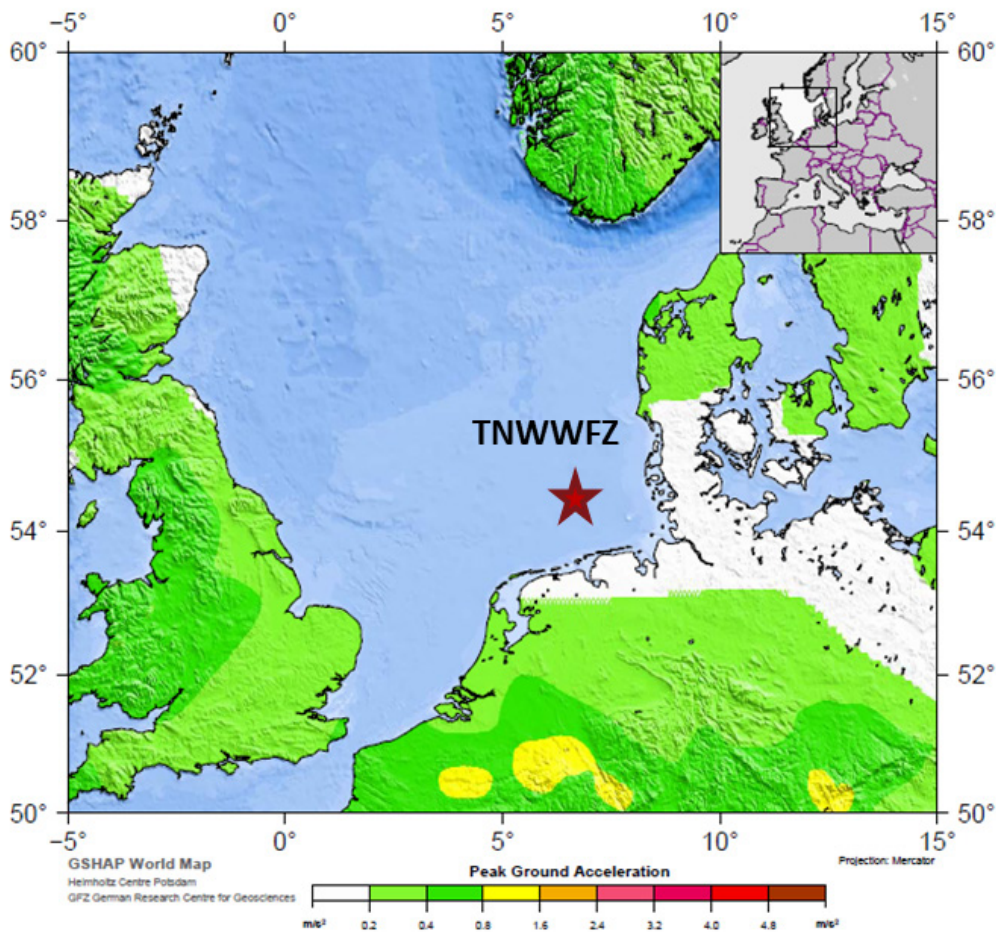


Figure 3-2 Seismic hazard map for a return period of 475 years on rock according to GSHAP (Grünthal et al., 1999)

3.2 Bungum et al. 2000

Bungum et al. (2000) developed a unified seismic hazard map for Norway, the North Sea and the U.K. Bungum et al. (1998) describe the model for the Norwegian sector of the North Sea and the report by EQE (2002) describes the model for the UK and UK sector of the North Sea. Bungum et al. (1998) use a coarse seismic source characterisation model consisting of 24 seismic source zones and a fine seismic source characterisation model consisting of 37 seismic source zones. The coarse model is the same as used for Norway in the GSHAP project (Grünthal et al., 1999). All source zones have three sets of activity rate and b-value pairs, with different weights implemented in a logic tree. EQE (2002) extended both seismic source models to the UK and developed 38 areal source zones for the fine model and 26 for the coarse model. Figure 3-3 shows the fine seismic source characterization model used in Bungum et al. (2000) and the peak ground acceleration (PGA) values for 475 year return period on rock. The TNW site is behind the legend of the plot, but if the contours are extrapolated, then Bungum et al. (2000) predict $PGA = 0.02 \text{ g}$ for rock and 475 year return period.

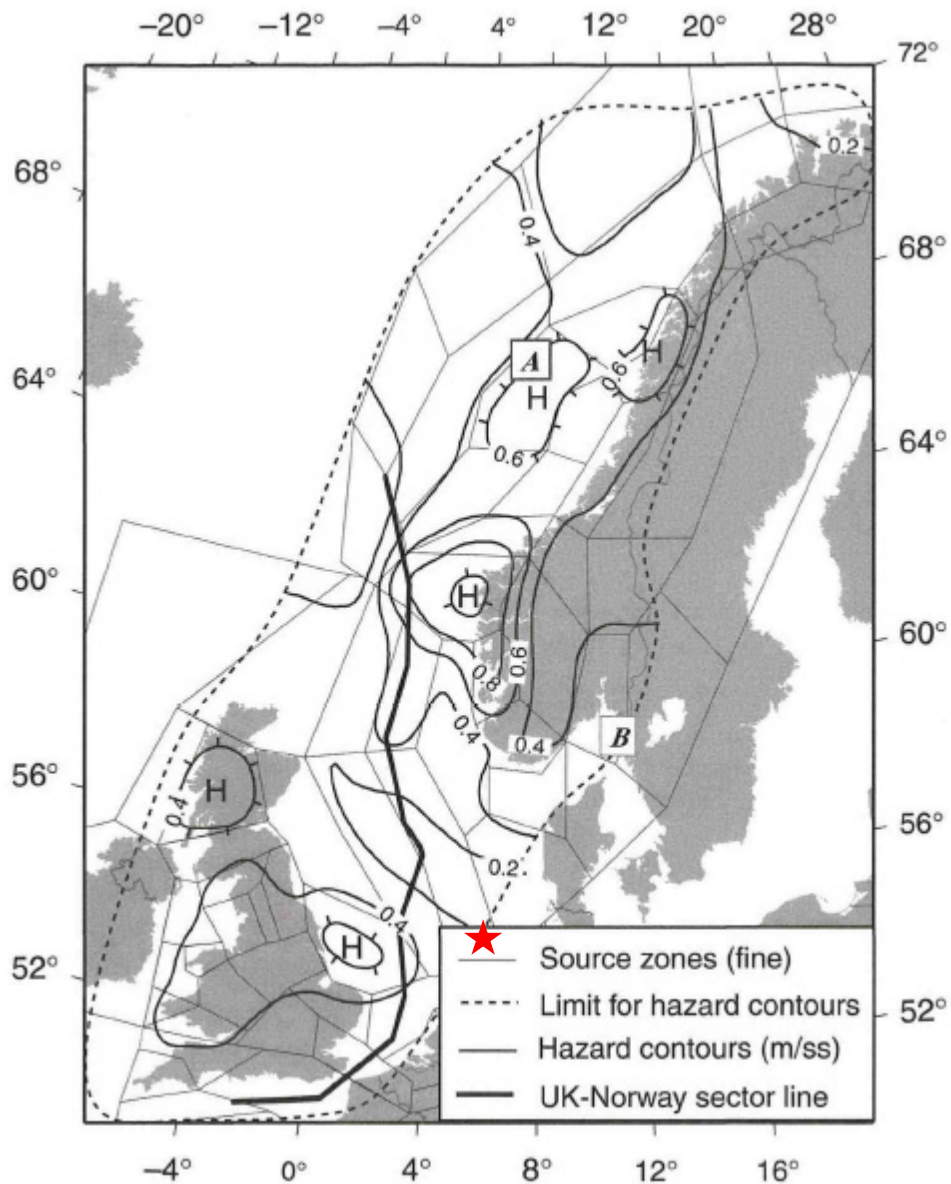


Figure 3-3 Fine seismic source model and resulting PGA (m/s^2) for 475 year return period on rock (Bungum et al., 2000). Red star is project location.

3.3 Seismic Hazard Harmonization in Europe (SHARE)

The SHARE project (Woessner et al., 2015) conducted a seismic hazard analysis for all of Europe (Figure 3-4). It was the first completed regional contribution to the Global Earthquake Model initiative. Woessner et al. (2015) used three different seismic source models; an areal source model, a fault source model with background seismicity, and an

area-smoothed model based on fault slip rate and past seismic activity. The areal seismic source zonation for the North Sea is mainly based on Bungum et al. (2000) and Musson and Sergeant (2007), with some adjustments. The SHARE project used four ground motion models for active shallow and oceanic crust, five for stable continental regions, two for deep seismicity in the Vrancea region, and one for volcanic and swarm type earthquakes. Figure 3-5 shows the PGA on rock for 475 year return period according to the SHARE project. For the project location, the SHARE map estimates $PGA < 0.025g$. The results of the SHARE project are currently being updated by the European Seismic Hazard Model 2020 (ESHM20), which operates under the Joint Research Activities of the Horizon 2020-funded project SERA (<http://www.efehr.org/en/Documentation/specific-hazard-models/europe/eshm2020-ongoing-work/>).

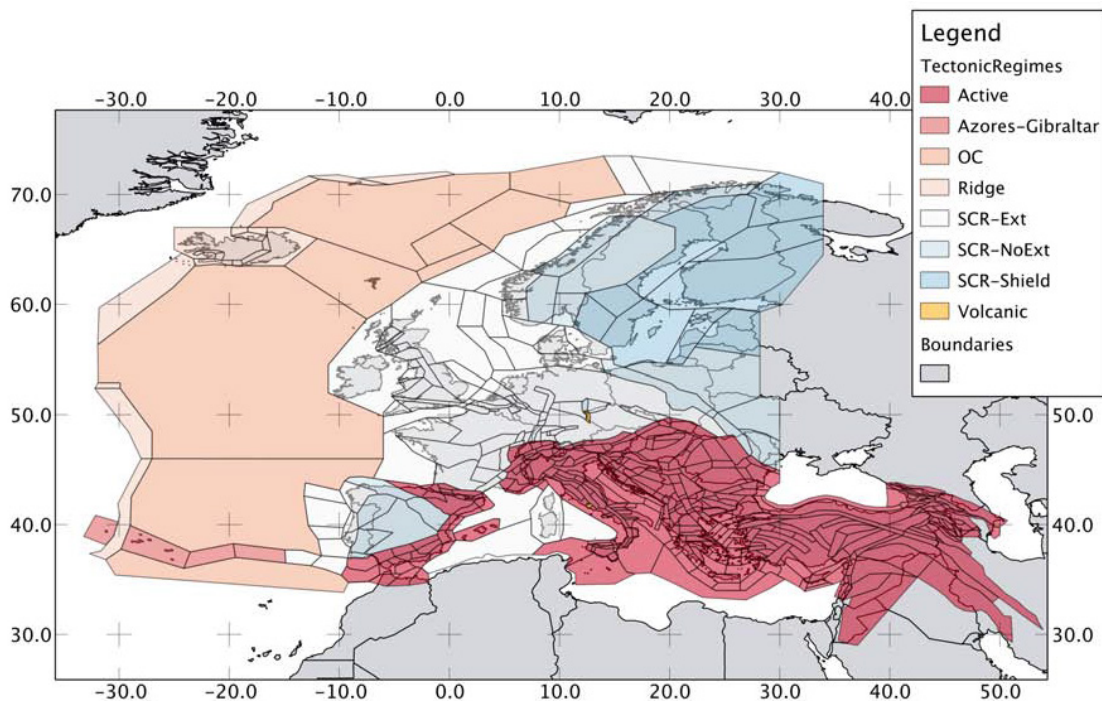


Figure 3-4 Areal source model used in the SHARE project (Woessner et al., 2015), showing the tectonic regimes of each of the areal sources.

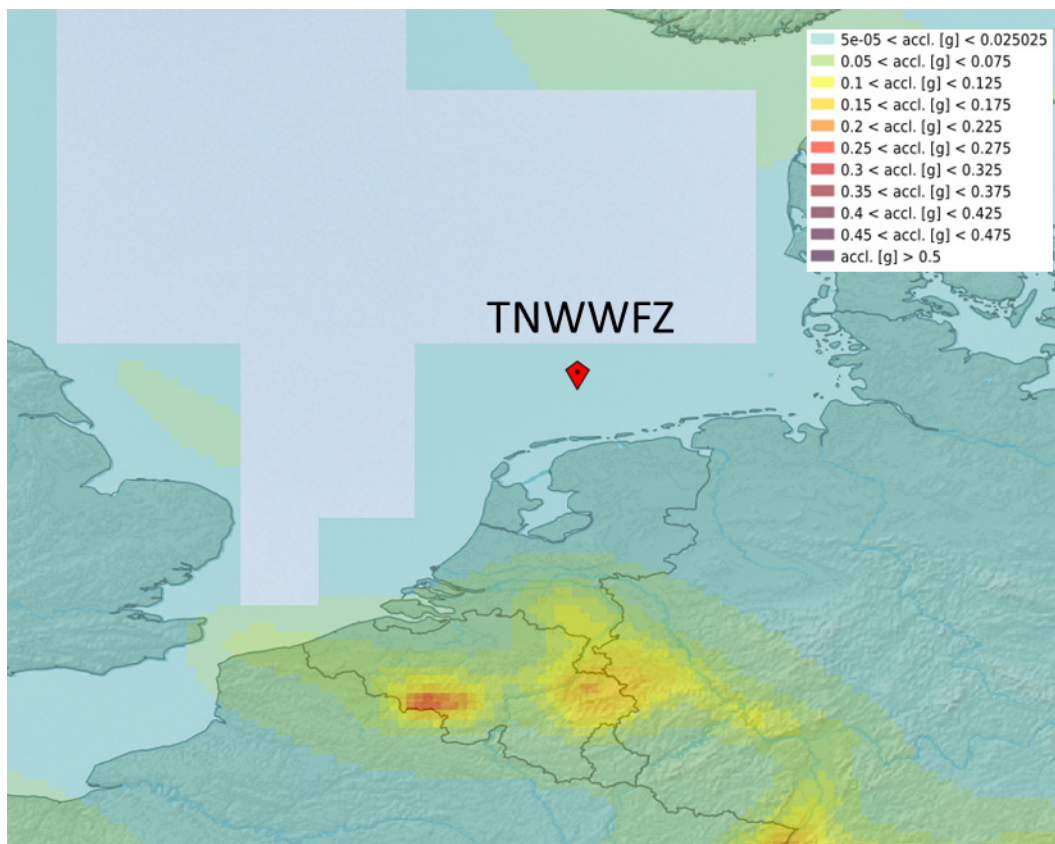


Figure 3-5 PGA on rock for 475-year return period from the SHARE project (Woessner et al., 2015)

3.4 HKW PSHA report

Fugro (2020) conducted a site specific PSHA for the Hollandse Kust West (HKW) Wind Farm Zone, which is about 200 km to the south-west of TNW off the coast of The Netherlands (Figure 3-6). They used three seismic source zones consisting of different areal sources and five ground motion models. Seismic source Model 1 is based mainly on the seismic hazard assessment of Le Dortz et al. (2019) for France and Grünthal et al. (2017, 2018) for Germany. Model 2 is based on the seismic hazard assessment of Belgium by Verbeek et al. (2009) and model D from Grünthal et al (2017, 2018) for Germany. Model 3 is based on model C from Grünthal et al (2017, 2018) for Germany. They used the traditional PSHA methodology coupled with Monte Carlo sampling of some branches of the logic tree to capture epistemic uncertainty. For 475 year return period and $V_{S30} = 300$ m/s, Fugro (2020) found $PGA = 0.0171$ g for HKW. Based on the three regional analyses described above, the HKW site should have a larger seismic hazard than the TNW site.

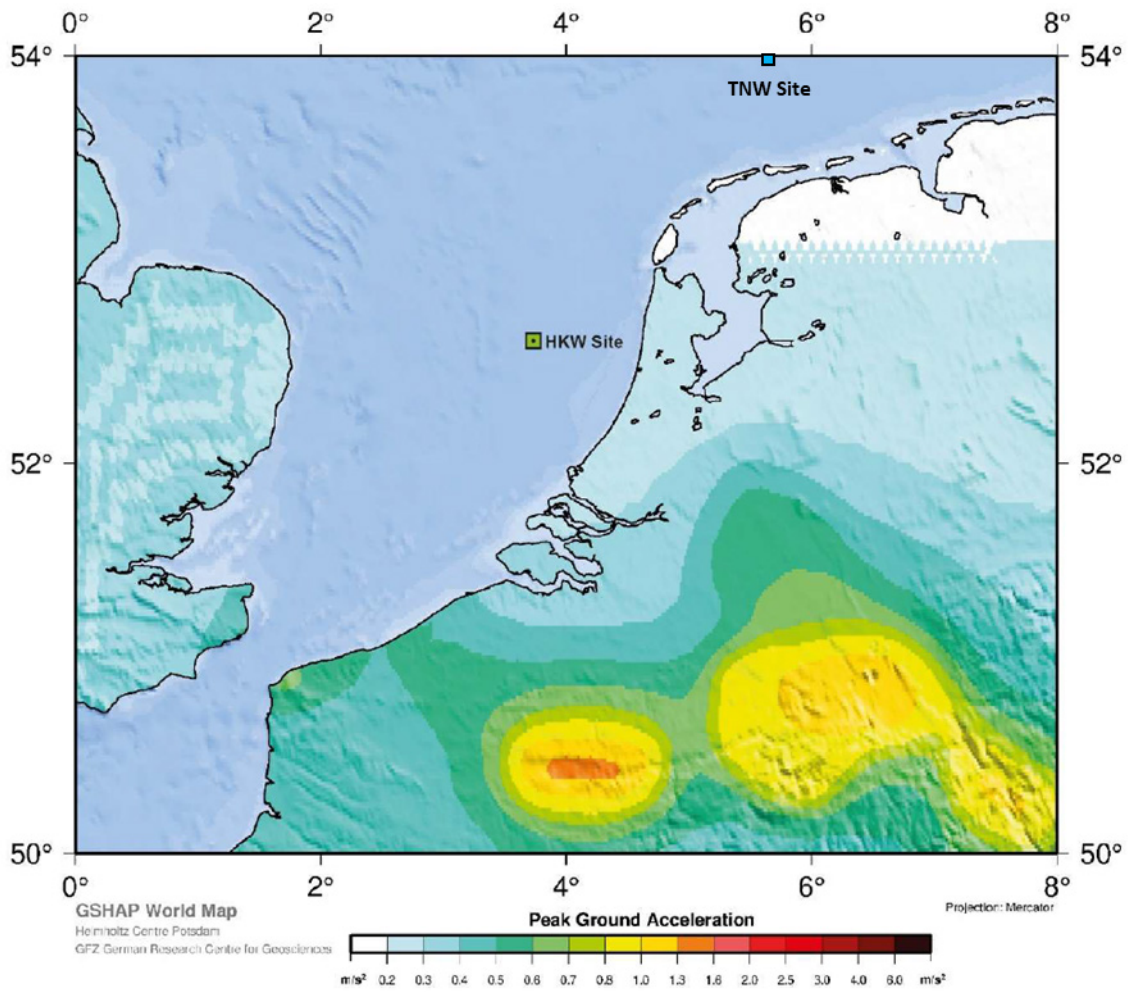


Figure 3-6 Location of HKW site compared to TNW with the GSHAP hazard model in the background (modified from Fugro (2020))

4 Overview of PSHA methodology

A detailed seismic action procedure as specified by ISO 19901-2:2017 and shown in Figure 1-1 consists of a site specific probabilistic seismic hazard analysis (PSHA) followed by a procedure to calculate the ALE and ELE return periods based on the hazard curve. This chapter provides an overview of PSHA methodology.

PSHA is a methodology that estimates the probability that an earthquake intensity measure will be exceeded at a given location in a set future time period. The main purpose of a PSHA is to aid in the decision of what level of an intensity measure to use in the design of a structure to ensure a desired performance state, and what magnitude and distance combination are most likely to produce the chosen level of the intensity measure.

NGI performed the PSHA calculations using the computer program HAZ45.2 developed by Professor Norman Abrahamson (Abrahamson, 2017; Hale et al., 2018). This program implements the PSHA methodology developed principally by Cornell (1968) and refined by McGuire (1974; 1978). This PSHA method has five basic components (Baker, 2008):

1. Identify all relevant earthquake sources.
2. Characterize the rates at which earthquakes of various magnitudes (M) are expected to occur for each source.
3. Characterize the distribution of source-to-site distances (R) for each source.
4. Predict the chosen intensity measure for all combinations of magnitude, distance and ϵ (the number of standard deviations of the ground motion model used to estimate the intensity measure) for each source.
5. Calculate the hazard curve at each spectral period.

Figure 4-1 shows the five components graphically. The design value of the intensity measure is chosen as the value corresponding to the hazard level deemed acceptable based on consequences of failure and societal risk. Acceptable hazard levels are often specified in codes or by local governments and are based on building type and importance.

In PSHA, many of the input parameters have uncertainty due to limited data or knowledge. This uncertainty, called epistemic uncertainty, is incorporated into the PSHA using a logic-tree framework (Kulkarni et al., 1984). Each branch of the logic tree represents an alternative credible model or parameter value and is given a weight. The weights at each branch tip are mutually exclusive and collectively exhaustive and must sum to one. The weights are based on engineering judgment of how accurate or 'credible' each alternative model is. In this way, the use of a logic tree allows multiple credible models to be included in the PSHA. When using a logic tree, a separate PSHA is conducted for each combination of alternative models (i.e. each final branch of the logic

tree). Then, all the different hazard curves are combined using the branch weights to estimate the mean hazard.

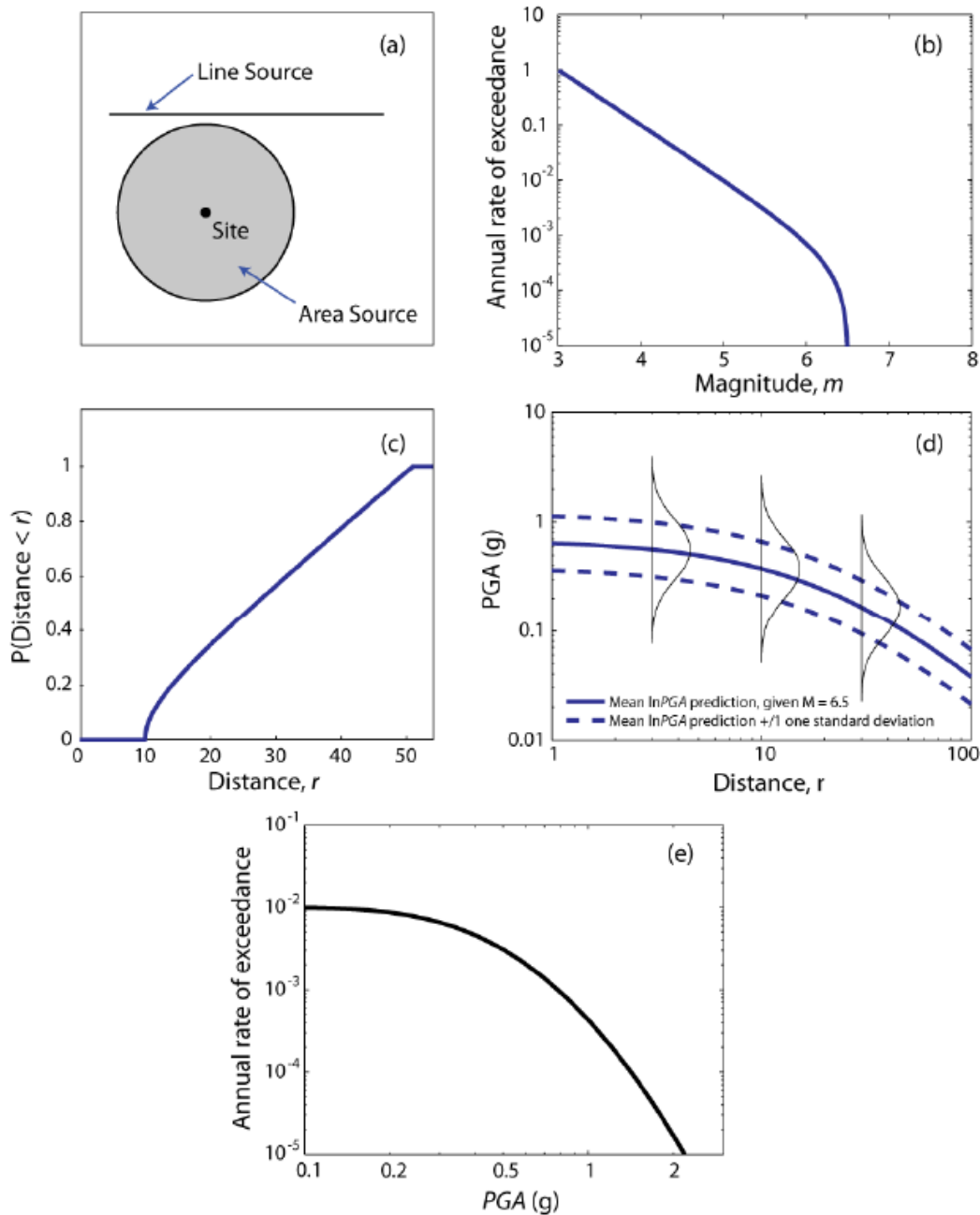


Figure 4-1 Schematic illustration of the five main components of a PSHA. (a) Identify earthquake sources. (b) Characterize the rate of occurrence of earthquake magnitudes for each source. (c) Characterize the distribution of source-to-site distances for each source. (d) Predict the intensity measure for all combinations of magnitude, distance and epsilon. (e) Combine information from parts a-d to compute the annual rate of exceedance for a given intensity measure (Baker, 2008)

5 Tectonic setting

5.1 Overview

The site is located in the North Sea in an extended stable continental region far from any tectonic plate boundaries. The closest boundaries are the Mid Atlantic Ridge over 1500 km to the north and west, and the boundary between the Eurasian and African plates almost 700 km to the south. The overall stress pattern of the project location is NW-SE, and mainly due to ridge push forces from the Mid-Atlantic Ridge and the collision of Africa and Europe (Grünthal and Stromeier, 1994; Fugro, 2020). On a global scale, the levels of seismic hazard are relatively low.

The tectonic development of the region is complex. Volcanic activity during the Triassic and Jurassic (roughly 250 Ma to 150 Ma) created a system of horsts and grabens in the North Sea, which are highs and lows separated by normal faults. This was followed by thermal subsidence during the Cretaceous (150 Ma to 65.5 Ma), which created an intracratonic sedimentary basin (Glennie and Underhill, 1998). In the Paleocene/Eocene (65.5 to 34 Ma), sea floor spreading began in the north Atlantic and mountain building in the Alps, and basin margins were uplifted due to inversion, producing a series of submarine fans (NPD, 2021). Over the last 2.5 million years large volumes of sediment were eroded and deposited in the North Sea by the movement of ice sheets during at least three different glacial periods (NGI, 2021). As the ice moved forwards and backwards push-moraines formed that were then subsequently overridden and eroded. The changes in climate also resulted in regional-scale oscillations in sea level and major changes in river drainage configurations (Lee et al., 2006).

5.2 Regional geologic structures

Figure 5-1 presents an overview of the principal tectonic structural units in central Europe. The TNW site sits at the southern end of the Central Graben, and is flanked by Doggerbank to the west and the Horn Graben to the east. All three of these structures are seismically inactive and formed due to rifting in the Jurassic. There is no evidence of a reactivation of the Central Graben after the Cretaceous (Ziegler, 1975). However, the Lower Rhine Graben, about 250 km from the site in the southern part of The Netherlands, is still seismically active. It is composed of several northwest–southeast oriented normal faults and exhibits moderate seismic activity (Vanneste et al., 2013). Vanneste et al. (2013) predict maximum magnitudes ranging from $M_w = 6.3-7.1$ with return periods of 6000 to 81500 years.

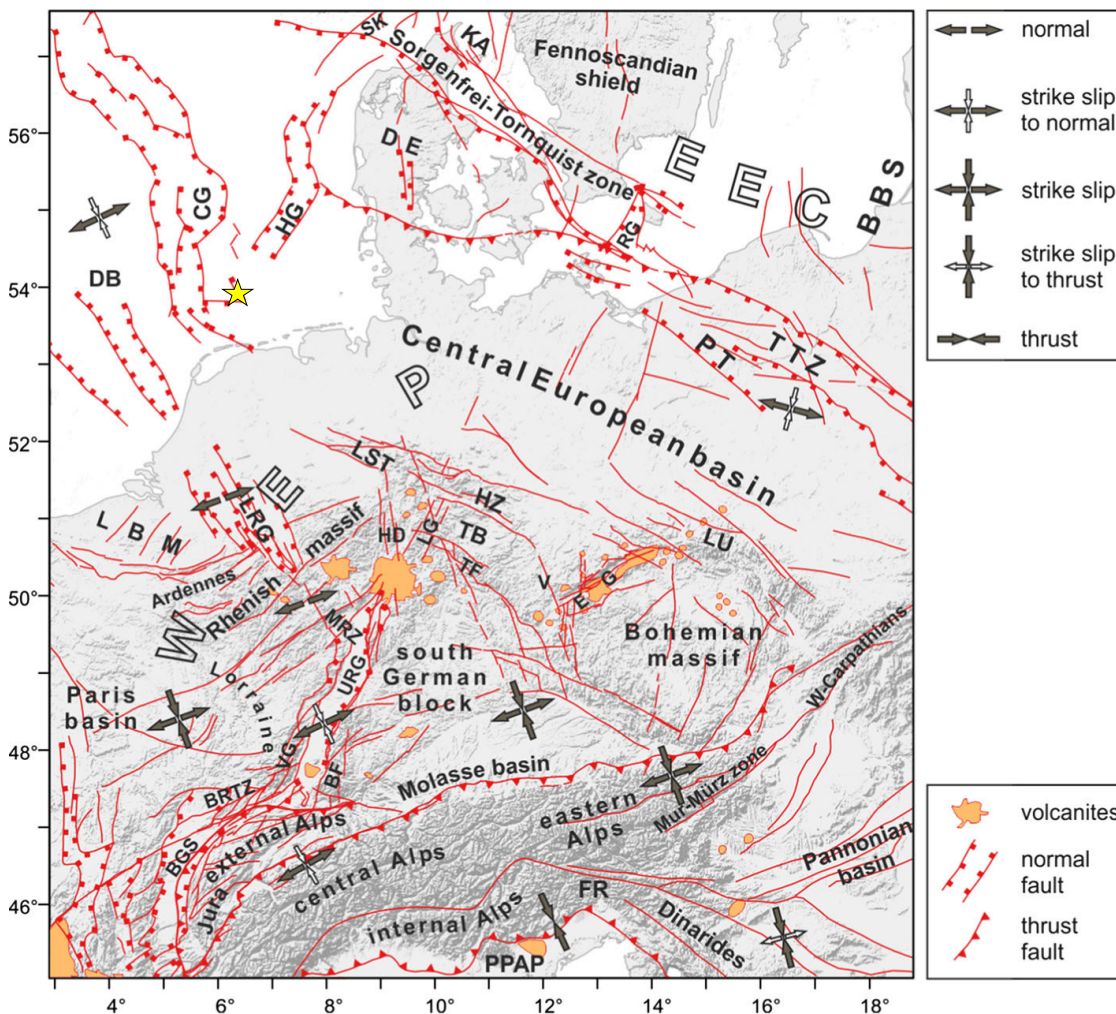


Figure 5-1 Overview of the principal tectonic structural units in central Europe (from Grünthal et al., 2018). Yellow star indicates the approximate location of the TNW wind farm zone. DB = Doggerbank, CG = Central Graben, HG = Horn Graben, LRG = Lower Rhine Graben.

5.3 Induced seismicity

The northern edge of the Groningen gas field is about 80 km to the south of the project in the north east of The Netherlands. It is a natural gas field that has been in operation since the 1960s. Potentially induced earthquakes first started in 1991 (Jansen and Herber, 2017), and the largest induced earthquake occurred on 16 August 2012 in Huizinge, with $M_L = 3.6$. Through 2020, there have been over 100 recorded induced earthquakes in the region (KNMI, 2021). The earthquakes occur inside the gas-bearing Rotliegend sandstone layer at about 3 km depth, and then radiate energy through the overlying Zechstein salt layer, which causes reflections and refractions of the waves (Kraaijpoel and Dost, 2013). Due to the large distance and small magnitudes of the induced earthquakes, they are not expected to significantly contribute to the seismic hazard at

the TNW site. In addition, induced earthquakes do not have the same recurrence characteristics as tectonic earthquakes, and therefore should not be used in PSHA.

Nevertheless, the client asked NGI to include them in the seismic hazard analysis. However, none of the induced earthquakes recorded so far is greater than 4.0, which is the lower limit on magnitude used in the PSHA. As a result, NGI artificially included one $M_w = 4.0$ earthquake at depth = 3 km at the northern edge of the Groningen gas field in the earthquake catalogue to represent seismic hazard due to induced earthquakes from this area. This affects Model 4 described in section 6.3 and is a conservative adjustment.

6 Source characterization

The seismic source model defines the earthquake sources, their geometry, and the rate that earthquakes of various magnitudes are expected to occur on each source (magnitude recurrence relation). NGI developed three seismic source models based on the three areal source models from Fugro (2020) for the HKW wind farm zone. In addition, NGI developed one model using smoothed gridded seismicity and an earthquake catalogue merged from The Netherlands, Belgian, German and British national seismic catalogues, as well as the ISC and EMEC catalogues.

6.1 Background

The second step in a PSHA calculation is to define the rate at which earthquakes of various magnitudes are expected to occur on each source.

A magnitude recurrence relation describes the rate at which earthquakes with magnitudes greater than or equal to M occur on a source $N(M)$. The recurrence relation is calculated by integrating the magnitude probability density function (f_m) and multiplying by the activity rate (N_{min}).

$$N(M) = N_{min} * \int_{m=M}^{M_{max}} f_m(m) dm \quad (6-1)$$

The magnitude probability density function (f_m), or magnitude distribution, gives the relative number that earthquakes of various magnitudes are expected to occur. Three common models used to describe the magnitude distribution are:

1. Truncated exponential (modified from Gutenberg and Richter, 1944)
2. Truncated normal (Schwartz and Coppersmith, 1984)
3. Composite (Youngs and Coppersmith, 1985)

Figure 6-1 shows examples of the three models. All three models require a minimum magnitude. The truncated exponential model also requires a maximum magnitude and a

b value, where b is the slope of the rate of earthquakes in log space and represents the ratio between large and small magnitude earthquakes for a source. The truncated normal model requires a mean magnitude, standard deviation and a maximum magnitude. The composite model requires a mean characteristic magnitude, maximum magnitude, boxcar width, and b value.

The magnitude probability density functions provide the relative rate of earthquake magnitudes on a source. To get the absolute rate the integral of the pdf must be multiplied by the activity rate (N_{min}), which is the rate of earthquakes above M_{min} as shown in equation (4-1). The two methods to estimate N_{min} and the b value are from instrumental and historical seismicity and from geologic or geodetic data.

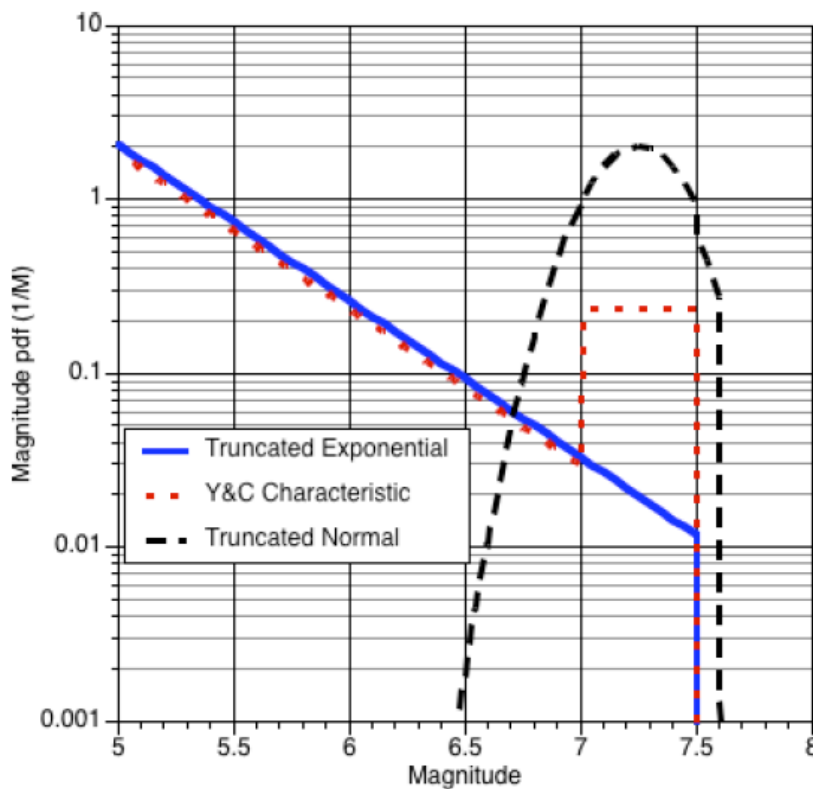


Figure 6-1 Comparison of magnitude probability density functions (f_m)

6.2 Source characterisation based on Fugro (2020)

Fugro (2020) conducted a site specific PSHA for the Hollandse Kust West (HKW) Wind Farm Zone, which is about 200 km to the south-west of TNW off the coast of The Netherlands. They used three different seismic source zones consisting of different areal sources. Seismic source Model 1 is based mainly on the seismic hazard assessment of Le Dortz et al. (2019) for France and Grünthal et al (2017, 2018) for Germany. Model 2 is based on the seismic hazard assessment of Belgium by Verbeek et al. (2009) and

model D from Grünthal et al. (2017, 2018) for Germany. Model 3 is based on model C from Grünthal et al. (2017, 2018) for Germany. NGI used the same three seismic source models as Fugro (2020), but extended them to the north and east to cover an area 300 km from the site. NGI used 300 km as a cut-off distance because this is the maximum valid distance of the ground motion models described in section 7, and possible earthquakes beyond this distance will have a negligible contribution to the seismic hazard. For all areal source zones NGI used the truncated exponential model, similar to Fugro (2020). Fugro (2020) used a minimum magnitude of 4.5, whereas NGI used a minimum magnitude of 4.0. Therefore, NGI adjusted the activity rates to reflect the lower value of M_{min} for all areal source zones.

NGI set the minimum magnitude at 4.0 because this is likely the minimum magnitude to cause damage to infrastructure (Bommer and Crowley, 2017), and to capture induced seismicity in the Groningen region.

6.2.1 Model 1

Figure 6-2 shows the geometry of seismic source Model 1. The areal source zones are the same as Model 1 for Fugro (2020), except NGI added zones GBAS977, NLAS037, DEAS980 and B05 to the north and east, and removed zones to the south and west that did not have a portion of the zone within 300 km of the site. Source zones GBAS977, NLAS037 and DEAS980 are modified from the areal source model of the SHARE project (Giardini et al., 2013), and source zone B05 from model B from Grünthal et al. (2017). NGI modified the added zones by adjusting their geometry to match with Model 1 from Fugro (2020) and recalculating the activity rate for $M_{min} = 4.0$ and the new size of the zone.

Table 6-1 lists the source parameters for Model 1. Fault Mech. is the fault mechanism, where SS = strike slip and N = normal faulting. The values under column 1st are given weights of 70% and the values under column 2nd are given 30% weight. These weights are based on the weights presented in Grünthal et al. (2017, 2018) for similar zones. M_{max} is the maximum magnitude for the given source zone. NGI gave both the minimum and maximum M_{max} values equal weight of 50%. NGI used a triangular distribution to describe the hypocentre depth. The min value represents the minimum depth and max represents the maximum depth. The peak value is the peak of the triangle and therefore the depth with the greatest weight in the triangular distribution. These values are based on the results of Fugro (2020), Grünthal et al. (2017, 2018), and the earthquake catalogue compiled by NGI (see section 6.3). $N(M_{min} = 4.0)$ is the activity rate for the given source zone when considering a minimum magnitude of 4.0 and b is the b value used in the truncated exponential magnitude recurrence model.

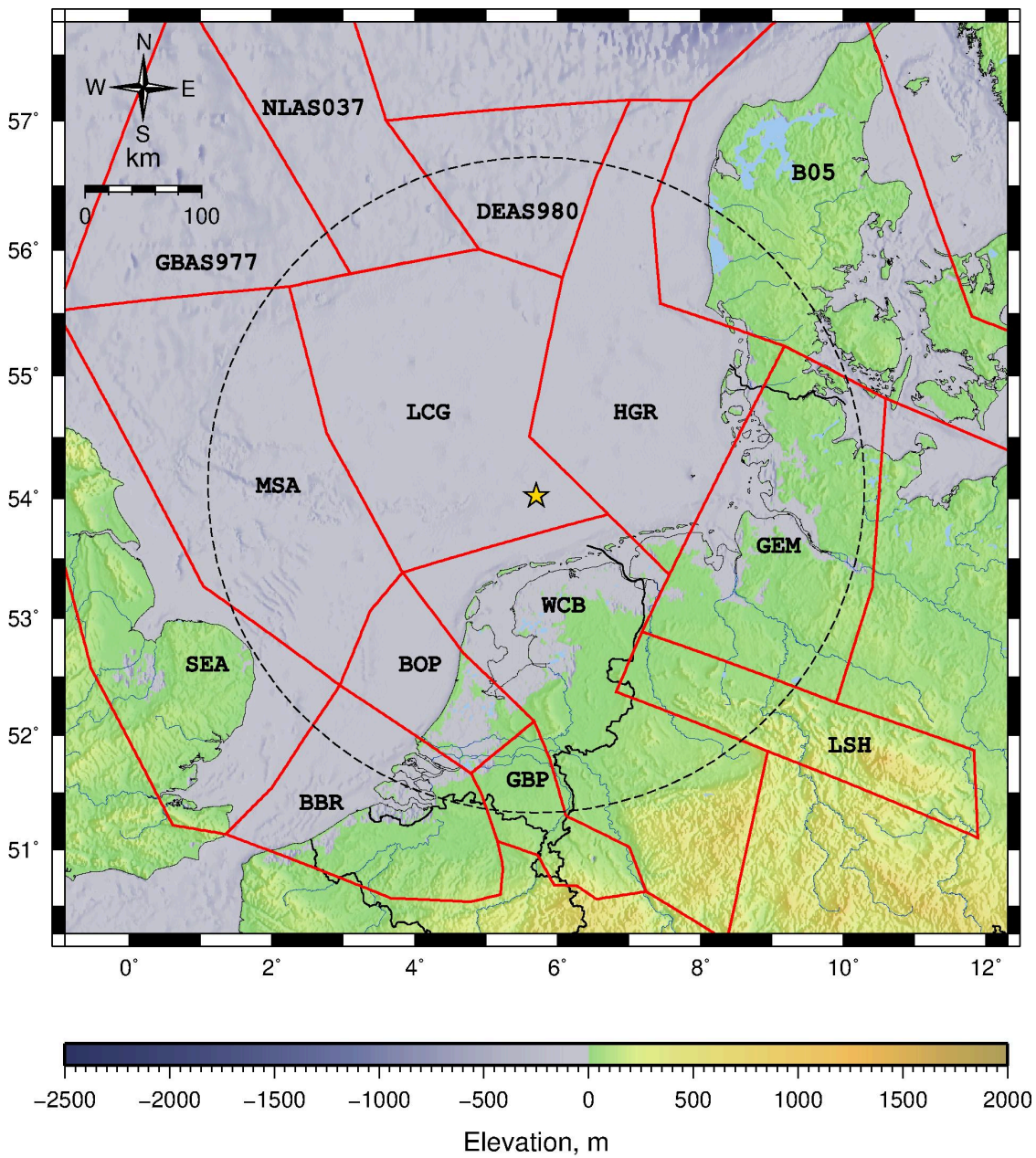


Figure 6-2 Seismic source model 1. Yellow star denotes project location. Dotted line indicates 300 km radius from the site.

Table 6-1 Source parameters for Model 1 (bold row indicates source zone where TNW is located)

Zone ID	Fault Mech.		Mmax		Depth (km)			N(M _{min} = 4.0)	b value
	1 st	2 nd	min	max	min	peak	max		
MSA	SS	N	6.2	6.8	0	10	25	0.0285	1.0345
BOP	N	SS	6.2	7	0	10	20	0.0066	0.9750
GBP	N	SS	6.2	7	0	10	20	0.0439	0.9248
WCB	SS	N	5.7	6.8	0	10	20	0.0167	1.0336
LSH	SS	N	5.7	6.8	0	10	25	0.0052	1.1341
GEM	SS	N	5.7	6.8	0	10	25	0.0244	0.8090
HGR	SS	N	5.7	6.8	0	10	25	0.0040	0.9812
LCG	SS	N	5.7	7.2	0	10	25	0.0110	1.1322
GBAS977	SS	N	6.5	7.1	0	10	20	0.0017	1.0000
NLAS037	SS	N	6.5	7.1	0	10	20	0.0321	1.0000
DEAS980	SS	N	6.5	7.1	0	10	20	0.0009	1.0000
B05	SS	N	5.7	6.83	0	10	32	0.0182	0.9530

6.2.2 Model 2

Figure 6-3 shows the geometry of seismic source Model 2. The areal source zones are the same as Model 2 for Fugro (2020), except NGI added zones D03, D04, D07 and D13 to the east, slightly adjusted the size of zones 20 and 21, and removed zones to the south and west that did not have a portion of the zone within 300 km of the site. The additional source zones are all from model D from Grünthal et al. (2017). Fugro (2020) based Model 2 partly on model D from Grünthal et al. (2017), therefore this is consistent with the original model. NGI adjusted zones 20 and 21 to match better with the new zones. NGI recalculated the activity rates for zones 20 and 21 based on their new size. Table 6-2 lists the source parameters for Model 2.

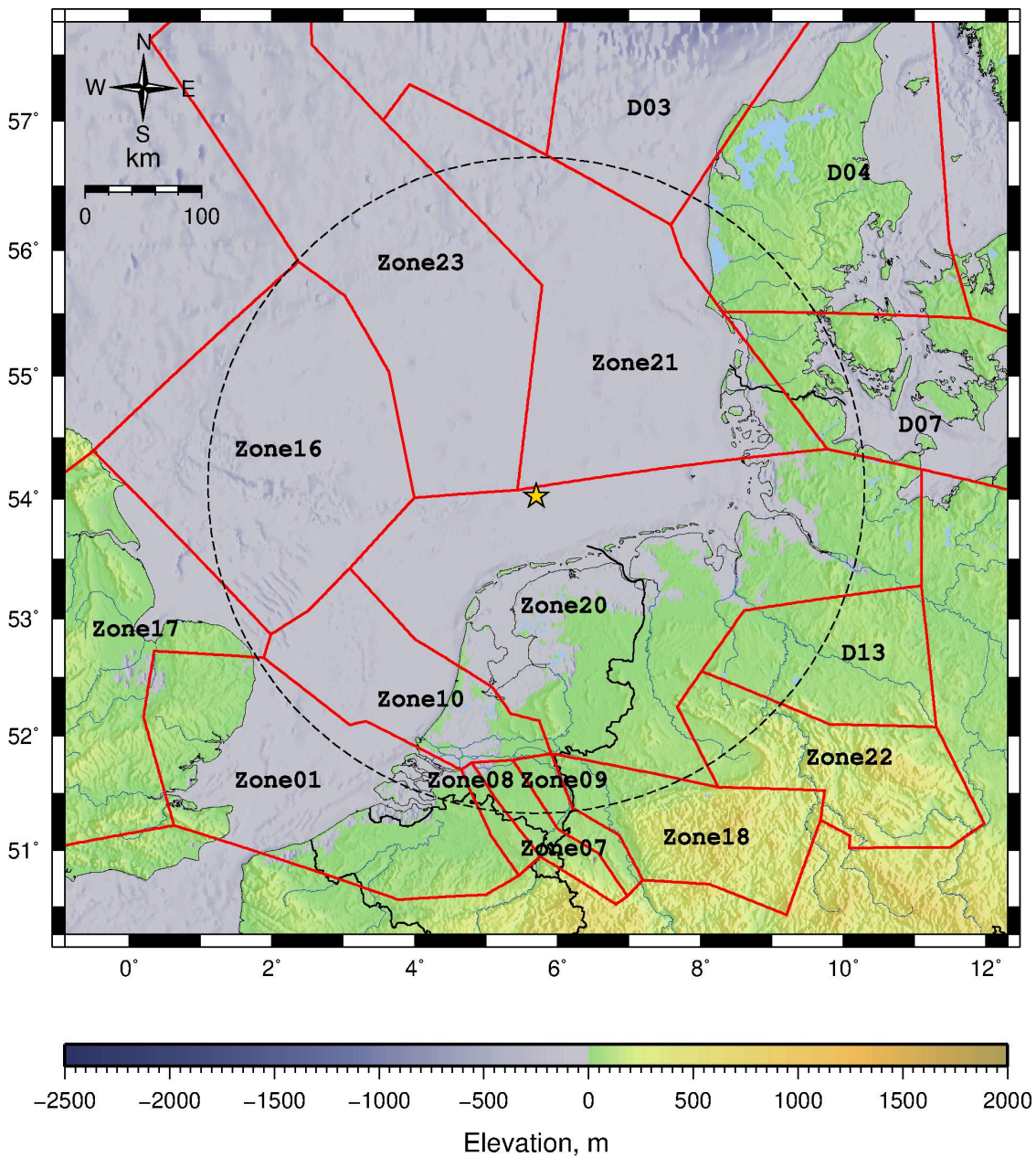


Figure 6-3 Seismic source model 2. Yellow star denotes project location. Dotted line indicates 300 km radius from the site.

Table 6-2 Source parameters for Model 2 (bold row indicates source zone where TNW is located)

Zone ID	Fault Mech.		Mmax		Depth (km)			N($M_{min} = 4.0$)	b value
	1 st	2 nd	min	max	min	peak	max		
Zone01	SS	N	5.67	6.82	0	10	23.1	0.0367	0.9390
Zone07	N	SS	6.74	7.32	0	10	20.9	0.0429	0.8995
Zone08	N	SS	6.74	7.32	0	10	20.9	0.0028	0.9601
Zone09	N	SS	6.74	7.32	0	10	20.9	0.0036	0.9401
Zone10	SS	N	5.70	6.83	0	10	32.0	0.0064	0.9567
Zone16	SS	N	5.89	6.79	0	10	23.9	0.0287	1.0196
Zone17	SS	N	5.89	6.79	0	10	23.9	0.0558	0.9636
Zone18	SS	N	5.70	6.83	0	10	32.0	0.0309	1.1764
Zone20	SS	N	5.70	6.83	0	10	32.0	0.0444	0.9861
Zone21	SS	N	5.70	6.83	0	10	32.0	0.0015	1.0178
Zone22	SS	N	5.69	6.83	0	10	32.7	0.0026	1.0556
Zone23	SS	N	5.69	7.19	0	10	32.0	0.0190	0.9830
D03	SS	N	5.65	6.80	0	10	32.0	0.1239	0.8060
D04	SS	N	5.76	6.83	0	10	32.0	0.0112	1.1120
D07	SS	N	5.82	6.83	0	10	32.0	0.0047	1.0200
D13	SS	N	5.76	6.83	0	10	32.0	0.0001	1.1120

6.2.3 Model 3

Figure 6-4 shows the geometry of seismic source Model 3. The areal source zones are the same as Model 3 for Fugro (2020), except NGI added zones C003, C004 and C011 to the east, and removed zones to the south and west that did not have a portion of the zone within 300 km of the site. The additional source zones are all from model C from Grünthal et al. (2017). Fugro (2020) based Model 3 model C from Grünthal et al. (2017), therefore this is consistent with the original model. Table 6-3 lists the source parameters for Model 3.

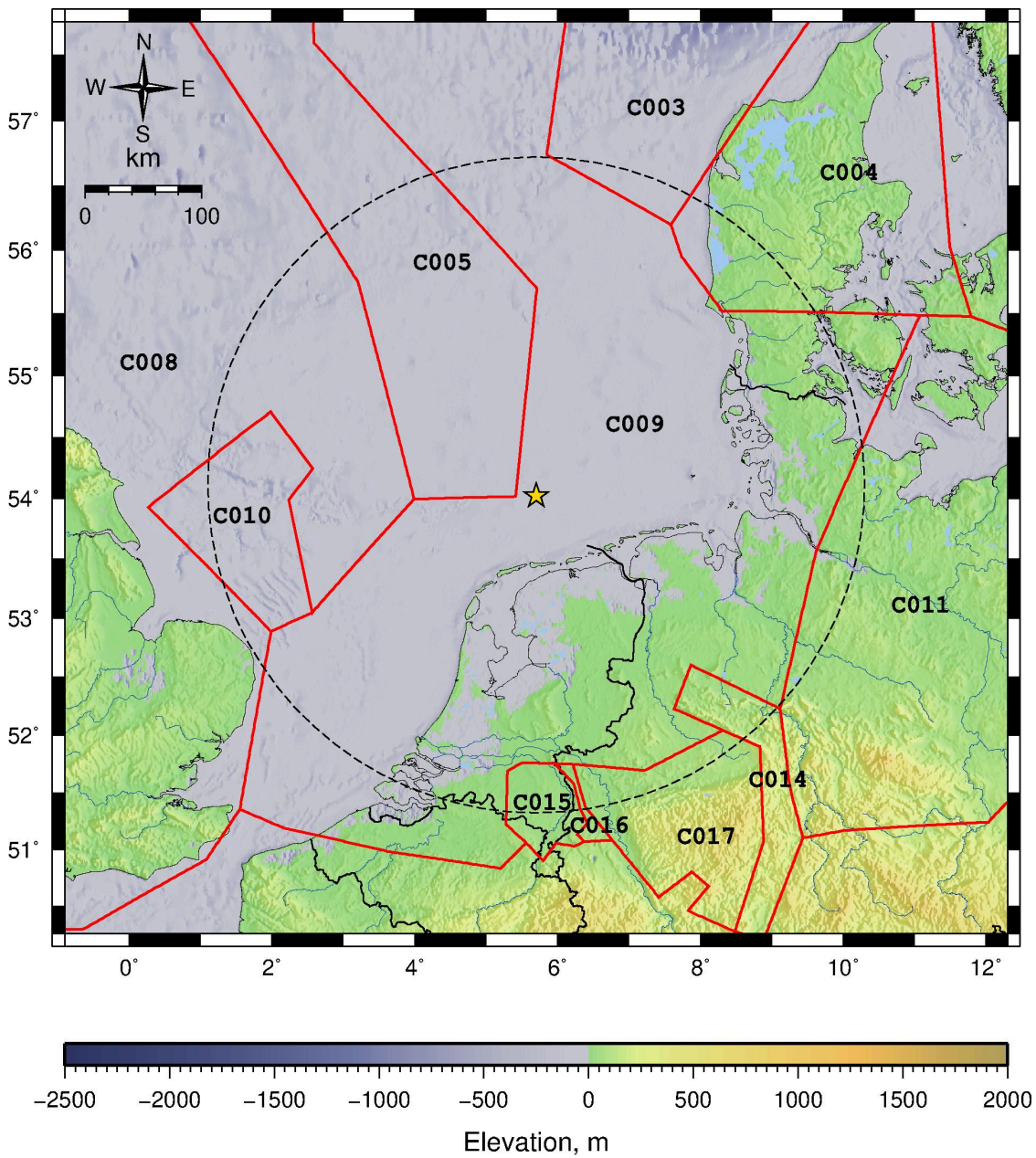


Figure 6-4 Seismic source model 3. Yellow star denotes project location. Dotted line indicates 300 km radius from the site.

Table 6-3 Source parameters for Model 3 (bold row indicates source zone where TNW is located)

Zone ID	Fault Mech.		Mmax		Depth (km)			N($M_{min} = 4.0$)	b value
	1 st	2 nd	min	max	min	peak	max		
C003	SS	N	5.65	6.80	0	10	32.0	0.1239	0.8060
C004	SS	N	5.76	6.83	0	10	32.0	0.0123	1.0860
C005	SS	N	5.69	7.19	0	10	32.0	0.0190	0.9830
C008	SS	N	5.89	6.79	0	10	15.5	0.1940	0.9647
C009	SS	N	5.70	6.83	0	10	32.0	0.0377	1.1024
C010	SS	N	5.89	6.79	0	10	15.5	0.0250	0.9267
C011	SS	N	5.76	6.83	0	10	32.0	0.0019	1.0860
C014	SS	N	5.69	6.83	0	10	32.7	0.0022	1.0319
C015	N	SS	6.74	7.32	0	10	20.9	0.0181	0.8442
C016	N	SS	6.74	7.32	0	10	20.9	0.0015	0.9376
C017	SS	N	5.70	6.83	0	10	32.0	0.0070	1.0285

6.3 Earthquake catalogue

6.3.1 Catalogue compilation

NGI compiled an earthquake catalogue of earthquakes occurring within a 300 km radius of the site from the International Seismological Centre on-line bulletin (ISC, 2021), British Geological Survey (BGS, 2021), Royal Netherlands Meteorological Institute (KNMI, 2021), Royal Observatory of Belgium (ROB, 2021), the German Federal Institute for Geosciences and Natural Resources (Leydecker 2011), and the European and Mediterranean Earthquake Catalogue (EMEC) (Grünthal and Wahlström, 2012). The ISC catalogue is an international catalogue containing earthquake data from all over the world. EMEC is a pan-European catalogue and an update to the CENEC catalogue (Grünthal et al., 2009). The other four catalogues are national databases focused on earthquakes recorded in or near their respective countries. NGI merged the catalogues and removed duplicates. Figure 6-5 shows the location and depth of the merged earthquake catalogue.

The largest earthquake in the database is the 1931 Dogger Bank earthquake (green pentagon at about 54° N and 1.5° E in Figure 6-5). According to the BGS catalogue, it occurred 274 km to the west of the site and had a local magnitude $M_L = 6.1$, whereas the ISC place the earthquake at 290 km from the site with a surface wave magnitude $M_S = 5.6$. NGI used the more conservative interpretation from the BGS in the final catalogue.

The second largest earthquake in the database is the 1932 $M_w = 5.2$ Uden earthquake, which occurred 261 km away from the site on the Lower Rhine Graben (red pentagon at about 51.7° N and 5.6° E in Figure 6-5). There are no other earthquakes with magnitude greater than five within 300 km of the site.

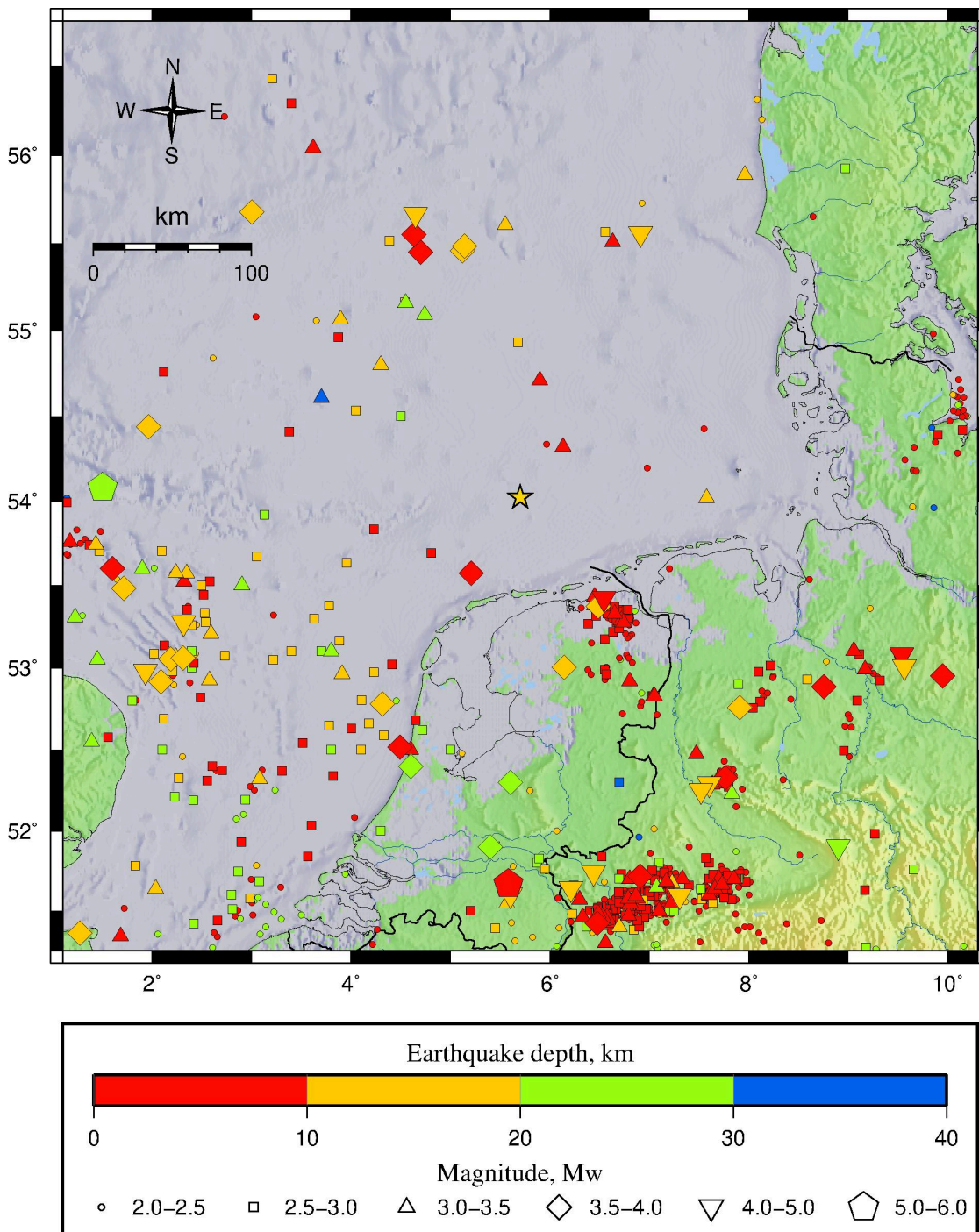


Figure 6-5 Location and depth of merged and magnitude converted earthquake catalogue

6.3.2 Magnitude conversion

There are many different types of magnitude scales and different agencies calculate the same magnitude scale differently. Therefore, when compiling an earthquake catalogue

from multiple sources, it is important to convert the magnitudes to the same scale. Because almost all ground motion models use moment magnitude (M_w) in their calculations, it is standard practice to convert to moment magnitude. Other common magnitude scales are:

- ↗ M_L , local magnitude
- ↗ M_b , body wave magnitude
- ↗ M_S , surface wave magnitude
- ↗ M_d , duration magnitude
- ↗ M_c , coda magnitude

The moment magnitude is based on the energy released during an earthquake. However, the other scales are based on certain features of recorded acceleration time series, properties of the specific recording instrument, and/or local geology. Due to the empirical nature of the other magnitude scales and uncertainties in magnitude calculation, conversion relations are also empirical. As a result, it is preferred to use region specific correlations based on data from the same area or the same tectonic region as the project.

Figure 6-6 presents a histogram of the number of earthquakes versus magnitude type for the merged catalogue. The catalogue mainly consists of earthquakes reported in local magnitude (932), followed by M_d (45), M_b (17) and M_S (1).

NGI converted the magnitudes to moment magnitude (M_w) using the conversions derived by Fugro (2020) for M_L , M_b , and M_S :

$$M_w = 0.0376 * M_L^2 + 0.646 * M_L + 0.53 \quad (6-2)$$

$$M_w = 2/3 * (M_S + 18.89) - 10.7 \quad (6-3)$$

$$M_w = 1.38 * M_b - 1.79 \quad (6-4)$$

and Grünthal et al. (2009) for M_d :

$$M_w = 1.472 * M_d - 1.49 \quad (6-5)$$

The Grünthal et al. (2009) equations were developed for central, northern and north-western Europe.

Figure 6-7 shows a histogram of the number of earthquakes versus magnitude for the merged and magnitude converted catalogue.

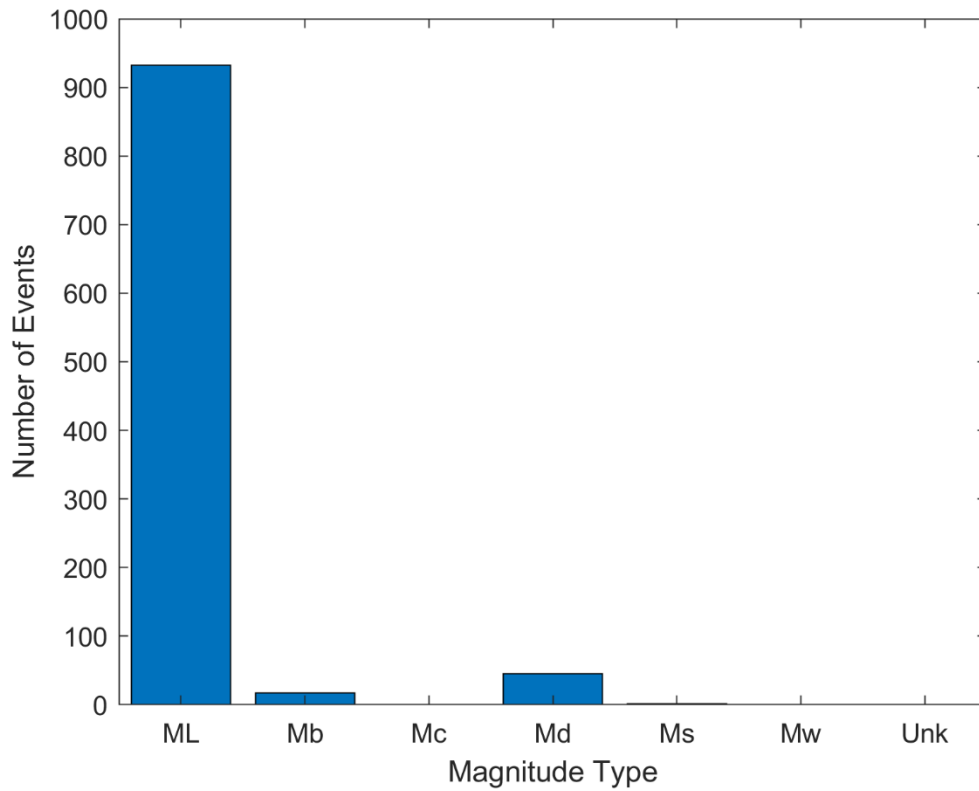


Figure 6-6 Histogram of magnitude type for the merged earthquake catalogue (Unk is unknown magnitude type)

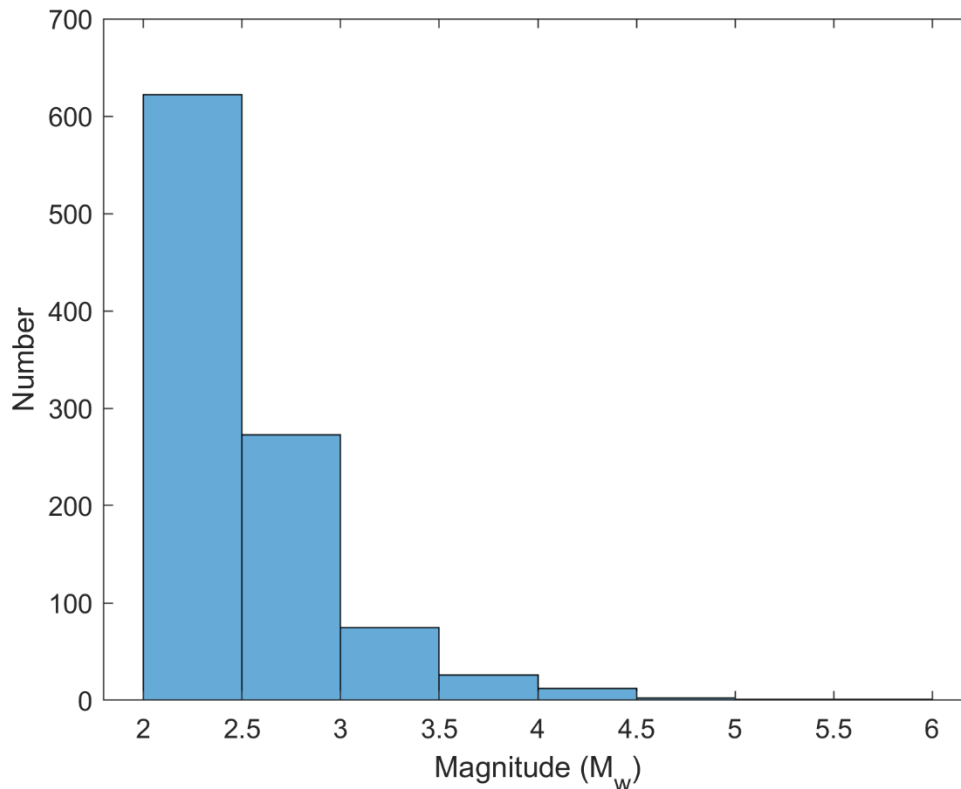


Figure 6-7 Histogram of magnitude for the merged and magnitude converted earthquake catalogue

6.3.3 Declustering

The second step in generating an earthquake catalogue is declustering. PSHA assumes that all earthquake events are independent, therefore, dependent events such as foreshocks and aftershocks must be removed. NGI used the declustering model of Grünthal (1985). The Grünthal (1985) method uses a magnitude dependent space and time window to define foreshocks and aftershocks. It is based on regression analyses of earthquakes from central Europe.

6.3.4 Completeness

The third step in preparing an earthquake catalogue is ensuring completeness. The activity rate (N_{min}) is the rate of earthquakes above M_{min} . Therefore, all earthquakes with $M > M_{min}$ that occurred in a given area and time period must be included in an earthquake catalogue to accurately predict N_{min} from the catalogue. If all earthquakes are not included, then the catalogue is incomplete. Normally, most catalogues are incomplete for smaller magnitude earthquakes because they are harder to detect without a strong ground motion station nearby. In most areas of the world, strong ground motion stations

were only first installed in the 1960's and 1970's, which severely limits the time period to estimate earthquake occurrence.

Stepp (1972) developed a method to evaluate earthquake catalogues for completeness for individual magnitude bins. This allows information for larger earthquakes from historical records to be used with information from instrument records that have a much shorter time period. The Stepp (1972) method assumes the earthquake sequence can be modelled as a Poisson distribution, and uses the statistical property that the variance of the estimate of a sample mean is inversely proportional to the number of observations in the sample. Therefore, rate of occurrence of earthquakes should be approximately constant and the catalogue is incomplete when it starts to decrease. However, the mean rate of occurrence and the standard deviation will only be stable and constant in the subinterval that is not only complete, but also long enough to give a good estimate (i.e. the sample size is statistically large enough). As a result, the data might fluctuate for the first years due to the small sample size. Larger magnitude earthquakes will have a longer unstable period because they occur less frequently than smaller magnitudes, but should have longer completeness times. For large magnitude earthquakes with very little data it is common practice to take the number of years since the earliest recorded earthquake as completeness time.

Figure 6-8 shows magnitude versus year for the merged, magnitude converted and declustered catalogue. There are no recordings of magnitude 3 or lower before 1960. The oldest earthquake in the catalogue is a $M = 3.1$ earthquake that occurred in 1757 in southeast England. NGI used the method of Stepp (1972) to estimate completeness of the earthquake catalogue. Table 6-3 lists the completeness years for different magnitude bins as well as the completeness years calculated by Fugro (2020) for the HKW site and the SHARE project for Northern Europe (Giardini et al., 2013). The completeness years in this study are similar to or smaller than those for the other studies. This is most likely because it is harder to detect small magnitude earthquakes offshore than onshore and the 300 km radius circle around TNW contains more sea than the other studies. Figure 6-9 shows the merged, magnitude converted, declustered and complete catalogue.

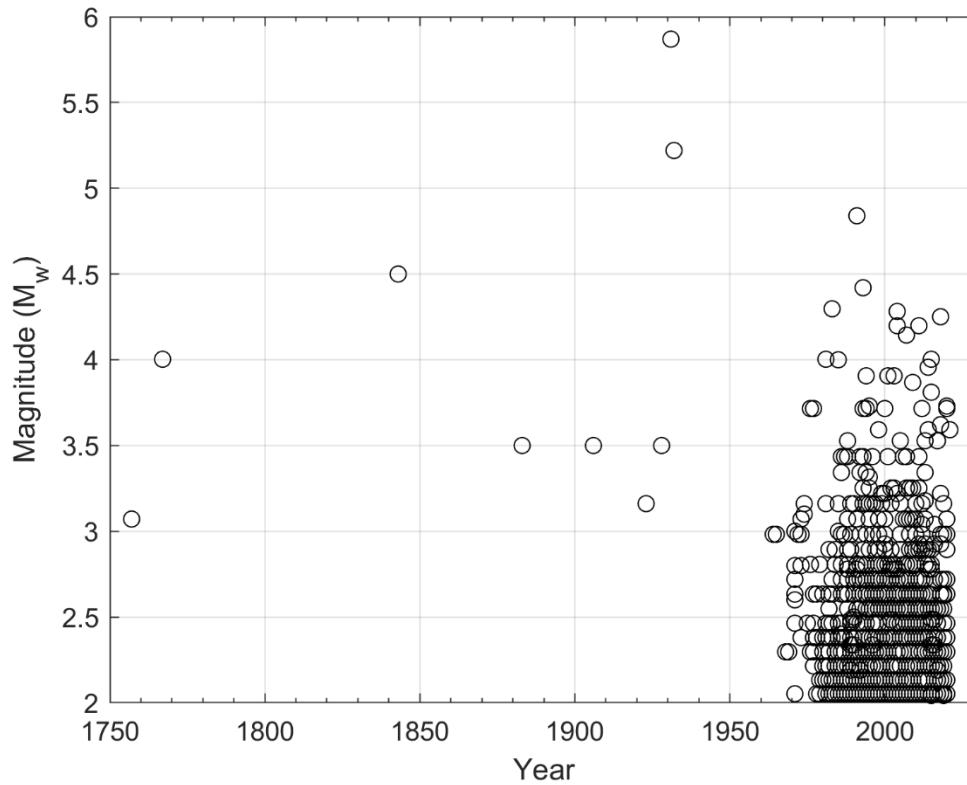


Figure 6-8 Earthquakes versus year for the merged, magnitude converted, declustered catalogue

Table 6-4 Completeness years for this study (TNW) compared with HKW (Fugro, 2020) and the SHARE project (Giardini et al., 2013) for Northern Europe

$\geq M$	TNW	HKW	SHARE
2.0	1985	1980	
2.5	1970	1975	
3.0	1970	1970	1970
3.5	1970	1950	
4.0	1960	1900	1890
4.5	1900	1850	
5.0	1800	1800	1800
5.5	1800	1800	1700

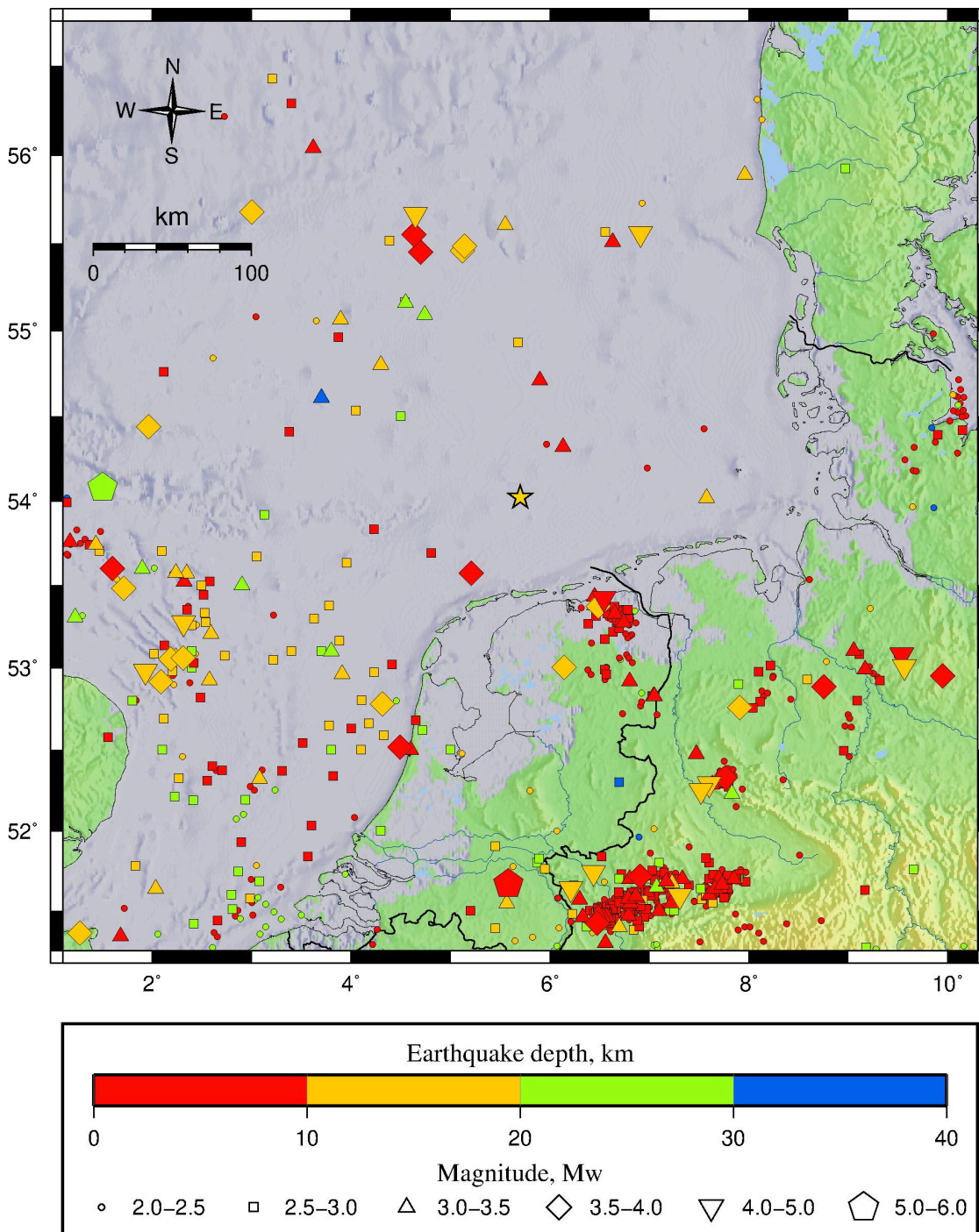


Figure 6-9 Merged, magnitude converted, declustered and complete catalogue for Mw > 2.0

6.3.5 Activity rates and b-values

After the earthquake catalogue was corrected for earthquake magnitude, dependent events and completeness, NGI calculated the activity rate, b-value and uncertainty

bounds using the maximum likelihood method of Weichert (1980). NGI then calculated an overall $N(M_{\min}=4) = 0.231$ and b -value = 1.0. Figure 6-10 shows the calculated magnitude recurrence relation versus cumulative annual rates of earthquakes in the declustered and complete catalogue with error bars.

NGI used one areal source zone 600 km by 600 km centred on the site. NGI used smoothed gridded seismicity to estimate relative activity rates across the larger areal source zone. Smoothed gridded seismicity is a grid of very small sub-sources with different activity rates but the same magnitude probability density function and b -value. The different activity rates represent the spatial variability of earthquake occurrence. The relative rates of each cell are based not just on the earthquakes that occurred in that cell, but a weighted average of the rates of the cell and the cells around it. NGI used a Gaussian distribution with a 50 kilometre radius and 0.2 by 0.2 degree grid cells to calculate the smoothed gridded seismicity. Figure 6-11 shows the declustered and complete earthquake catalogue for $M_w > 4.0$, and Figure 6-12 shows the corresponding smoothed gridded seismicity source model.

NGI used a truncated exponential model for the magnitude recurrence relation and minimum magnitude of $M_w = 4.0$, similar to seismic source models 1-3. NGI used maximum magnitudes of 6.1, 6.5, 6.9 and 7.2 with weights of 0.2, 0.5, 0.2 and 0.1 in a logic tree framework. NGI based these values on the maximum magnitudes used for seismic source models 1-3. The largest earthquake in the database is the 1931 Dogger Bank earthquake, which had a $M_w = 5.87$ ($M_L = 6.1$) and is less than these values. Figure 6-13 shows a histogram of earthquake hypocentre depths for the merged, magnitude converted, desclustered and complete earthquake catalogue for $M_w \geq 4.0$. Based on this figure, NGI modelled aleatory variability of the hypocentre depth for Model 4 as a triangular distribution with $\min = 0$, $\max = 24$ km, and $\text{peak} = 10$ km.

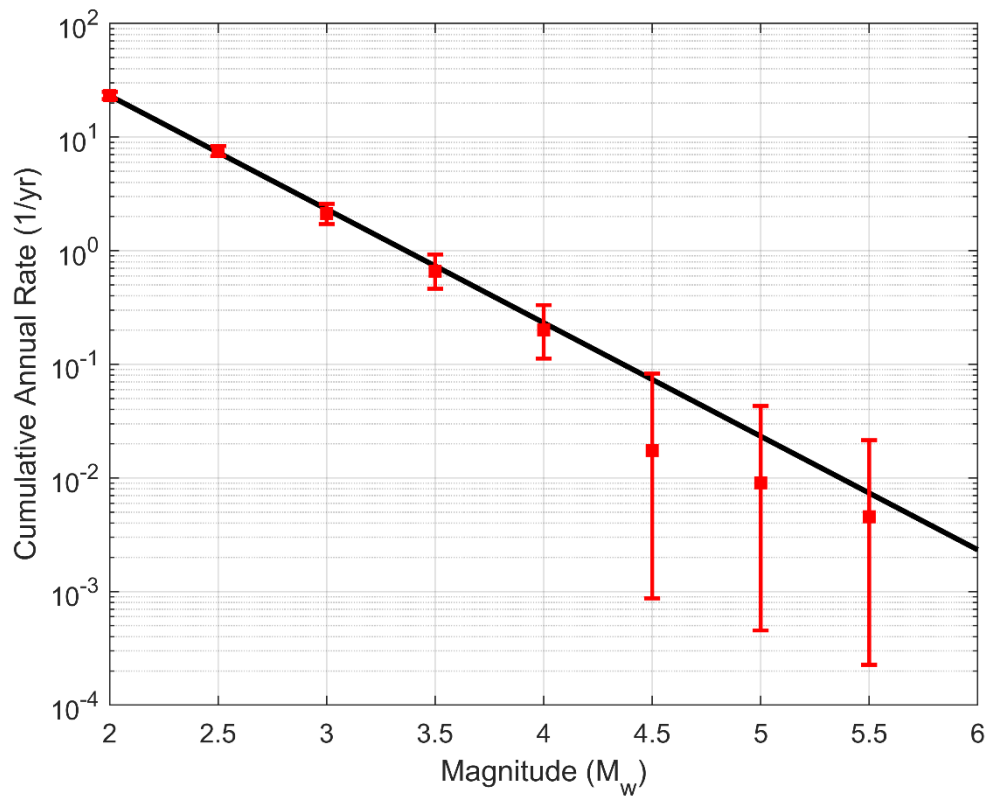


Figure 6-10 Magnitude recurrence relation (black line) versus cumulative annual rates of earthquakes in the declustered and complete catalogue (red squares) with error bars

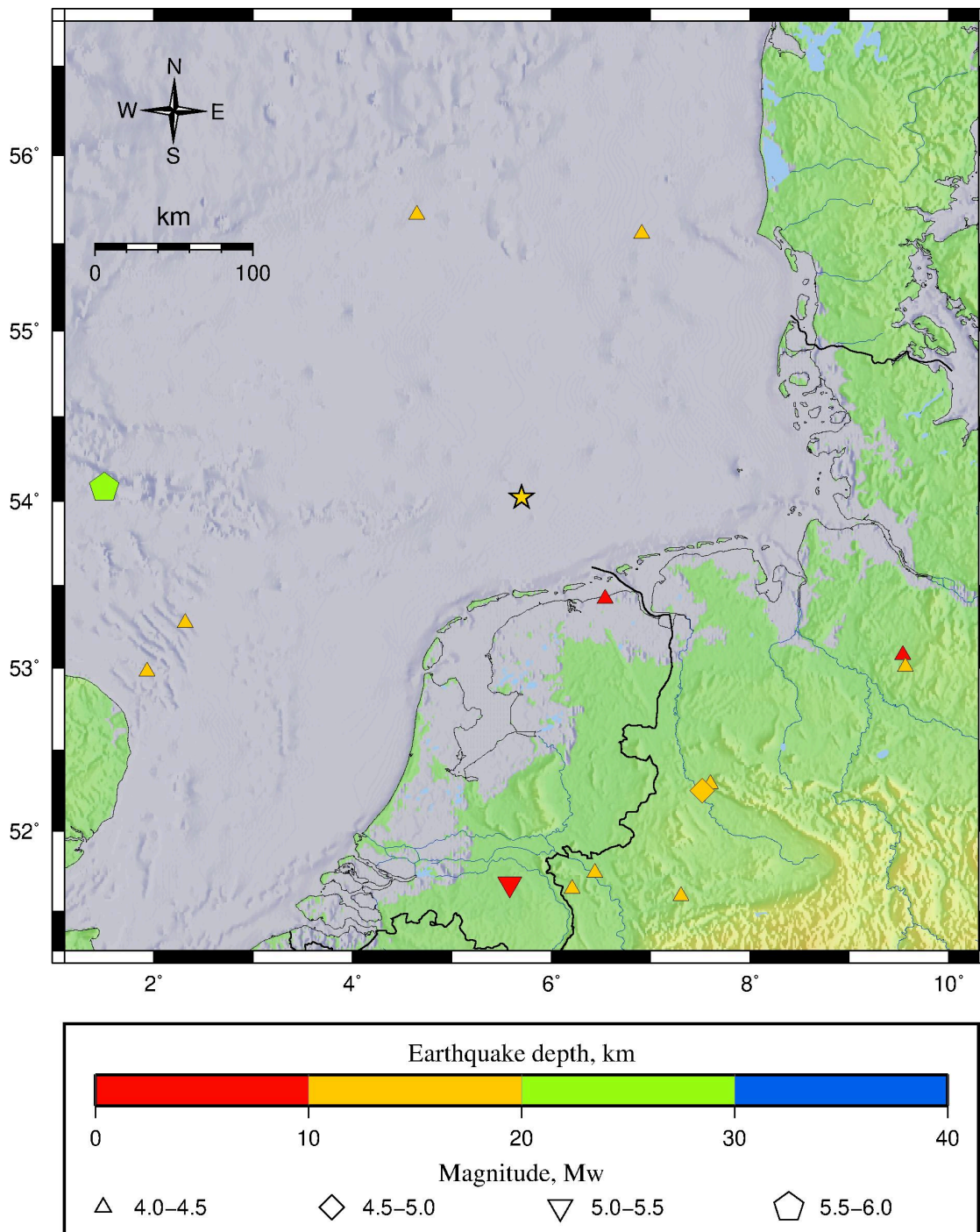


Figure 6-11 Merged, magnitude converted, declustered and complete catalogue for Mw > 4.0

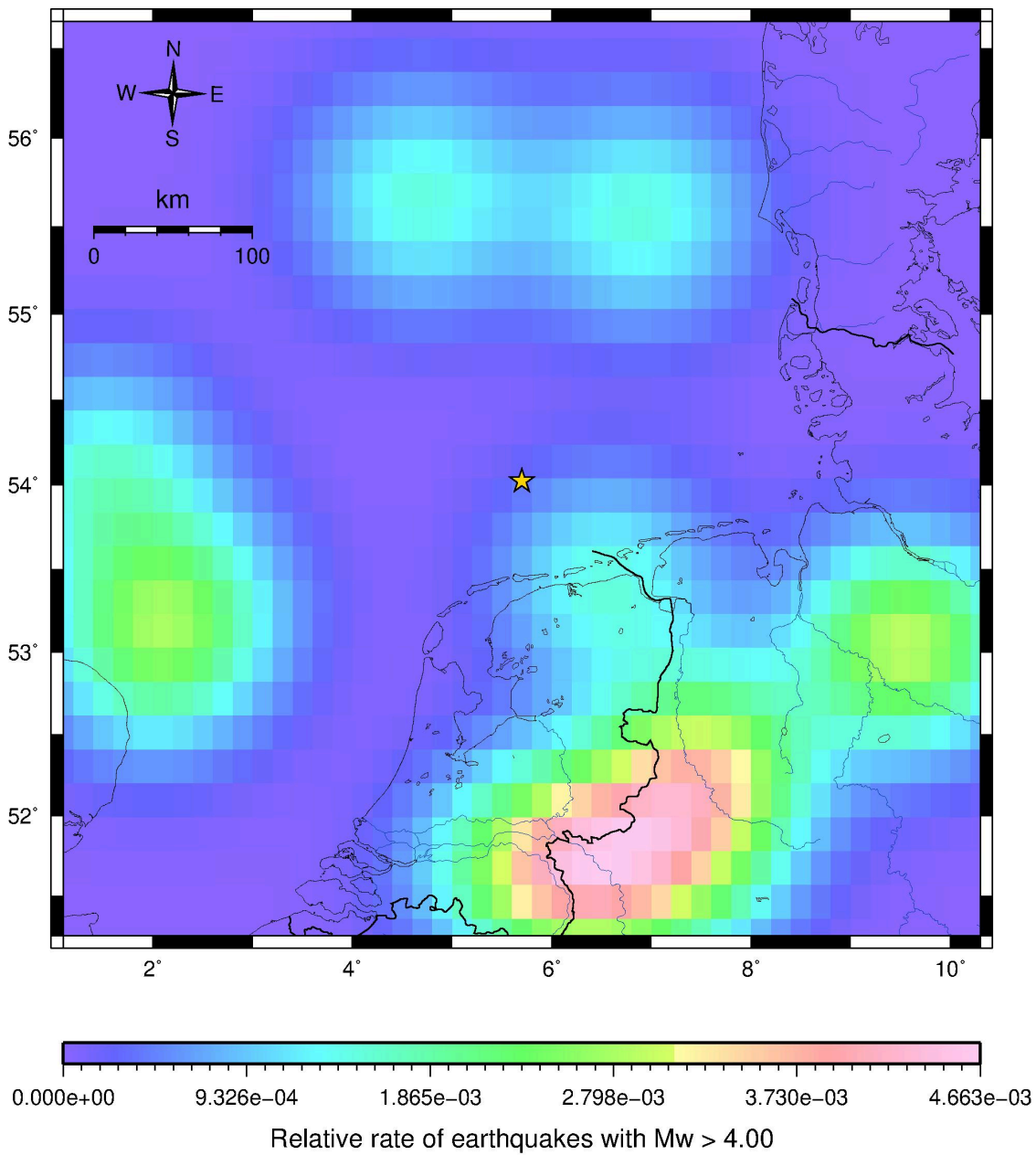


Figure 6-12 Smoothed gridded seismicity heat map for Mw > 4.0 showing the relative activity rate. Yellow star is the site location.

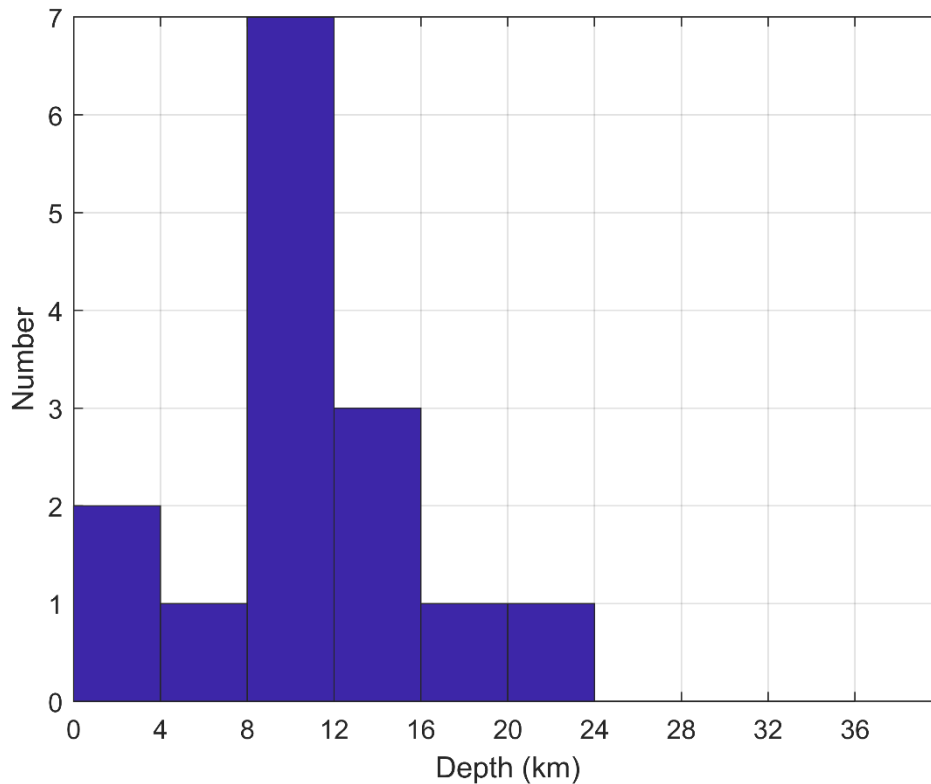


Figure 6-13 Histogram of earthquake hypocentre depths for the merged, magnitude converted, desclustered and complete earthquake catalogue for $M_w \geq 4.0$.

7 Ground motion models

7.1 Background

Ground motion models (GMMs) are empirical models that predict the expected range of an earthquake intensity measure (IM) at a site from a given earthquake scenario based on source, path, and site effects. The simplest models represent source effects by moment magnitude (M_w), path effects by the distance from the rupture zone to the site (R_{RUP}) and site effects by the time averaged shear wave velocity over the top 30 meters (V_{s30}). Most GMMs assume a log normal distribution and predict a mean value and standard deviation to estimate the variability of the IM given the earthquake scenario.

In this report the IM is selected as the spectral acceleration (Sa) at a given period (T) and the peak ground acceleration (PGA). In general, most PSHAs are conducted for these IMs. However, PSHA can be conducted for other IMs such as the Arias intensity, peak ground velocity, or peak ground displacement.

Normally, GMMs are developed for earthquakes from three different seismic regions:

- Shallow crustal earthquakes in active tectonic regions (e.g. California, Italy, Turkey, Greece)
- Shallow crustal earthquakes in stable continental regions (e.g. Australia, Eastern North America, Northern Europe)
- Interface and intraslab earthquakes from subduction zones (e.g. Japan, Chile, New Zealand)

7.2 Selected GMMs

NGI used the same five ground motion models (GMMs) with the same logic tree weights as Fugro (2020) for the HKW wind farm zone. Table 7-1 lists the references and weights used in the logic tree calculation for each ground motion model, as well as the minimum and maximum magnitude, distance and period ranges for which each ground motion model was developed. A brief description of each model is presented below:

- Akkar et al. (2014): This model is an update to the Akkar and Bommer (2010) ground motion model and was designed for crustal earthquakes in southern Europe and the Mediterranean region. They use a subset of the ground motions from the Reference Database for Seismic Ground-Motion in Europe (RESORCE) developed for the Seismic Ground Motion Assessment (SIGMA) project (Akkar et al. 2013) that have measured values of V_{S30} .
- Bindi et al. (2017): This model was developed for the PSHA of Germany conducted by Grünthal et al. (2017, 2018). They used a subset of the NGA-West2 ground motion database (Ancheta et al., 2014). One of the criteria in selecting the database subset was $V_{S30} > 360$ m/s, which is larger than the target $V_{S30} = 265$ m/s used for TNW. In addition, Bindi et al. (2017) recommend their model only for short return periods (e.g. 475 years). However, NGI believe that their model is still relevant for the TNW site because it was specifically tuned for a similar nearby region (Germany). In addition, as shown in section 9.1, the results using this model at longer return periods are not that much different from the other selected ground motions models.
- Campbell and Bozorgnia (2014): This model is one of the NGA West 2 ground motion models and an update to the 2008 NGA West 1 study. It uses a large, uniformly processed database of ground motions from active crustal regions all over the world.
- Cauzzi et al. (2015): This model is an update of the Cauzzi and Faccioli (2008) model. It attempts to develop an empirical ground motion model based on a different dataset than the NGA West 2 database (e.g. Campbell and Bozorgnia, 2014; Bindi et al., 2017) and the RESORCE database (e.g. Akkar et al., 2014) to capture epistemic uncertainty in PSHA. The database consists of ground motions mostly from Italy, Iceland, Japan, Greece, Turkey and Iran, with a few from California, Alaska, Taiwan and China.
- Yenier and Atkinson (2015): This model is a "plug and play" model that can be adapted to any region in the world by adjusting a few key parameters. The key

parameters are magnitude, distance, stress parameter, geometrical spreading rate, anelastic attenuation and an additional calibration factor. The form of the model is based on results from equivalent point-source simulations calibrated to empirical data in California. In this report, NGI used the Yenier and Atkinson (2015) model adapted to Central and Eastern North America, as described in the same paper. While this is not technically valid for Northern Europe, the model provides conservative estimates and only has a small effect on the hazard results due to its small weight in the logic tree. The model does not include aleatory variability, therefore, NGI used the standard deviation from the Atkinson and Boore (2006, 2011) model, similar to Fugro (2020) for the HKW site.

The models of Akkar et al. (2014), Bindi et al. (2017) and Cauzzi et al. (2015) were also used in the PSHA for Germany (Grünthal et al., 2018). In addition, Brooks et al. (2020) evaluated the fit of 16 ground motion models to recorded earthquakes from the northern North Sea region. They found that the model of Akkar et al. (2014) had the best fit to the data for PGA and most spectral periods, with the model of Cauzzi et al. (2015) providing a moderate fit for some but not all spectral periods. Villani et al (2019) evaluated GMMs for use in the UK, and they also recommended using Cauzzi et al. (2015) and one of the NGA West 2 ground motion models. This shows that the chosen GMMs agree with those used in similar studies for surrounding regions.

Some of the ground motion models use RotD50 spectral acceleration and some the geometric mean. However, Boore and Kishida (2017) show that the difference between these two is less than 7% for all periods. Therefore, NGI did not adjust any of the GMMs based on spectral acceleration type.

In this study, NGI set the minimum magnitude at $M_w = 4.0$, which is lower than the minimum magnitude of the Cauzzi et al. (2015) model, and the maximum distance as 300 km, which is larger than the maximum distance of the Akkar et al. (2014) and Cauzzi et al. (2015) ground motion models. Therefore, to ensure that these models behave reasonably when extrapolated outside of their intended ranges, NGI plotted response spectra for various combinations of magnitude and distance. Figure 7-1 through Figure 7-4 show the response spectra predicted by the selected ground motion models for the minimum and maximum magnitude and distance values. The maximum magnitude considered in this study is 7.32 and within the magnitude range of all the ground motion models. All of the models predict reasonable response spectra. The Yenier and Atkinson (2015) model tends to predict larger spectral acceleration values than all other models for all cases except large magnitude and short distance.

Table 7-1 Epistemic weights, minimum and maximum magnitude, distance and period ranges of the selected ground motion models

Reference	Weight	Magnitude (Mw)		Distance (km)		Period (s)	
		min	max	min	max	min	max
Akkar et al. (2014)	0.25	4.0	7.6	1	200	0.01	4
Bindi et al. (2017)	0.25	3.0	8.0	0	300	0.01	4
Campbell and Bozorgnia (2014)	0.20	3.3	8.5	0	300	0.01	10
Cauzzi et al. (2015)	0.20	4.5	7.9	0	150	0.01	10
Yenier and Atkinson (2015)	0.10	3.0	8.0	1	600	0.01	10

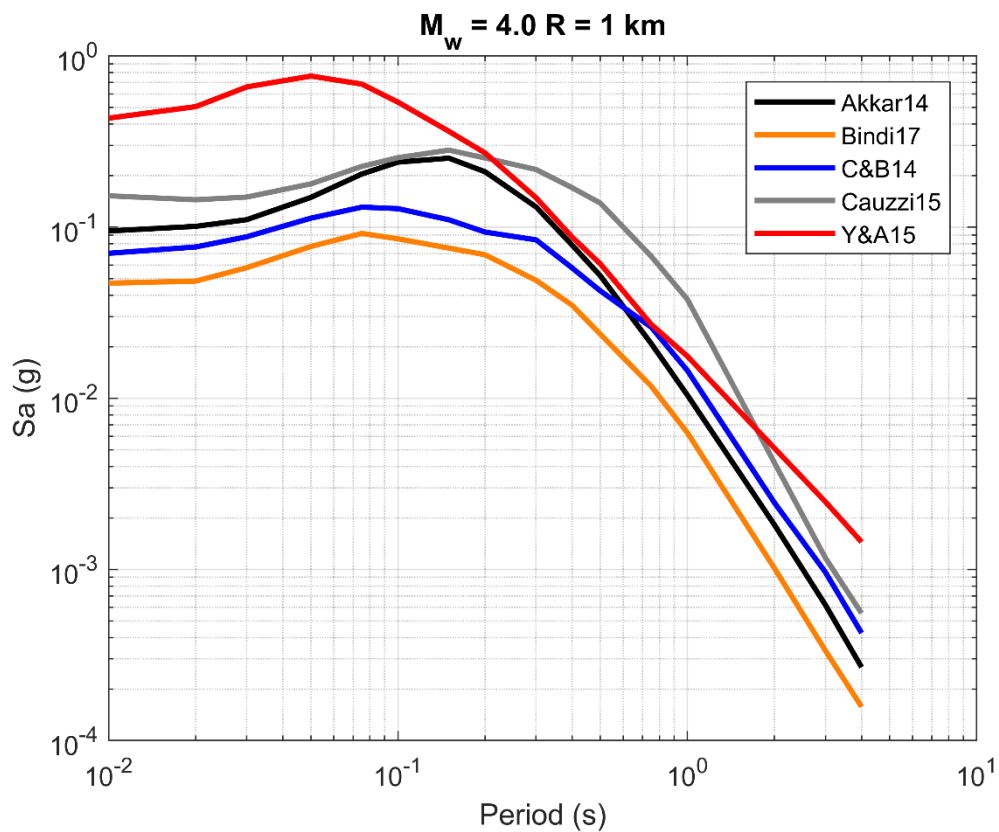


Figure 7-1 Response spectra predicted by the selected ground motion models for $V_{s30} = 265$ and lower bound magnitude ($M_w = 4.0$) and distance ($R = 1$ km)

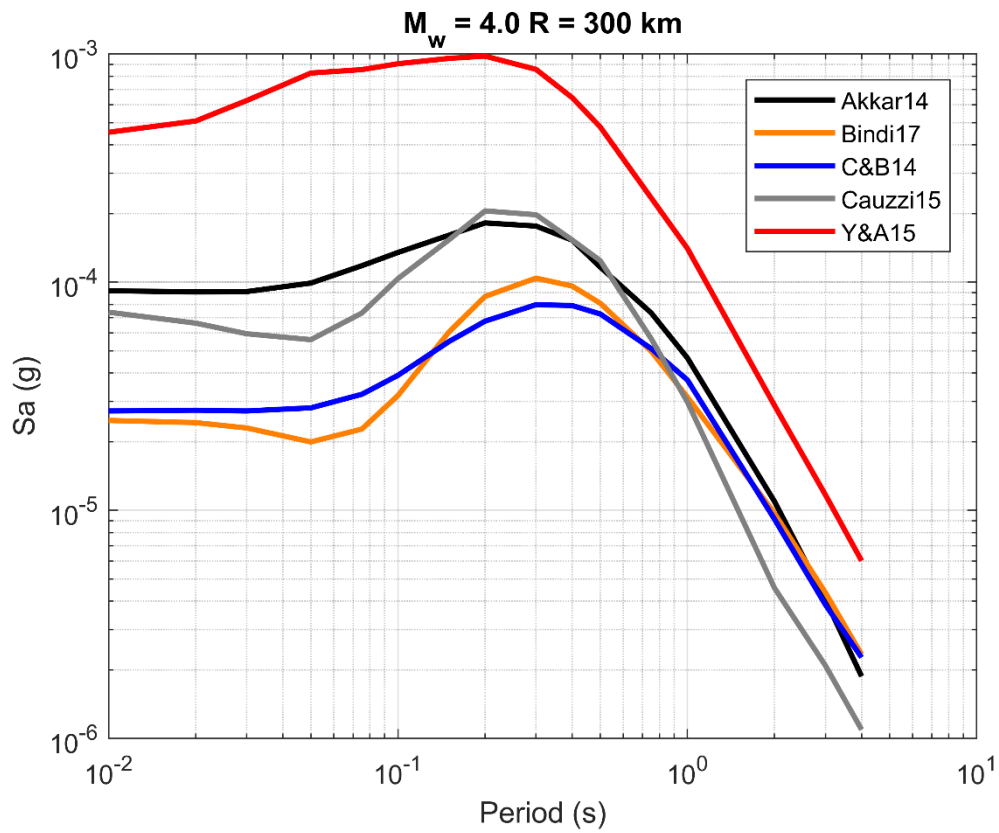


Figure 7-2 Response spectra predicted by the selected ground motion models for $V_{s30} = 265$ and lower bound magnitude ($M_w = 4.0$) and upper bound distance ($R = 300$ km)

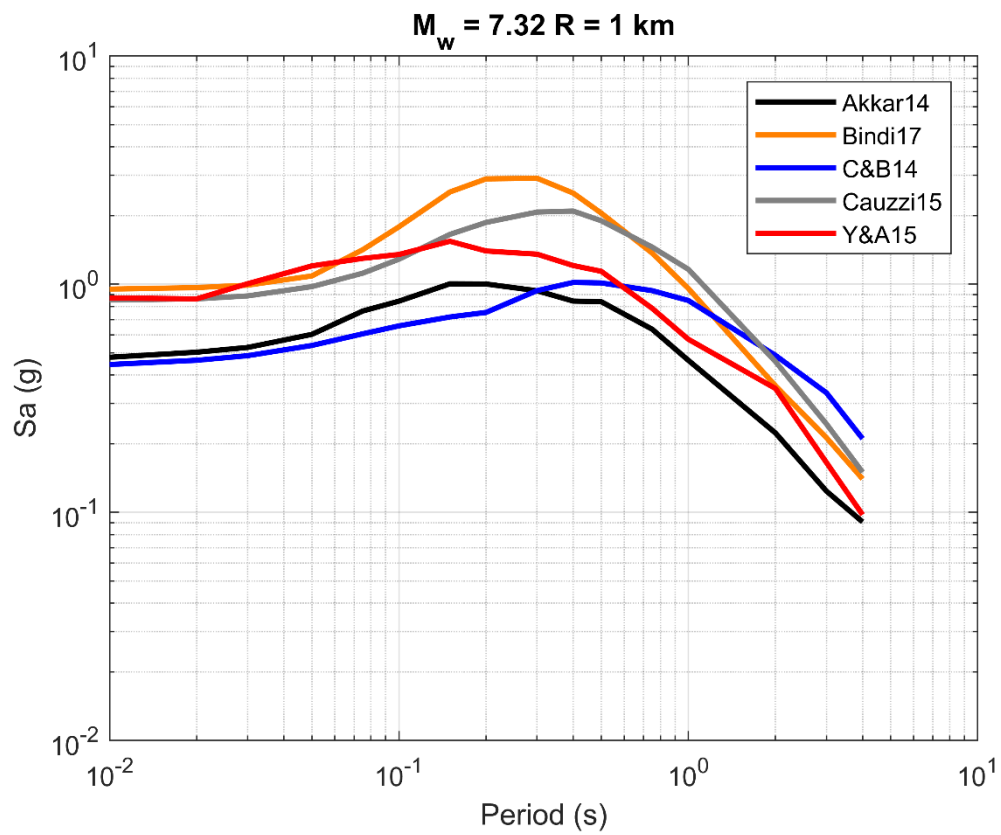


Figure 7-3 Response spectra predicted by the selected ground motion models for $V_{s30} = 265$ and upper bound magnitude ($M_w = 7.32$) and lower bound distance ($R = 1$ km)

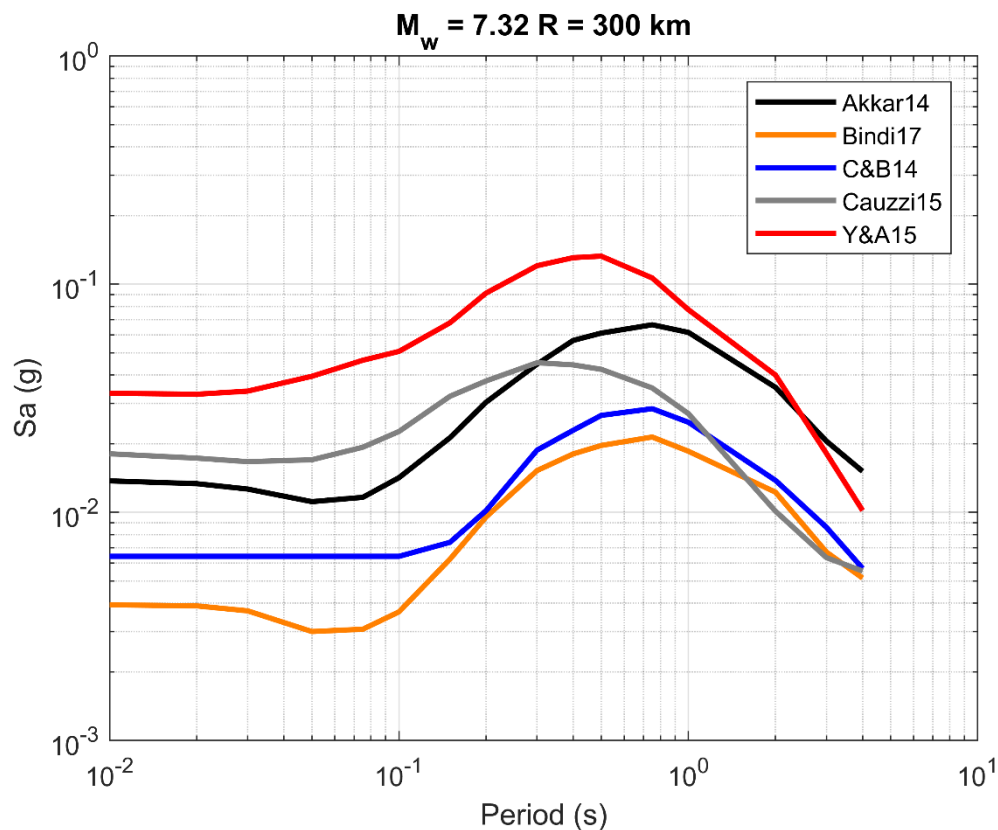


Figure 7-4 Response spectra predicted by the selected ground motion models for $V_{s30} = 265$ and upper bound magnitude ($M_w = 7.32$) and distance ($R = 300$ km)

8 Characterisation of uncertainty

8.1 Aleatory variability and epistemic uncertainty

In PSHA there are two main types of uncertainty; aleatory variability and epistemic uncertainty. Aleatory variability is the natural randomness in a process. As more data is collected the aleatory variability does not necessarily increase or decrease, it just becomes more accurate and closer to the true randomness of the process. In PSHA, probability density functions (e.g. for earthquake magnitude or depth) and standard deviations (e.g. for ground motion models) characterise aleatory variability. Aleatory variability controls the shape of the hazard curve.

Epistemic uncertainty is the scientific uncertainty in a model due to limited data or knowledge. In theory, as more data is collected epistemic uncertainty should decrease. Examples of epistemic uncertainty in PSHA are alternate seismic source models and ground motion models, and different maximum magnitudes, widths and faulting types

of a given source. Hazard curve fractiles (see section 10.3) represent the epistemic uncertainty.

One way to distinguish between aleatory variability and epistemic uncertainty is to ask if the parameter sometimes has one value and sometimes another, then it is aleatory variability. However, if the parameter has either one value or another, but we are not sure which, then the parameter has epistemic uncertainty.

8.2 Logic tree

Epistemic uncertainty is considered in PSHA by using a logic tree framework (Kulkarni et al., 1984). Each branch of the logic tree represents an alternative credible model or parameter value and is given a weight. The weights at each branch tip are mutually exclusive and collectively exhaustive and must sum to one. The weights are based on engineering judgment of how accurate or 'credible' each alternative model is. In this way, the use of a logic tree allows multiple credible models to be included in the PSHA. When using a logic tree, a separate PSHA is conducted for each combination of alternative models (i.e. each final branch of the logic tree). Then, all the different hazard curves are combined using the branch weights to estimate the mean hazard.

In this project, NGI considered epistemic uncertainty for the following parameters:

- ↴ Seismic source model
- ↴ Maximum magnitude
- ↴ Fault mechanism
- ↴ Ground motion model

9 Design hazard levels

ISO 19901-2:2017 requires offshore structures to satisfy the design criteria for Extreme Level Earthquakes (ELE) and Abnormal Level Earthquakes (ALE). The annual probability of exceedance P_f for these two events are calculated as follows:

1. Plot the hazard curve for $S_a(T_{dom})$ on a log-log scale, where $S_a(T_{dom})$ is the spectral acceleration for the dominant modal period of the structure. If there is no specific information about the structure, $T_{dom} = 1$ second may be used.
2. Calculate the value of $S_{aP_f}(T_{dom})$ from the hazard curve, where $S_{aP_f}(T_{dom})$ is the spectral acceleration at period T_{dom} and annual probability of exceedance P_f . Table 9-1 lists the values of P_f for each exposure level.

3. Estimate the slope of the seismic hazard curve a_R for the point corresponding to $S_{Pf}(T_{dom})$. The value of a_R is calculated as $a_R = Sa_1/Sa_2$, where Sa_1 is a spectral acceleration greater than $S_{Pf}(T_{dom})$, and Sa_2 is a spectral acceleration less than $S_{Pf}(T_{dom})$ with an annual probability of failure 10 times greater than Sa_1 . See Figure 9-1 for details.
4. Determine the correction factor C_C corresponding to a_R from Table 9-2.
5. Calculate the ALE spectral acceleration as $Sa_{ALE}(T_{dom}) = C_C * S_{Pf}(T_{dom})$.
6. The annual probability of exceedance for the ALE (P_{ALE}) is the annual probability of exceedance corresponding to $Sa_{ALE}(T_{dom})$.
7. The ELE spectral acceleration is then calculated as $Sa_{ELE}(T_{dom}) = Sa_{ALE}(T_{dom}) / C_r$, where C_r is the seismic reserve capacity factor for the structural system.
8. The annual probability of exceedance for the ELE (P_{ELE}) is the annual probability of exceedance corresponding to $Sa_{ELE}(T_{dom})$.
9. Calculate the return period for the ALE and ELE as $RP_{ALE} = 1/P_{ALE}$ and $RP_{ELE} = 1/P_{ELE}$.
10. The minimum return periods for ELE are 200 years, 100 years, and 50 years for exposure levels 1, 2 and 3, respectively. If RP_{ELE} is less than the minimum value, then the minimum value will be used.

For this project, NGI used $T_{dom} = 1$ second and $C_r = 1.1$ for deep pile foundations made of steel (i.e. monopile) and $C_r = 1.4$ for shallow concrete foundations. Table 9-3 lists the ELE and ALE design return periods for exposure levels L1 and L2 and $C_r = 1.1$ and 1.4. In addition, the client requested return periods of 95 years and 475 years.

Table 9-1 Target annual probability of exceedance, P_f (from ISO 19901-2)

Exposure Level	P_f
L1	$4 \times 10^{-4} = 1/2500$
L2	$1 \times 10^{-3} = 1/1000$
L3	$2.5 \times 10^{-3} = 1/400$

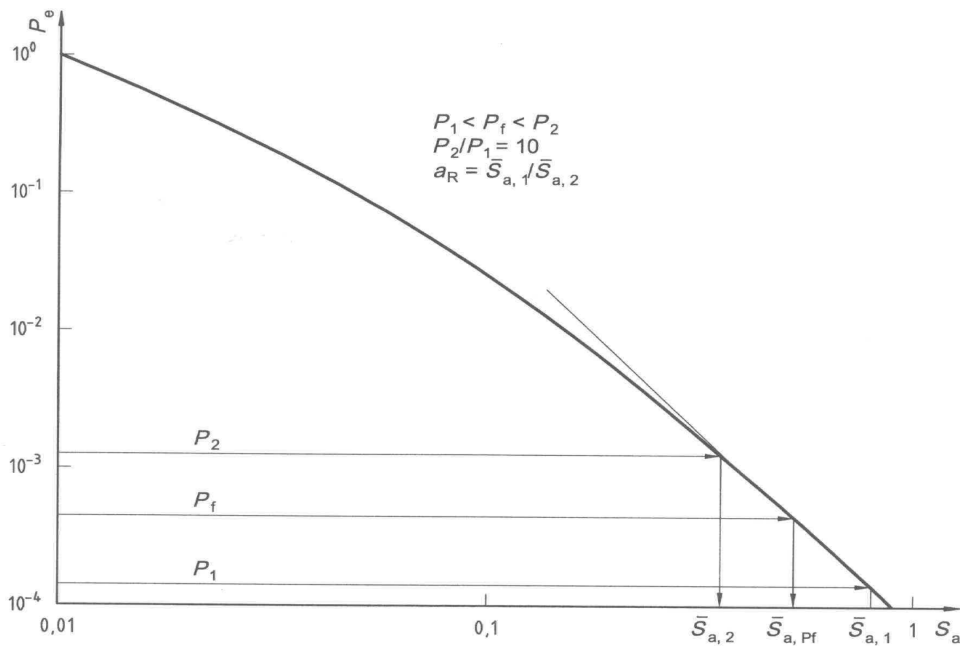


Figure 9-1 Procedure to estimate a_R (ISO 19901-2)

Table 9-2 Correction factor C_C (ISO 19901-2)

a_R	1.75	2.0	2.5	3.0	3.5
C_C	1.2	1.15	1.12	1.10	1.10

Table 9-3 Design return periods (years)

Design Level	L1 Deep	L2 Deep	L1 Shallow	L2 Shallow
ELE	2500	1000	1675	700
ALE	3000	1150	3000	1150

10 PSHA results

10.1 Hazard curves

Figure 10-1 shows the mean hazard for PGA and the unweighted hazard curves for the four different source models. Model 4, the smoothed seismicity model, predicts the largest hazard for return periods less than about 1000 years (annual rate of exceedance = 10^{-3}), and Model 2 predicts the largest hazard for return periods greater than 1000 years. Model 4 most likely predicts the largest hazard at short return periods due to the inclusion of induced seismicity. Models 1 and 3 predict similar hazard at all return periods. The total hazard, which is the weighted average of the four models following

the logic tree approach, plots between the four models because they are all given equal weight. The results are similar for other spectral periods.

Figure 10-2, Figure 10-3, and Figure 10-4 show the contribution of each source zone to the hazard for Models 1, 2 and 3. In general, the areal source zone where the site is located dominates the seismic hazard, especially at longer return periods. This is because these zones have a higher chance of producing a large magnitude earthquake close to the site, which is what drives the hazard for PGA at long return periods. Figure 10-2 shows that LCG (the zone the site is located in) and WCB dominate the hazard for return periods greater than 150 years, whereas MSA, GBP and GEM control the hazard for return periods less than 150 years. This is because the latter three source zones have the highest activity rates, and therefore more chance of producing small magnitude earthquakes. Figure 10-3 shows that the source most contributing to the hazard for Model 2 is zone 20 (the zone the site is located in), followed by source zones 23 and 16. The site is near the border of zones 23 and 21, however, zone 21 has the smallest activity rate, and therefore does not contribute significantly to the seismic hazard except at very long return periods. Figure 10-4 shows that source C009 controls the hazard at all return periods for Model 3. This is the zone that the site is located in, and in addition, it comprises a majority of the area within the 300 km radius of the PSHA calculation. Source C005 also contributes to the hazard for the same reasons.

Figure 10-5 shows the mean hazard for PGA and the unweighted hazard curves for the different ground motion models. The model of Yenier and Atkinson (2015) predicts significantly larger hazard than the other models. This was also seen in section 7. The reason is that the Yenier and Atkinson (2015) model was developed for Eastern North America and therefore predicts much less attenuation than the other models. However, the Yenier and Atkinson (2015) model does not significantly increase the total mean hazard because it is only given a weight of 0.10. The other four ground motions models predict similar results to each other. Figure 10-6 shows the mean hazard for spectral acceleration at one second ($Sa(T=1)$) and the unweighted hazard curves for the different ground motion models. The Yenier and Atkinson (2015) model still predicts the largest hazard, but the difference is not as great for long periods as for short periods. In addition, at long periods the Cauzzi et al. (2015) model starts to predict less hazard than the other three models.

Figure 10-7 shows the mean hazard for all 16 spectral periods investigated. Figure 10-7 shows spectral periods of 0.2 and 0.3 seconds predict the largest hazard for return periods of about 100 years or less, and 0.15 to 0.2 seconds for longer return periods.

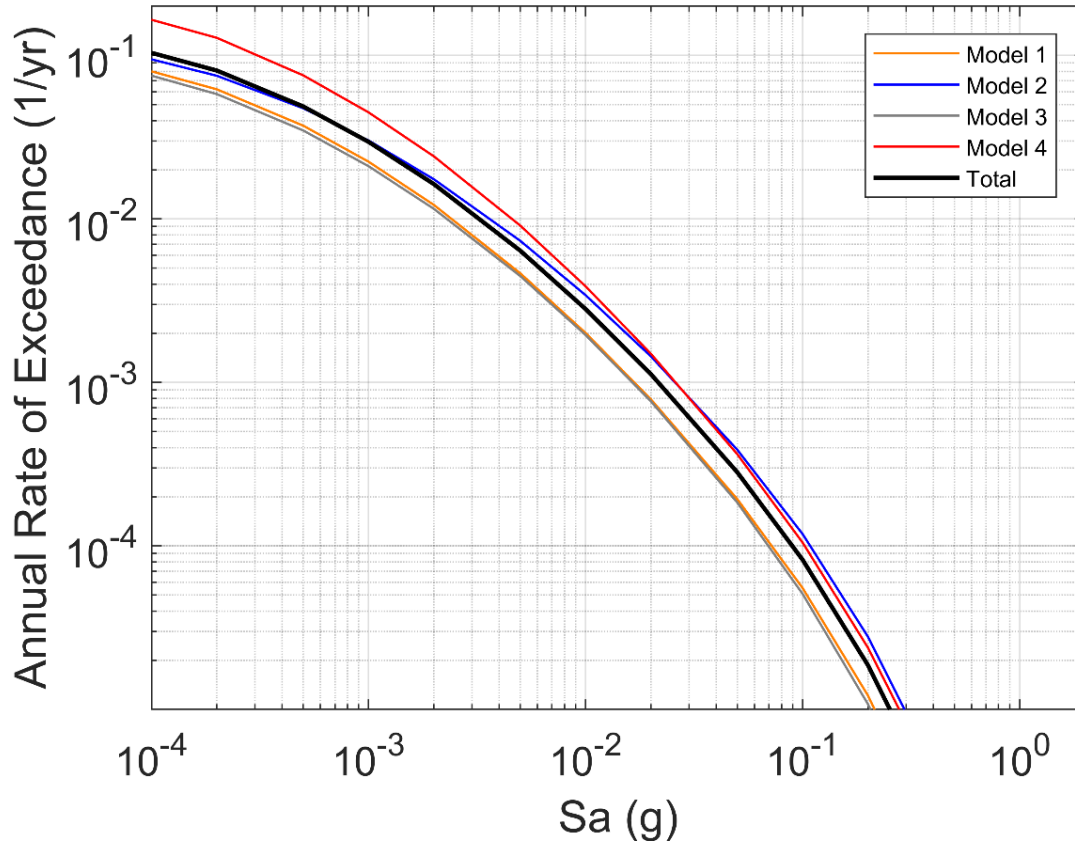


Figure 10-1 Mean hazard curves for PGA showing the unweighted hazard curves for the four seismic source models and the weighted total hazard curve.

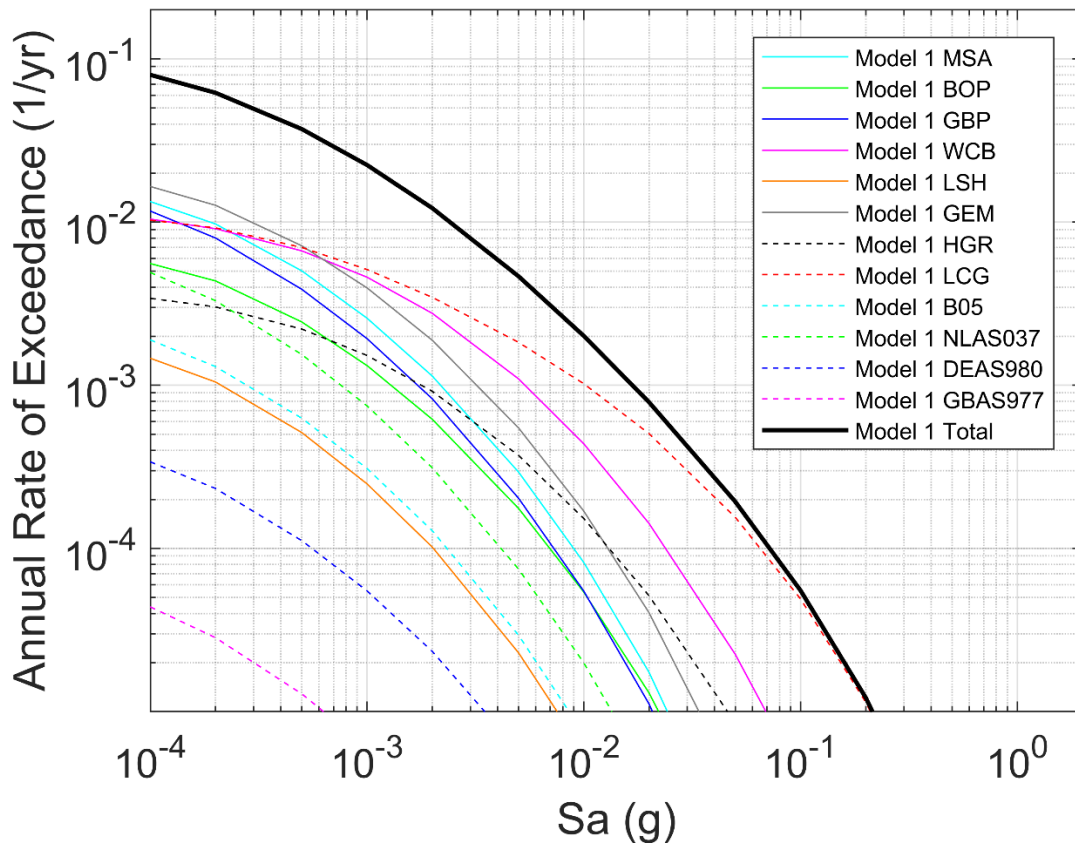


Figure 10-2 Mean hazard curves for PGA showing the contribution of the different areal source zones to Model 1

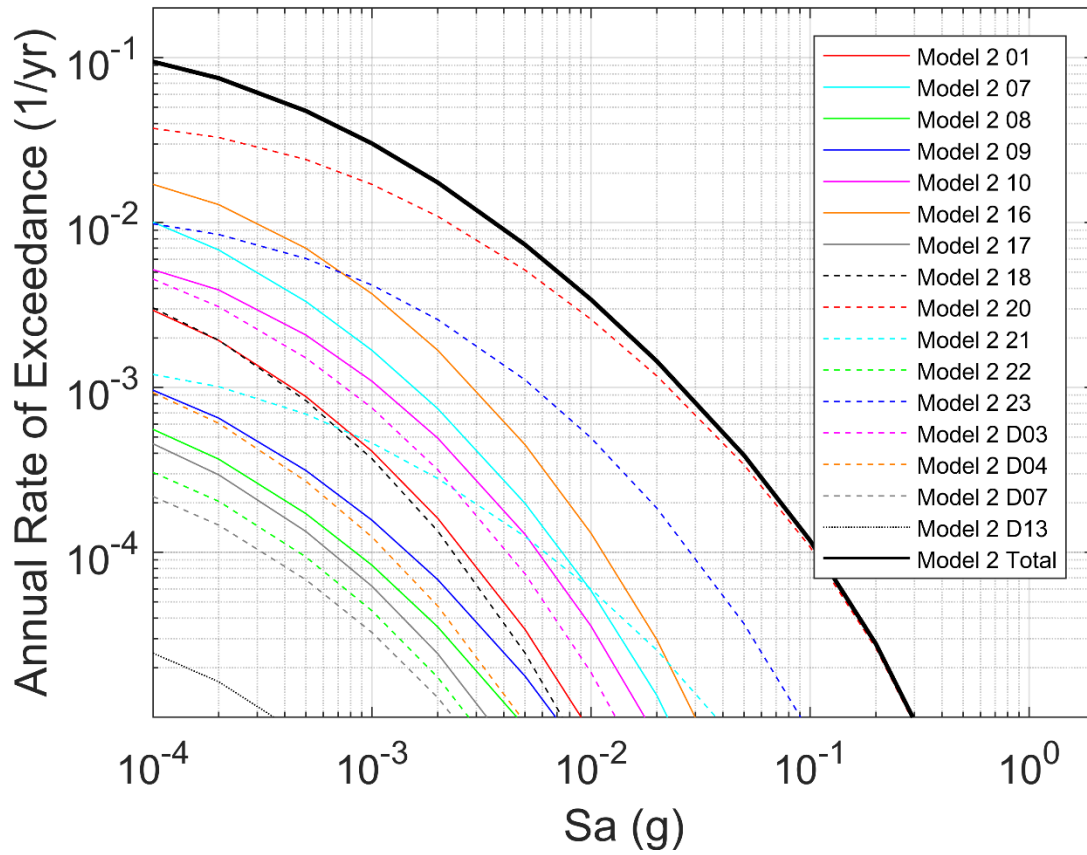


Figure 10-3 Mean hazard curves for PGA showing the contribution of the different areal source zones to Model 2

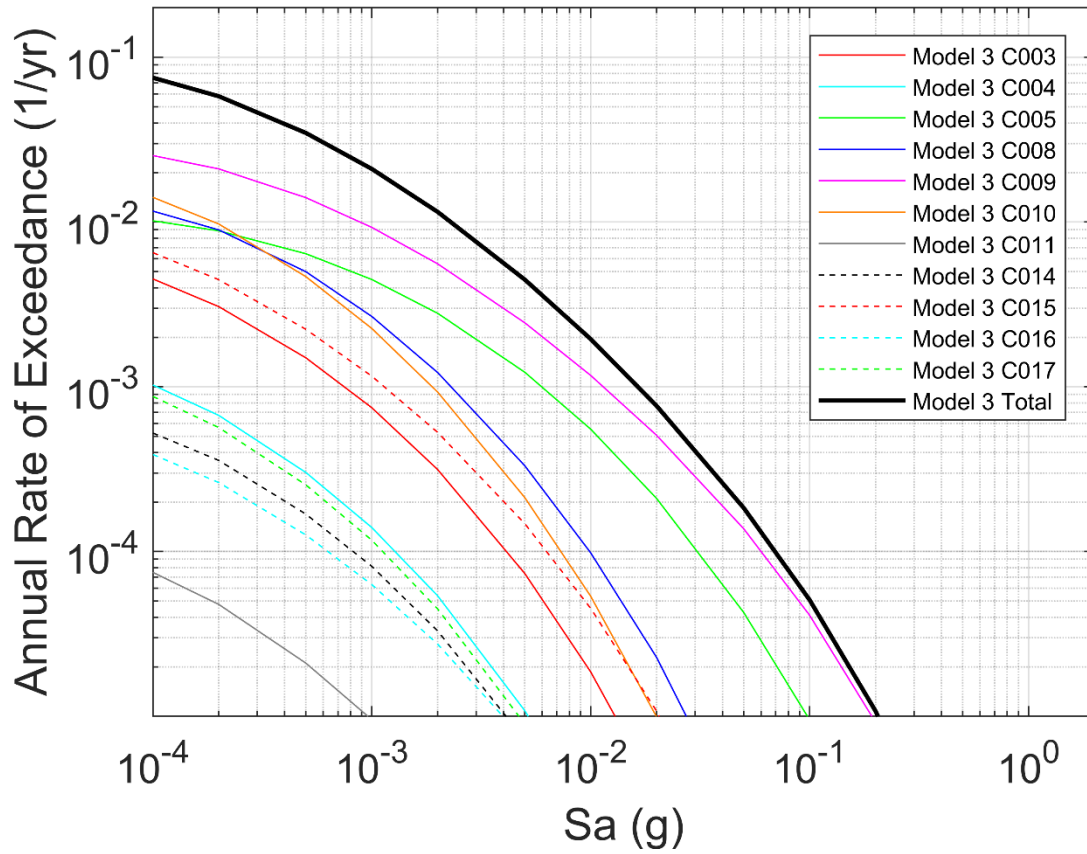


Figure 10-4 Mean hazard curves for PGA showing the contribution of the different areal source zones to Model 3

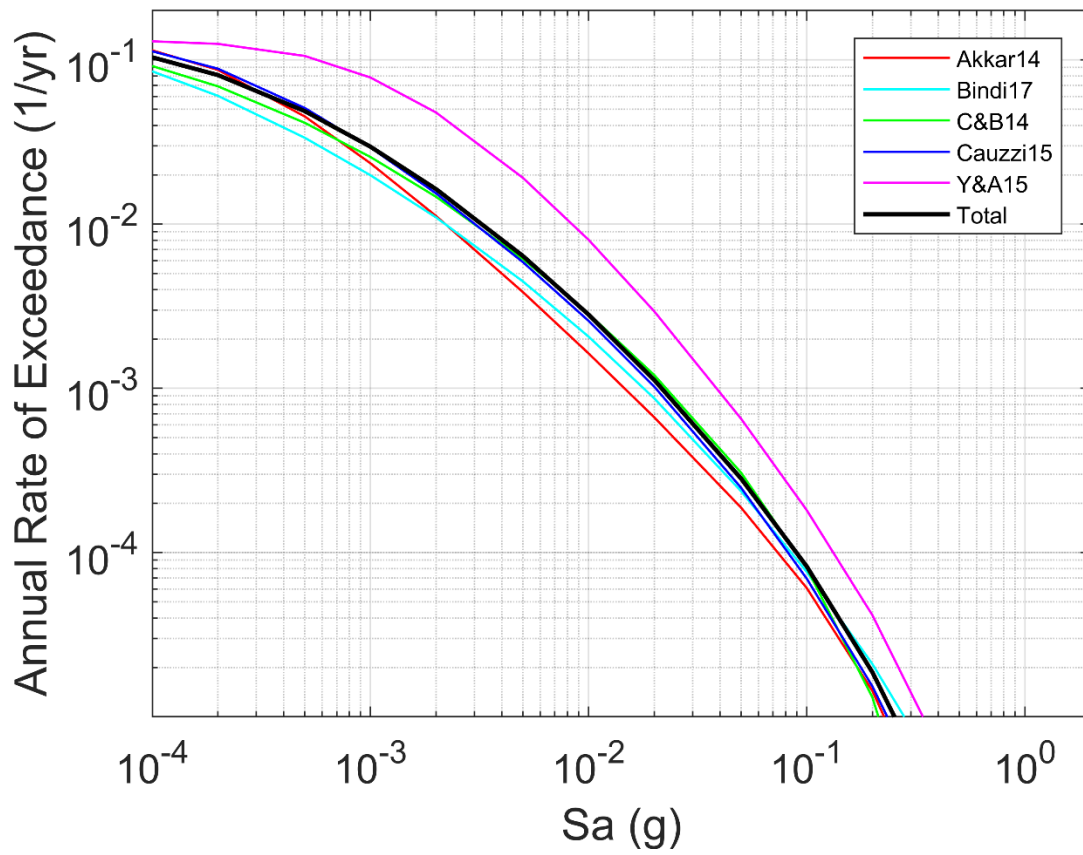


Figure 10-5 Mean hazard curves for PGA showing the unweighted hazard curves for each ground motion model and the weighted total hazard curve

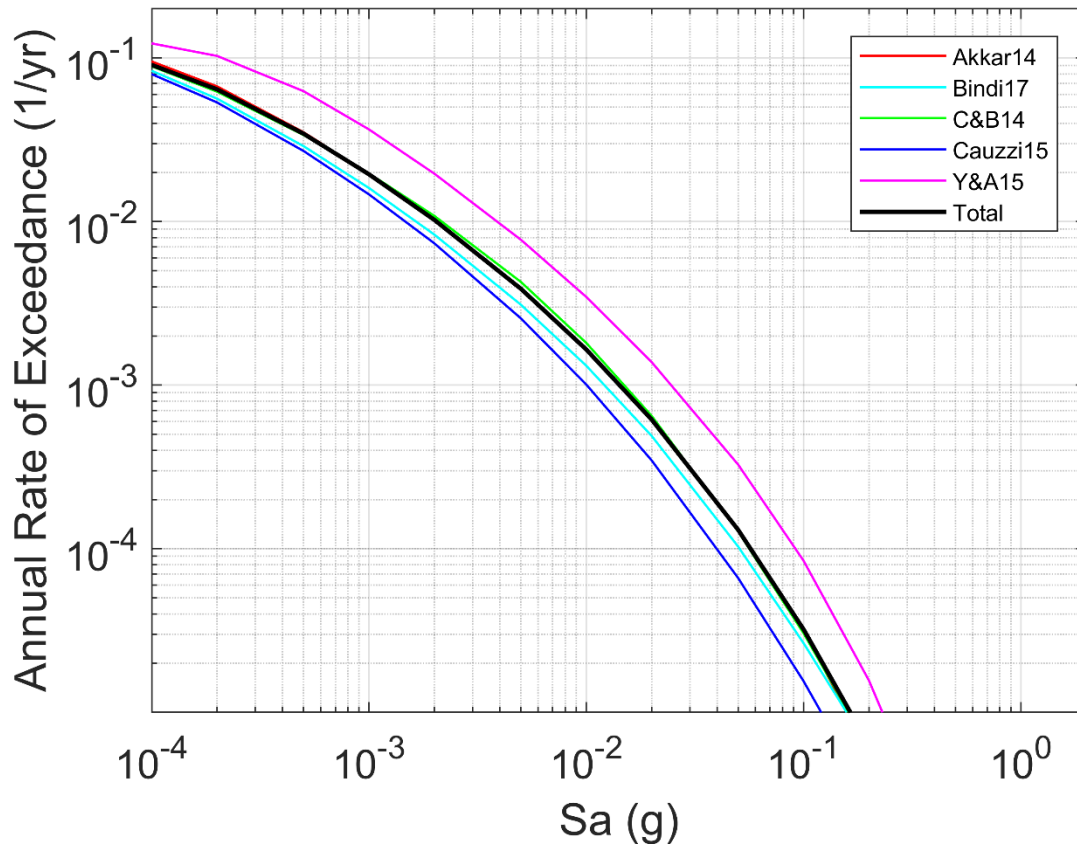


Figure 10-6 Mean hazard curves for S_a ($T=1$ second) showing the unweighted hazard curves for each ground motion model and the weighted total hazard curve

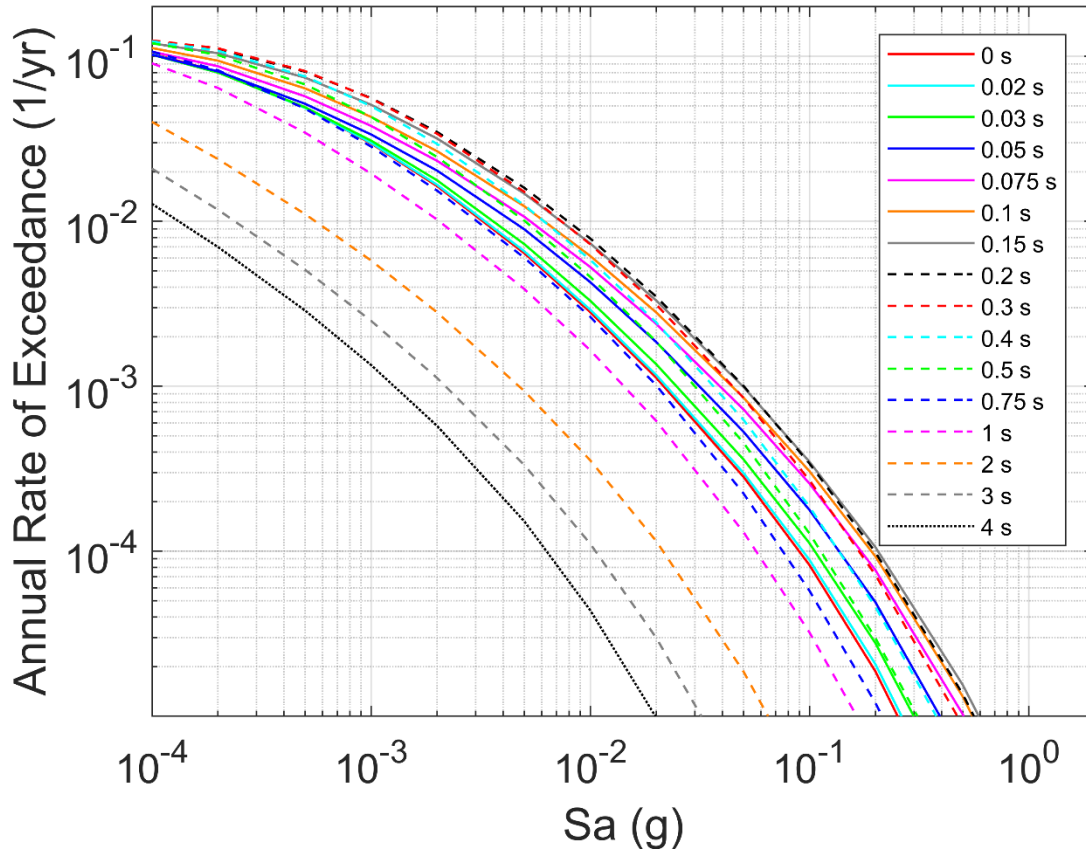


Figure 10-7 Mean hazard curves for all spectral periods

10.2 Horizontal design uniform hazard spectra (UHS)

Uniform Hazard Spectra (UHS) are response spectra with equal probability of exceedance at all periods. In other words, there is an equal probability to meet or exceed the given spectral acceleration value, S_a , at one period as there is at another. UHS are calculated by taking the S_a value at each period for a given hazard level. Because the hazard is computed independently for each period, UHS do not represent the response spectrum from one earthquake, and they do not give the probability of meeting or exceeding the S_a value at multiple periods. The short-period spectral values are often dominated by nearby moderate earthquakes and the long-period spectral values by distant larger magnitude earthquakes (Figure 10-16 and Figure 10-17). Another way to think of a UHS is as an envelope of response spectra for multiple scenarios. Figure 10-8 and Table 10-1 present the horizontal uniform hazard spectra (UHS) for the eight different design return periods.

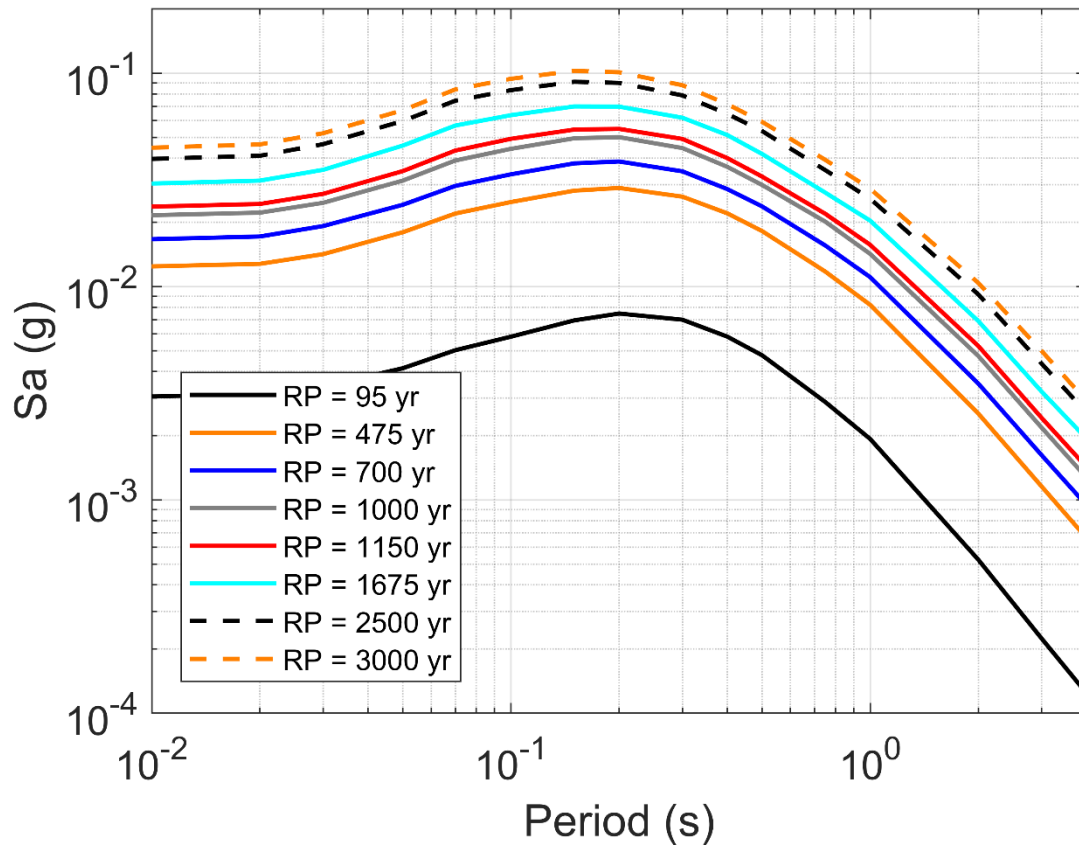


Figure 10-8 Horizontal, mean Uniform Hazard Spectra for different return periods (5% damping)

Table 10-1 Horizontal, mean uniform hazard spectra (g) for different return periods (year) and 5% damping

Period (s)	95	475	700	1000	1150	1675	2500	3000
PGA	0.0031	0.0124	0.0167	0.0216	0.0237	0.0304	0.0397	0.0448
0.02	0.0031	0.0128	0.0172	0.0222	0.0244	0.0314	0.0411	0.0464
0.03	0.0034	0.0142	0.0192	0.0247	0.0272	0.0353	0.0465	0.0524
0.05	0.0041	0.0180	0.0242	0.0314	0.0348	0.0458	0.0598	0.0671
0.07	0.0050	0.0220	0.0297	0.0390	0.0434	0.0569	0.0744	0.0840
0.1	0.0058	0.0249	0.0336	0.0443	0.0493	0.0636	0.0833	0.0942
0.15	0.0069	0.0282	0.0378	0.0496	0.0545	0.0699	0.0912	0.1026
0.2	0.0075	0.0290	0.0386	0.0502	0.0549	0.0698	0.0901	0.1011
0.3	0.0070	0.0264	0.0347	0.0446	0.0492	0.0619	0.0788	0.0879
0.4	0.0058	0.0221	0.0286	0.0364	0.0400	0.0513	0.0646	0.0717
0.5	0.0048	0.0182	0.0238	0.0300	0.0328	0.0419	0.0536	0.0592
0.75	0.0029	0.0118	0.0156	0.0202	0.0219	0.0276	0.0352	0.0393
1	0.0019	0.0082	0.0111	0.0142	0.0157	0.0204	0.0258	0.0287
2	0.0005	0.0025	0.0035	0.0047	0.0053	0.0069	0.0092	0.0104
3	0.0002	0.0012	0.0016	0.0022	0.0024	0.0032	0.0044	0.0050
4	0.0001	0.0007	0.0009	0.0013	0.0014	0.0019	0.0026	0.0029

10.3 Hazard fractiles

When using a logic tree, a separate PSHA is conducted for each combination of alternative models (i.e. each final branch of the logic tree). Then, all the different hazard curves are combined using the branch weights to estimate the mean hazard. It is common practice when using a logic tree to take the mean hazard curve. The advantages to taking the mean hazard curve are that the mean hazard combined with the mean fragility gives the mean risk and the mean hazard curve is more conservative as the uncertainty increases. However, it is also possible to calculate the median hazard curve or any hazard fractile (percentile). The different hazard curve fractiles represent the epistemic uncertainty in the hazard curve based on the logic tree weights (Abrahamson and Bommer, 2005). Fractiles show the percentage of the logic tree branch tips that give results above or below. For example, the 84th fractile shows a hazard curve where 84% of the branch tips predicted lower hazard curves and 16% above. Fractile plots help understand the total epistemic uncertainty based on all the different models used in the PSHA.

Figure 10-10 and Figure 10-11 show the mean and 5th, 16th, 50th (median), 84th, and 95th fractile hazard curves for PGA and spectral acceleration at one second ($S_a(T=1)$), respectively. The mean hazard is slightly larger than the median hazard. Figure 10-11 and Figure 10-12 show the mean and 5th, 16th, 50th (median), 84th, and 95th UHS for 475 year and 3000 year return periods, respectively.

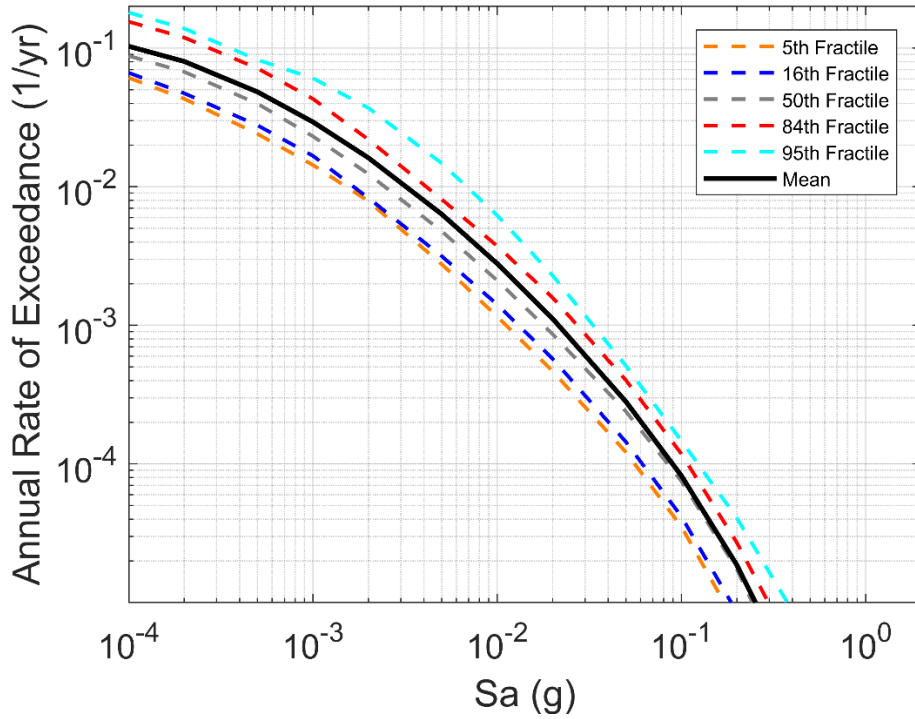


Figure 10-9 Mean hazard curve and hazard curve fractiles for PGA

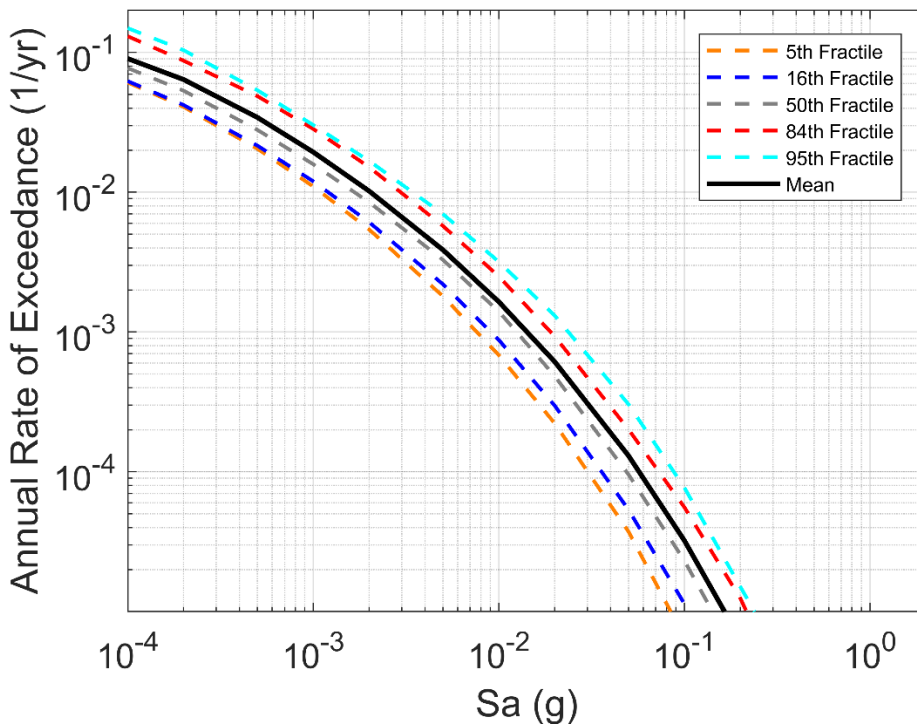


Figure 10-10 Mean hazard curve and hazard curve fractiles for Sa (T=1 second)

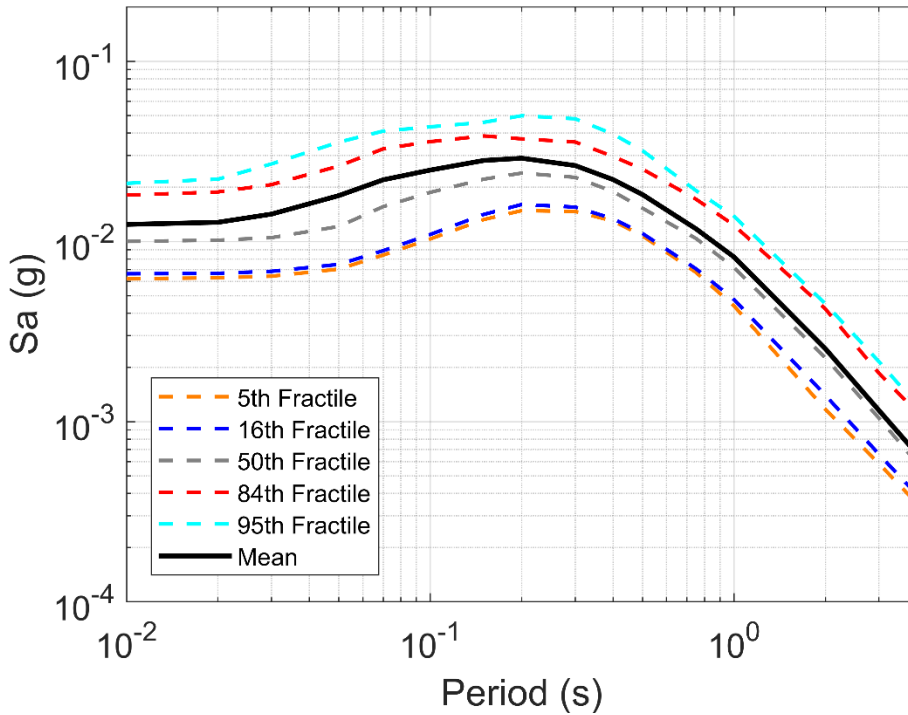


Figure 10-11 Mean UHS and UHS fractiles for 475 year return period

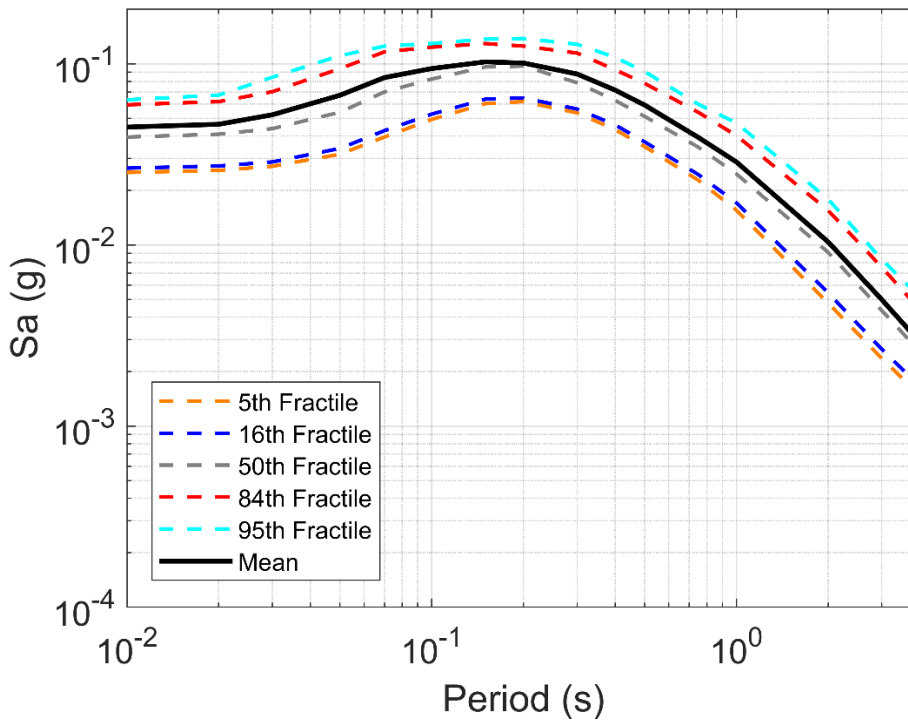


Figure 10-12 Mean UHS and UHS fractiles for 3000 year return period

10.4 Deaggregation

The hazard deaggregation shows the percent contribution for different magnitude and distance bins to the overall hazard at a given spectral period and return period. Figure 10-13, Figure 10-14 and Figure 10-15 show the hazard deaggregation for PGA and a spectral period of $T = 1.0$ seconds for return periods of 95 years, 475 years, and 3,000 years, respectively. Figure 10-16 and Figure 10-17 show the mean magnitude and mean distance contributing to the hazard for the eight design return periods. These figures show that as the spectral periods increase, the mean magnitude and distance increase, and as the return period increases, the mean magnitude increases and the mean distance decreases. This is a common result for PSHA with no strong fault activity. For a return period of 95 years, the controlling scenario at short spectral periods is $M_w = 4.9$ and $R = 140$ km, and at long spectral periods it is $M_w = 5.2$ and $R = 180$ km. For a return period of 495 years, the controlling scenario at short spectral periods is $M_w = 5.0$ and $R = 90$ km, and at long spectral periods it is $M_w = 5.7$ and $R = 170$ km. For a return period of 3000 years, the controlling scenario at short spectral periods is $M_w = 5.0$ and $R = 50$ km, and at long spectral periods it is $M_w = 6.0$ and $R = 170$ km.

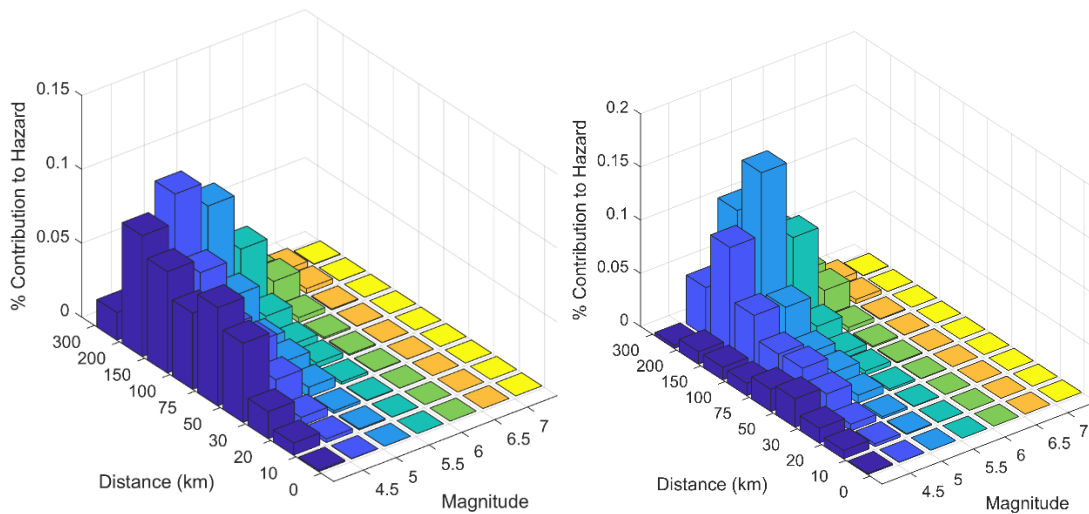


Figure 10-13 Hazard deaggregation for PGA (left) and $S_a(T=1)$ (right) for 95 year RP

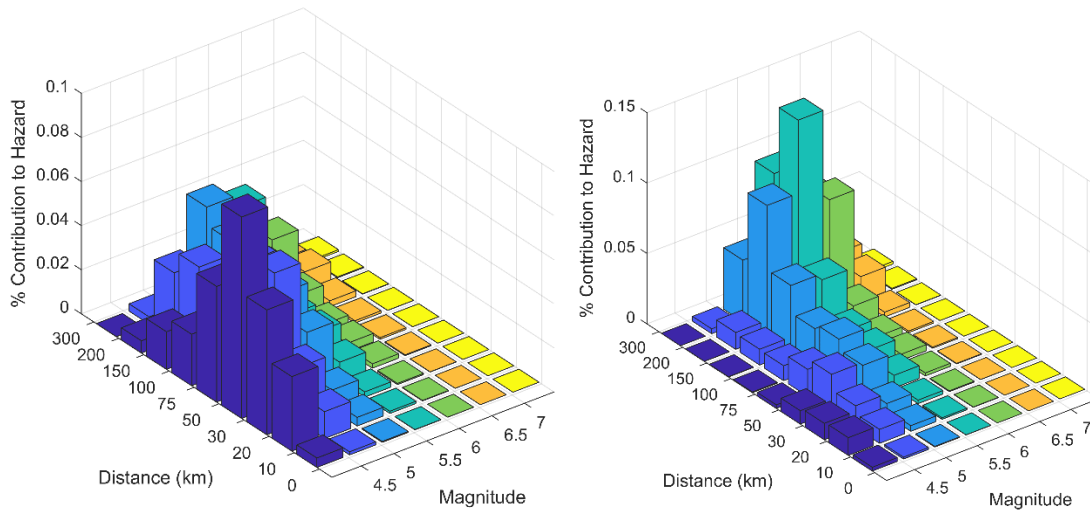


Figure 10-14 Hazard deaggregation for PGA (left) and Sa(T=1) (right) for 475 year RP

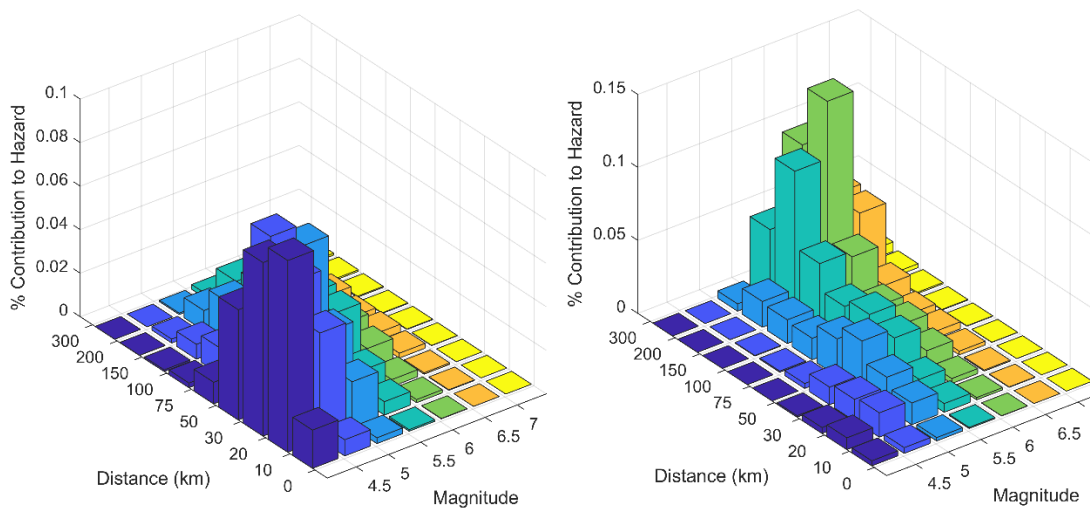


Figure 10-15 Hazard deaggregation for PGA (left) and Sa(T=1) (right) on rock for 3000 year RP

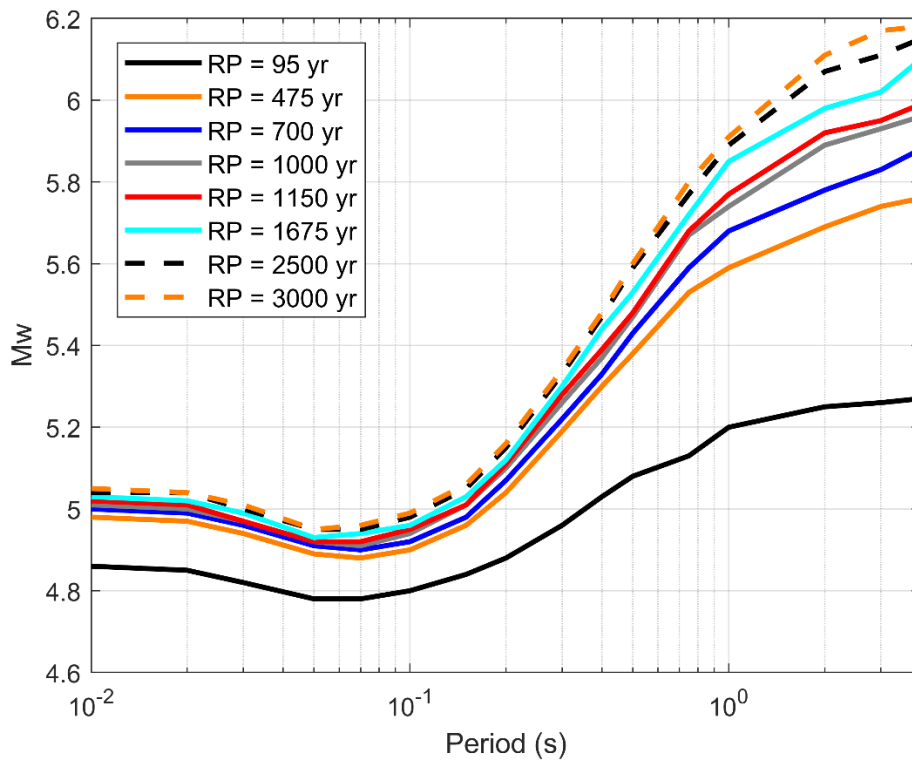


Figure 10-16 Mean magnitude contributing to the hazard at different spectral and return periods

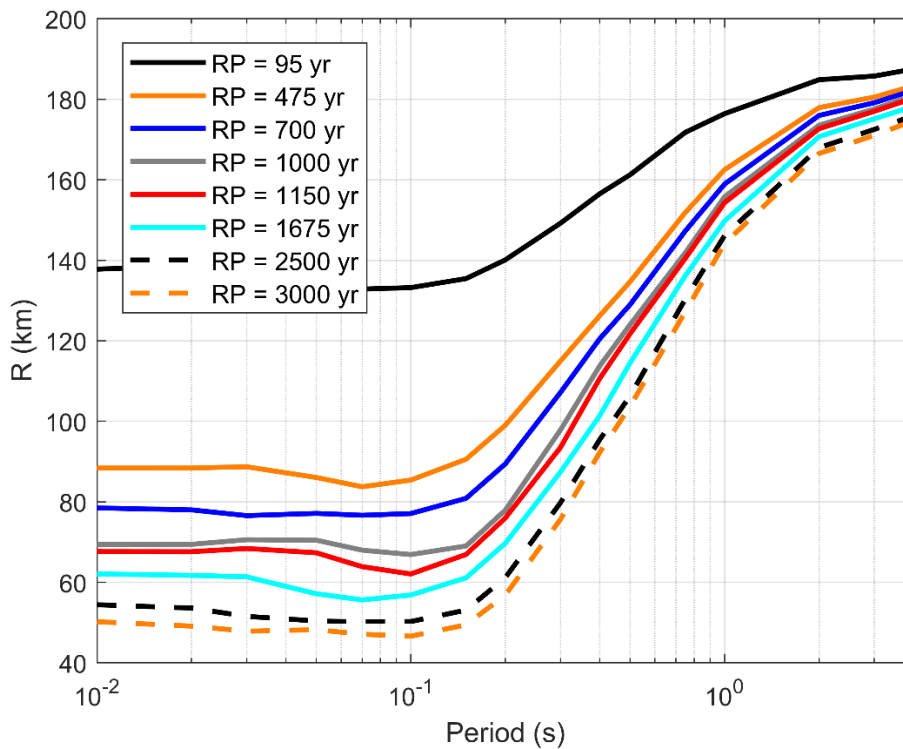


Figure 10-17 Mean distance contributing to the hazard at different spectral and return periods

10.5 Comparison with other studies

NGI calculated $PGA = 0.0124$ (Table 10-1) for 475 year return period and site conditions of $V_{S30} = 265$ m/s. This is comparable to the values estimated by Grünthal et al. (1999) (section 3.1) of 0-0.02 g, Bungum et al. (2000) (section 3.2) of 0.02 g, and Woessner et al. (2015) (section 3.3) of 0-0.025 g. However, these values were estimated for $V_{S30} = 760-800$ m/s. Therefore, for $V_{S30} = 265$ m/s, these values would be larger due to site amplification.

Figure 10-18 compares the mean UHS from this study for the TNW wind farm zone with the mean UHS from Fugro (2020) for the HKW wind farm zone for the four return periods specified in Fugro (2020). The values at the TNW site are about 70% of those for the HKW site. This is logical, because all three regional studies discussed in section 3 predict lower hazard for TNW than for HKW. The shape of the UHS is also very similar, which is due to the same ground motion models and similar seismic source zones used in both reports, and similar site conditions ($V_{S30} = 265$ m/s for TNW and $V_{S30} = 300$ m/s for HKW).

Figure 10-19 compares mean UHS calculated according to the PSHA (i.e. detailed seismic action procedure in ISO 19901-2:2017) and the simplified seismic action procedure described in section 2 for both exposure levels (L1 and L2) and both deep steel foundations and shallow concrete foundations. In all cases the simplified seismic action procedure predicts larger ground motions than the detailed seismic action procedure. This is also expected because the simplified seismic action procedure is designed to be conservative.

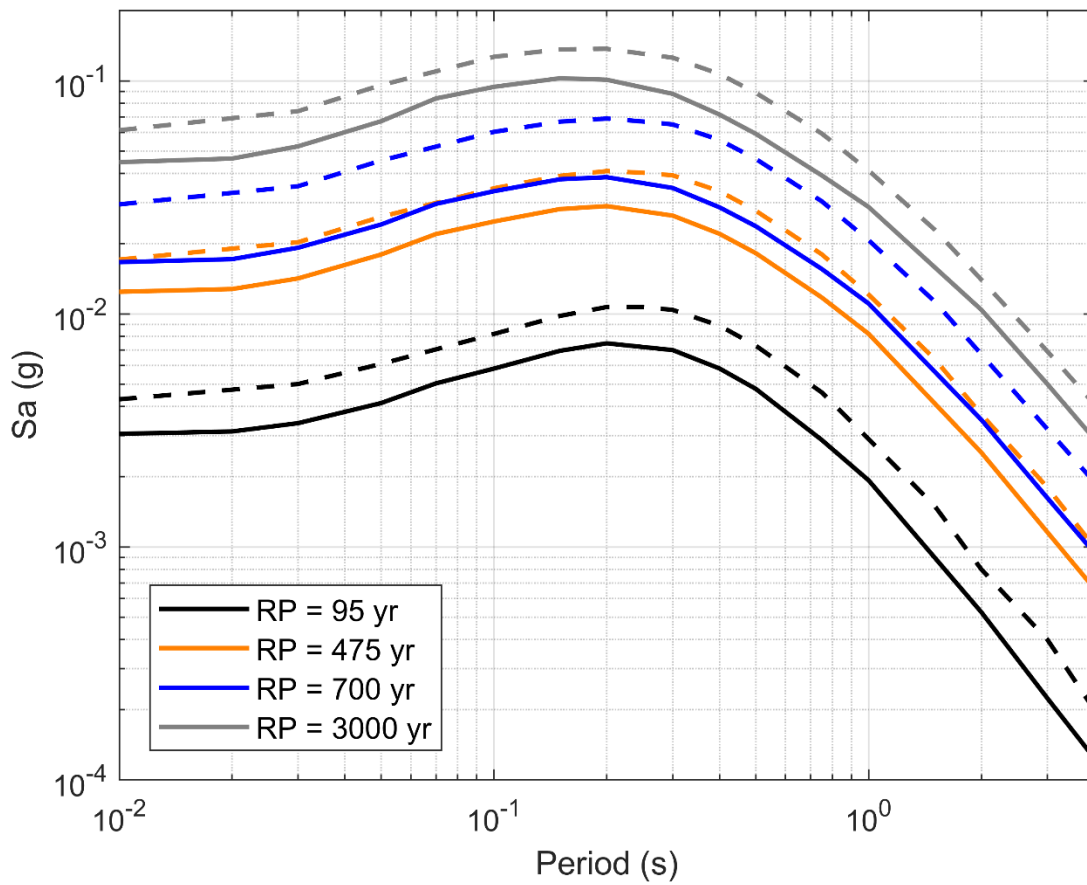


Figure 10-18 Comparison of mean UHS between TNW (solid lines) and HKW (dashed lines) for four different return periods. Note: Values shown for HKW site 700 year return period are for the closest available return period of 624 years. HKW used $V_{s30} = 300$ m/s and TNW used $V_{s30} = 265$ m/s.

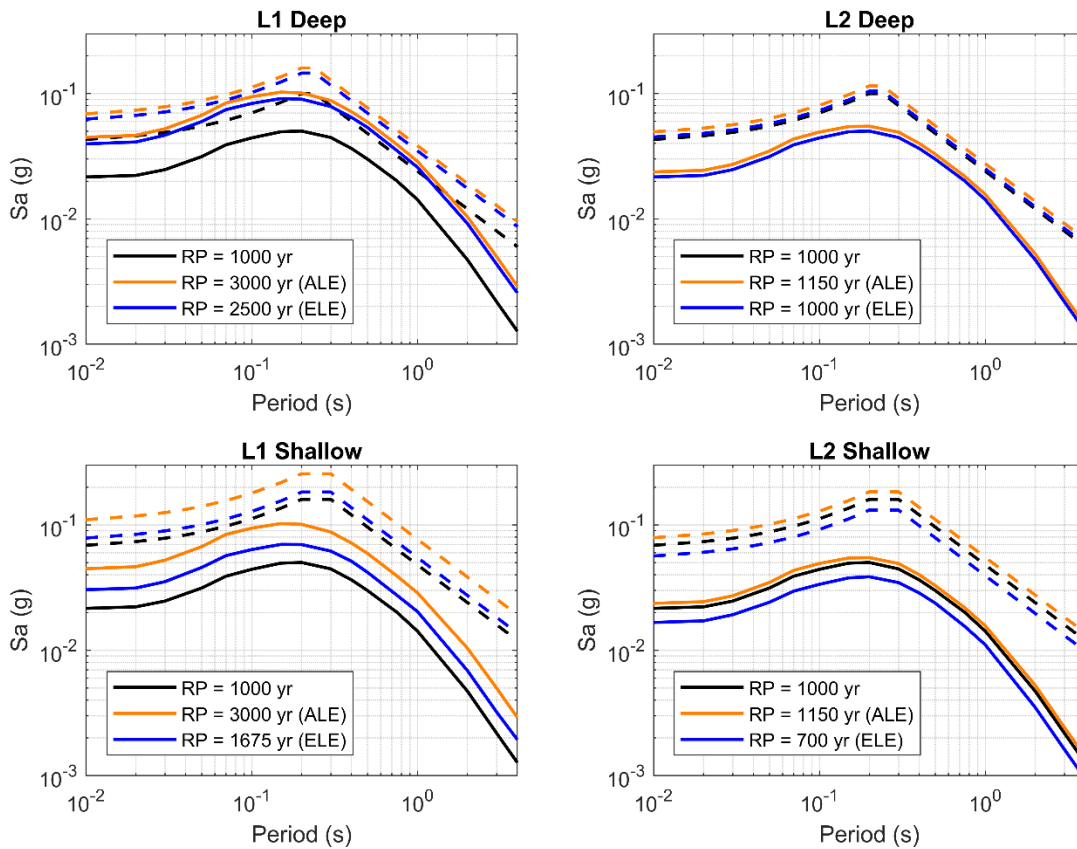


Figure 10-19 Comparison of mean UHS from the detailed seismic action procedure (solid lines) and design spectra from simplified seismic action procedure (dashed lines) for different exposure levels and foundation types.

10.6 Vertical design spectra and spectra for other damping ratios

NGI recommends taking vertical design spectra as $\frac{1}{2}$ the horizontal design spectra, as recommended by ISO19901-2:2017 for sites where $S_{a,map}(1.0) < 0.25$ g (for TNW $S_{a,map}(1.0) = 0.02$ g).

For design spectra at other damping ratios than 5%, NGI recommends using the correction factor given by ISO19901-2:2017:

$$D = \frac{\ln(100/\eta)}{\ln(20)} \quad (10-1)$$

where η is the damping ratio in percent and D is the correction factor with which to multiply the spectral acceleration values at 5% given in Table 10-1.

11 Conclusions

NGI performed a simplified and detailed seismic action procedure according to ISO 19901-2:2017 for the middle (5.699° East 54.022° North) of the Ten Noorden van de Waddeneilanden (TNW) Wind Farm Zone off the north coast of The Netherlands. NGI performed analyses for the Extreme Level Earthquake (ELE) and Abnormal Level Earthquake (ALE), L1 and L2 exposure levels, and assuming both deep steel foundations and shallow concrete foundations. These correspond to return periods of 700, 1000, 1150, 1675, 2500 and 3000 years. In addition, the client requested results for return periods of 95 and 475 years. The main conclusions from the analyses are:

- Based on seismic CPT data, NGI calculated an average $V_{S30} = 265$ m/s for TNW. The SCPT show similar velocity profiles across the site, therefore, NGI used only one representative value of V_{S30} .
- Model 4, the smoothed seismicity model, predicts the largest hazard for return periods less than about 1000 years, and Model 2 predicts the largest hazard for return periods greater than 1000 years. Model 4 most likely predicts the largest hazard at short return periods due to the inclusion of induced seismicity in the model development.
- In general, the areal source zone where the site is located dominates the seismic hazard, especially at longer return periods. This is because these zones have a higher chance of producing a large magnitude earthquake close to the site, which is what drives the hazard for PGA at long return periods.
- The ground motion model of Yenier and Atkinson (2015) predicts significantly larger hazard than the other models. The reason is that the Yenier and Atkinson (2015) model was developed for Eastern North America and therefore predicts much less attenuation than the other models. However, the Yenier and Atkinson (2015) model does not significantly increase the total mean hazard because it is only given a weight of 0.10, and including it provides conservative estimates (see Figure 7-1 through Figure 7-4).
- Spectral periods of 0.2 and 0.3 seconds predict the largest hazard for return periods of about 100 years or less, whereas spectral periods of 0.15 to 0.2 seconds predict the largest hazard for longer return periods.
- As the spectral period increases, the mean magnitude and distance increase, and as the return period increases, the mean magnitude increases and the mean distance decreases. This is a common result for PSHA with no strong fault activity.
- The controlling magnitude-distance scenario for short spectral periods is $M_w = 4.8-5.3$ and $R = 50-90$ km, and for long spectral periods is $M_w = 5.6-6.1$ and $R = 140-180$ km.
- The values at the TNW site are about 70% of those for the HKW site, which is expected based on past regional studies.
- In all cases the simplified seismic action procedure predicts larger ground motions than the detailed seismic action procedure. This is expected because the simplified seismic action procedure is designed to be conservative.

12 References

- Abrahamson, N. (2017). HAZ45.2, <https://github.com/abrahamson/HAZ>.
- Abrahamson, N. & Bommer, J. (2005). Probability and uncertainty in seismic hazard analysis. *Earthquake Spectra*, 21(2), 603-607.
- Akkar, S. & Bommer, J. (2010). Empirical equations for the prediction of PGA, PGV and spectral accelerations in Europe, the Mediterranean and the Middle East. *Seismol Res Lett* 81:195–206.
- Akkar S., Sandıkkaya M.A., Senyurt, M. & Azari S.A., Ay BÖ (2013). Reference database for seismic ground-motion in Europe (RESORCE). *Bull Earthq. Eng.* 12, 1, 311-339.
- Akkar, S., Sandıkkaya & M.A., Bommer, J.J. (2014). Empirical ground motion models for point- and extended-source crustal earthquake scenarios in Europe and the Middle East. *Bull Earthq Eng* 12:359–387.
- Atkinson, G. & Boore, D. (2006). Earthquake ground-motion prediction equations for eastern North America, *Bull. Seismol. Soc. Am.* 96, 2181–2205.
- Atkinson, G.M. & Boore, D.M. (2011). Modifications to Existing Ground-Motion Prediction Equations in Light of New Data. *Bulletin of the Seismological Society of America*, 101(3), 1121-1135.
- Baker, J. (2008). An introduction to Probabilistic Seismic Hazard Analysis (PSHA). [https://web.stanford.edu/~bakerjw/Publications/Baker_\(2008\)_Intro_to_PSHA_v1_3.pdf](https://web.stanford.edu/~bakerjw/Publications/Baker_(2008)_Intro_to_PSHA_v1_3.pdf)
- Bindi, D., M. Massa, L. Luzi, G. Ameri, F. Pacor, R. Puglia & P. Augiera (2014). Pan-European ground-motion prediction equations for the average horizontal component of PGA, PGV, and 5%-damped PSA at spectral periods up to 3.0 s using the RESORCE dataset, *Bull Earthq. Eng.* 12, no. 1, 391–430.
- Bindi, D., Cotton, F., Kohta, S.R., Bosse, C., Stromeyer, D. & Grünthal, G. (2017). Application-driven ground motion prediction equation for seismic hazard assessments in non-cratonic moderate-seismicity areas. *J Seismol* (2017) 21:1201–1218.
- Bommer, J.J. & Crowley, H. (2017). The Purpose and Definition of the Minimum Magnitude Limit in PSHA Calculations. *Seismological Research Letters* 88 (4) 1097–1106.
- Boore D.M. & Kishida T. (2017). Relations between some horizontal component ground-motion intensity measures used in practice. *Bull Seismol Soc Am* 107:334–343.

British Geological Survey (2021). BGS Earthquake database search. <http://www.earthquakes.bgs.ac.uk/earthquakes/dataSearch.html>

Brooks, C., Douglas, J. & Shipton, Z. (2020). Improving earthquake ground-motion predictions for the North Sea. *J Seismol* (2020) 24:343–362.

Bungum, H., Lindholm, C.D., Dahle, A., Hicks, E., Høgden, S., Nadim, F., Holme, J.K. & Harbitz, C. (1998). Development of Seismic Zonation for Norway: Final Report. Report for the Norwegian Council for Building Standardization (NBR), 187 pp.

Bungum, H., Lindholm, C.D., Dahle, A., Woo, G., Nadim, F., Holme, J.K., Gudmestad, O.T., Hagberg, T. & Karthigeyan, K. (2000). New seismic zoning maps for Norway, the North Sea, and the United Kingdom. *Seismological research letters*, 71, 687-697.

Campbell K.W. & Bozorgnia Y. (2014). NGA-West2 ground motion model for the average horizontal components of PGA, PGV, and 5% damped linear acceleration response spectra. *Earthquake Spectra* 30(3):1087–1115.

Cauzzi C. & Faccioli E. (2008). Broadband (0.05 to 20 s) prediction of displacement response spectra based on worldwide digital records. *J. Seismol.* 12:453–475.

Cauzzi, C., Faccioli, E., Vanini, M. & Bianchini, A. (2015). Updated predictive equations for broadband (0.01–10 s) horizontal response spectra and peak ground motions, based on a global dataset of digital acceleration records. *Bull Earthq Eng* 13: 1587–1612.

Cornell, C.A. (1968). Engineering seismic risk analysis. *Bulletin of the Seismological Society of America*, 58, p. 1583-1606.

Fugro (2020). Site-Specific Probabilistic Seismic Hazard Assessment for the Hollandse Kust (west) Wind Farm Zone. Final Report P904711/SHA 02. 1 October.

Giardini, D. et al. (2013). Seismic Hazard Harmonization in Europe (SHARE): Online Data Resource, <http://portal.share-eu.org:8080/jetspeed/portal/>, doi: 10.12686/SED-00000001-SHARE, 2013.

Glennie, K.W., Underhill & J.R. Origin (1998). Development and Evolution of Structural Styles. *Petroleum Geology of the North Sea: Basic Concepts and Recent Advances*. Wiley online library.

Grünthal, G. (1985). The up-dated earthquake catalogue for the German Democratic Republic and adjacent areas – statistical data characteristics and conclusions for hazard assessment. 3rd International Symposium on the Analysis of Seismicity and Seismic Risk, Liblice, Czechia, 17–22 June.

- Grünthal, G. & Stromeyer, D. (1994). The recent crustal stress field in Central Europe sensu lato and its quantitative modelling. *Geologie en Mijnbouw*, 73, p. 173-180.
- Grünthal, G. & the GSHAP Region 3 Working Group (1999). Seismic hazard assessment for Central, North and Northwest Europe: GSHAP Region 3. *Annali di Geofisica*, 42(6), p. 999-1011.
- Grünthal, G., Wahlström, R. & Stromeyer, D. (2009). The unified catalogue of earthquakes in central, northern, and northwestern Europe (CENEC)—updated and expanded to the last millennium. *Journal of Seismology*, 13, 517–541.
- Grünthal, G., & Wahlström, R. (2012). The European-Mediterranean earthquake catalogue (EMEC) for the last millennium. *J. Seismol.*, 16(3): p. 535–570
- Grünthal, G., Stromeyer, D., Bosse, C. (2017). The data set of the earthquake model for the probabilistic seismic hazard assessment of Germany, version 2016. Report on supplementary material for the respective publication. Scientific technical report STR - Data; 17/05.
- Grünthal, G., Stromeyer, D., Bosse, C. Cotton, F. & Bindi, D. (2018). The probabilistic seismic hazard assessment of Germany — version 2016, considering the range of epistemic uncertainties and aleatory variability “. *Bulletin of Earthquake Engineering*. <https://doi.org/10.1007/s10518-018-0315-y>.
- Gutenberg, B. & Richter, C.F. (1944). Frequency of earthquakes in California. *Bulletin of the Seismological Society of America*, 34(4), 185-188.
- Hale, C., Abrahamson, N. & Bozorgnia, Y. (2018). Probabilistic Seismic Hazard Analysis Code Verification. Pacific Earthquake Engineering Research Center, PEER Report No. 2018/03.
- ISC (2021). International Seismological Centre Online Bulletin. <http://www.isc.ac.uk/iscbulletin/search/bulletin/>
- ISO 19901-2 (2017). Petroleum and natural gas industries – Specific requirements for offshore structures – Part 2: Seismic action procedures and criteria. International Organization for Standardization, Geneva, Switzerland.
- ISO 19902 (2020). Petroleum and natural gas industries — Fixed steel offshore structures. International Organization for Standardization, Geneva, Switzerland.
- ISO 19903 (2019). Petroleum and natural gas industries — Concrete offshore structures. International Organization for Standardization, Geneva, Switzerland.

Jansen J.D. & Herber, R. (2017). Research into induced seismicity in the Groningen field: further studies. *Netherl J Geosci.*, 96(5): 279-284.

KNMI (2021). Seismic catalogue. <http://rdsa.knmi.nl/dataportal/>.

Kraaijpoel D. & Dost, B. (2013). Implications of salt-related propagation and mode conversion effects on the analysis of induced seismicity. *J Seismol* 17(1):95–107.

Kulkarni, R.B., Youngs, R.R. & Coppersmith, K.J. (1984). Assessment of confidence intervals for results of seismic hazard analysis, in *Proc. Of the Eighth World Conf. on Earthquake Engineering*, San Francisco, California, Vol. 1, 263–270.

Le Dortz K., Combres P. & Carbon D. (2019). An alternative seismotectonic zonation for probabilistic and deterministic seismic hazard assessment for Metropolitan France, 10ème Colloque National AFPS.

Lee, J.R., J. Rose & I.A.N. Candy et al. (2006). Sea-level changes, river activity, soil development and glaciation around the western margins of the southern North Sea Basin during the Early and early Middle Pleistocene: evidence from Pakefield, Suffolk, UK. *Journal of Quaternary Science* 21: 155–179.

Leydecker, G. (2011): Earthquake catalogue for Germany and adjacent areas for the years 800 to 2008). – *Geol. Jb.*, E 59; 198 S., 12 Abb., 5 Tab., 9 Anhaenge, 1 CD; BGR Hannover; Vertrieb: E. Schweizerbart'sche Verlagsbuchhandlung, Stuttgart. https://www.bgr.bund.de/EN/Themen/Seismologie/Erdbebenauswertung_en/Erdbeben_kataloge_en/historische_Kataloge/germany_en.html

McGuire, R.K. (1974). Seismic structural response risk analysis incorporating peak response regressions on earthquake magnitude and distance. Massachusetts Institute of Technology Department of Civil Engineering/Research Report R74-51.

McGuire, R.K. (1978). FRISK: Computer program for seismic risk analysis using faults as earthquake sources. U.S. Geological Survey Open-File Report 78-1007.

Musson, R.M.W. & Sargeant, S.L. (2007). Eurocode 8 seismic hazard zoning maps for the UK. British Geological Survey: Seismology and geomagnetism programme technical report CR/07/125, pp. 70.

NGI (2021). Ten Noorden van de Waddeneilanden Wind Farm Zone: Geological Ground Model report. NGI report 20190798-02-R, DRAFT, 25 March.

NPD (2021). CO2 Atlas for the Norwegian Continental Shelf - Chapter 4.1: Geology of the North Sea. Norwegian Petroleum Directorate. <https://www.npd.no/en/facts/publications/co2-atlases/co2-atlas-for-the-norwegian-continental-shelf/4-the-norwegian-north-sea/4.1-geology-of-the-north-sea/>

ROB, (2021). Royal Observatory of Belgium earthquake catalogue and database. <https://www.geo.be/catalog/details/799f9119-77f1-4931-b4e0-4615839ee1c4?l=en>

Schwartz, D.P. & Coppersmith, K.J. (1984). Fault behavior and characteristic earthquakes: Examples from the Wasatch and San Andreas fault zones. *Journal of geophysical research*, 89(B7), 5681-5698.

Stepp, J.C. (1972). Analysis of completeness of the earthquake sample in the Puget Sound Area and its effect on statistical estimates of earthquake hazard. In proceedings of 1st International Conference on Microzonation, Seattle, USA.

Tromans, I.J., Aldama-Bustos, G., Douglas, J., Lessi-Cheimariou, A., Hunt, S., Daví, M., Musson, R.M.W., Garrard, G., Strasser, F.O. & Robertson, C. (2019). Probabilistic seismic hazard assessment for a new-build nuclear power plant site in the UK, *Bulletin of Earthquake Engineering* 17 1–36.

Vanneste, K., Camelbeeck, T. & Verbeek, K. (2013). A Model of Composite Seismic Sources for the Lower Rhine Graben, Northwest Europe. *Bulletin of the Seismological Society of America*, Vol. 103, No. 2A, p. 984–1007.

Verbeek, K., Vanneste K. & Camelbeeck, T. (2009). Seismotectonic zones for probabilistic seismic-hazard assessment in Belgium. ONDRAF/NIRAS report, Belgium agency for radioactive waste and enriched fissile materials. NIROND-TR Report 2008-31E. 61 pp.

Villani, M., Polidoro, B., Ader, T., McCully, R., Lubkowski, Z., Courtney, T.J. & Walsh, M. (2019). A selection of GMPEs for the UK based on ground motion and macroseismic datasets. *Bull Seismol Soc Am* 109(4):1378–1400.

Weichert, D.H. (1980). Estimation of the earthquake recurrence parameters for unequal observation periods for different magnitudes. *Bulletin of the Seismological Society of America*, 70(4), 1337-1346.

Woessner, J., Laurentiu, D., Giardini, D., Crowley, H., Cotton, F., Gruenthal, G., Valensise, G., Arvidsson, R., Basili, R., Demircioglu, M.B., Hiemer, S., Meletti, C., Musson, R.W., Rovida, A.N., Sesetyan, K. & Stucchi, M. (2015). The 2013 European Seismic Hazard Model: key components and results. *Bulletin of Earthquake Engineering* 13, p. 3553-3596.

Yenier, E. & Atkinson, G.M. (2015). Regionally Adjustable Generic Ground-Motion Prediction Equation Based on Equivalent Point-Source Simulations: Application to Central and Eastern North America. *Bulletin of the Seismological Society of America*, Vol. 105, No. 4, pp. 1989–2009.

Youngs, R.R. & Coppersmith, K.J. (1985). Implications of fault slip rates and earthquake recurrence models to probabilistic seismic hazard analysis. *Bulletin of the Seismological Society of America*, 75(4), 939-964.

Ziegler, P.A. (1975). The geological evolution of the North Sea area in the tectonic framework of North-Western Europe. *Norges geol. Unders.* 316, 1-27.

Dokumentinformasjon/Document information		
Dokumenttittel/Document title Seismic hazard assessment		Dokumentnr./Document no. 20190798-03-TN
Dokumenttype/Type of document Teknisk notat / Technical note	Oppdragsgiver/Client Ministerie van Economische Zaken en Klimaat, Rijksdienst voor	Dato/Date 2021-05-26
Rettigheter til dokumentet iht kontrakt/ Proprietary rights to the document according to contract Oppdragsgiver / Client		Rev.nr.&dato/Rev.no.&date 0 /
Distribusjon/Distribution BEGRENSET: Distribueres til oppdragsgiver og er tilgjengelig for NGIs ansatte / LIMITED: Distributed to client and available for NGI employees		
Emneord/Keywords PSHA, offshore wind		

Stedfesting/Geographical information	
Land, fylke/Country The Netherlands	Havområde/Offshore area
Kommune/Municipality	Felt navn/Field name
Sted/Location	Sted/Location
Kartblad/Map	Felt, blokknr./Field, Block No.
UTM-koordinater/UTM-coordinates Zone: 31N East: 687217.8 North: 5987845.7	Koordinater/Coordinates Projection, datum: East: North:

Dokumentkontroll/Document control					
Kvalitetssikring i henhold til/Quality assurance according to NS-EN ISO9001					
Rev/ Rev.	Revisjonsgrunnlag/Reason for revision	Egenkontroll av/ Self review by:	Sidemanns- kontroll av/ Colleague review by:	Uavhengig kontroll av/ Independent review by:	Tverrfaglig kontroll av/ Interdisciplinary review by:
	DRAFT document	2021-03-24 Brian Carlton	2021-03-25 Amir M Kaynia		
0	Revised according to RVO and DNV comments	2021-05-21 Brian Carlton			

Dokument godkjent for utsendelse/ Document approved for release	Dato/Date 26 May 2021	Prosjektleder/Project Manager Carl Fredrik Forsberg
--	---------------------------------	---

2015-10-16, 043 n/e, rev.03

NGI (Norwegian Geotechnical Institute) is a leading international centre for research and consulting within the geosciences. NGI develops optimum solutions for society and offers expertise on the behaviour of soil, rock and snow and their interaction with the natural and built environment.

NGI works within the following sectors: Offshore energy – Building, Construction and Transportation – Natural Hazards – Environmental Engineering.

NGI is a private foundation with office and laboratories in Oslo, a branch office in Trondheim and daughter companies in Houston, Texas, USA and in Perth, Western Australia

www.ngi.no

NGI (Norges Geotekniske Institutt) er et internasjonalt ledende senter for forskning og rådgivning innen ingeniørrelaterte geofag. Vi tilbyr ekspertise om jord, berg og snø og deres påvirkning på miljøet, konstruksjoner og anlegg, og hvordan jord og berg kan benyttes som byggegrunn og byggemateriale.

Vi arbeider i følgende markeder: Offshore energi – Bygg, anlegg og samferdsel – Naturfare – Miljøteknologi.

NGI er en privat næringsdrivende stiftelse med kontor og laboratorier i Oslo, avdelingskontor i Trondheim og datterselskaper i Houston, Texas, USA og i Perth, Western Australia.

www.ngi.no

Neither the confidentiality nor the integrity of this document can be guaranteed following electronic transmission. The addressee should consider this risk and take full responsibility for use of this document.

This document shall not be used in parts, or for other purposes than the document was prepared for. The document shall not be copied, in parts or in whole, or be given to a third party without the owner's consent. No changes to the document shall be made without consent from NGI.

Ved elektronisk overføring kan ikke konfidensialiteten eller autentisiteten av dette dokumentet garanteres. Adressaten bør vurdere denne risikoen og ta fullt ansvar for bruk av dette dokumentet.

Dokumentet skal ikke benyttes i utdrag eller til andre formål enn det dokumentet omhandler. Dokumentet må ikke reproduseres eller leveres til tredjemann uten eiers samtykke. Dokumentet må ikke endres uten samtykke fra NGI.



The creative commons license terms 4.0 CC BY apply to this material.
Please take notice of the general terms "Creative Commons Attribution 4.0 International public License" before starting to use the license. These terms can be accessed by clicking on this link <https://creativecommons.org/licenses/>

This investigation was carried out by NGI, commissioned by RVO, an agency of the Ministry of Economic Affairs and Climate Policy.

Whilst a great deal of care has been taken in compiling the contents of this investigation, RVO can not be held liable for any damages resulting from any inaccuracies and/or outdated information.

The information in this document is valid at the time of publishing (see month/year). Updates will be published on the website <https://offshorewind.rvo.nl/> at the relevant sitemap (TNW), General Information, submap Revision Log and Q & A. In the Revision Log is indicated which versions are the latest and what the changes are in relation to previous versions. The documents can be found at the relevant sites, indicated in the List of all reports and deliverables.

Contacts
Netherlands Enterprise Agency (RVO)
Croeselaan 15 | 3521 BJ | Utrecht
P.O. Box 8242 | 3503 RE | Utrecht
www.rvo.nl | <https://english.rvo.nl>

Netherlands Enterprise Agency (RVO) | November 2021